AN EXPERIMENTAL INVESTIGATION OF INTERFACE BOND STRENGTH OF CONCRETE USING LARGE POWDER-DRIVEN NAILS

by

Donguk Choi, B.S.E., M. Arch., M.S.E.

Dissertation

Presented to the Faculty of the Graduate School of

The University of Texas at Austin

in Partial Fulfillment

of the Requirements

for the Degree of

Doctor of Philosophy

The University of Texas at Austin

May 1996

AN EXPERIMENTAL INVESTIGATION OF INTERFACE

BOND STRENGTH OF CONCRETE USING

LARGE POWDER-DRIVEN NAILS

APPROVED BY
DISSERTATION COMMITTEE:

_____
David W. Fowler

_____
James O. Jirsa

_____
Dan L. Wheat

_____
Frank B. McCullough

_____
Morris Stern

Dedicated to my family

ACKNOWLEDGEMENTS

I would like to express thanks to my supervising professors Dr. David W. Fowler and Dr. James O. Jirsa for their generous support. Thoughtful and hard working Dr. Fowler has always been inspiring. Knowledgeable and friendly Dr. Jirsa enabled me to make progress toward accomplishing a meaningful work. Thanks are due to my committee members, Dr. Dan Wheat, Dr. Frank McCullough, and Dr. Morris Stern for their interest and comments. My thanks are extended to other professors in the Department of Civil Engineering for their wonderful classroom instructions which were always full of invaluable information.

The assistance of David Whitney, Paul Walters, Rose Rung, and other technical staffs at the Construction Materials Research Group and that of Blake Stasney, Raymond Madonna, Wayne Fontenot, Patrick Ball, Ryan Green, Wayne Little, and other staffs at the Ferguson Structural Engineering Laboratory are acknowledged.

I am indebted to Reverend Eunkyu Park and fellow members of the Korean Presbyterian Church at Austin for their friendship and encouragement. I thank my parents for their concern and support. I acknowledge with gratitude the unlimited support of my children, Yangho and Yoonjo, and my wife, Chaeoak. Love and peace have always been at home thanks to wonderful experiences that we have shared together in our services to God.

February 1996 Donguk Choi

Austin, Texas

AN EXPERIMENTAL INVESTIGATION OF INTERFACE BOND STRENGTH OF CONCRETE USING LARGE POWDER-DRIVEN NAILS

Publication No. _____

Donguk Choi, Ph.D.
The University of Texas at Austin, 1996

Supervisors: David W. Fowler and James O. Jirsa

Delaminations of freshly placed overlays from existing concrete substrates have been reported in bonded concrete overlays (BCOs). An experimental study was undertaken to determine the performance of special large powder-driven nails used to provide positive bonding for BCOs. The investigation consisted of four parts. (1) Nail pull-out strength was investigated (366 tests). Test variables were strength of concrete and nail location with regard to cracks and test slab edges. (2) Interface shear strengths and mechanism of shear transfer with and without nails were investigated by push-off tests (116 tests). Test variables included concrete strength, interface roughness (shotblasted, sandblasted, and troweled), bonded versus unbonded interface, interface reinforcement, and crack effects. Interface strengths were also tested at early ages. (3) Beam fatigue tests were conducted to determine the interface shear strength deterioration. (4) A full-scale experimental BCO was constructed near El Paso, Texas, and nails were used in two of eight test sections. The condition of overlays in sections with and without nails was

compared in terms of overlay drying shrinkage crack and interface strength development and extension of delaminated interfaces. In the laboratory studies, nail pull-out strengths of 36 kN and 44 kN were determined in normal strength concrete and high strength concrete, respectively. The push-off test results indicated that nails were effective in improving the interface shear strengths of bonded-rough interfaces. An unbonded-rough interface with nails effectively resisted the shear force and limited the interface slip. Overlay curing methods at early ages significantly influenced the strength development. Interface strength did not deteriorate after 3,000,000 fatigue cycles in tests with nails and bonded-rough interfaces, but deterioration of composite action of unbonded interfaces with nails was observed after half a million cycles. In the experimental BCO, good bond (1,360 kPa or higher in tension) was developed in the slab interior region but interface delaminations and low bond strengths were determined near cracks and slab corners and edges. Test sections with nails performed significantly better than those without nails in terms of overlay drying shrinkage crack and interface bond strength development. The study results were used to make recommendations regarding the use of nails in a BCO to be constructed on IH-10 in downtown El Paso.

TABLE OF CONTENTS

APPENDICES

LIST OF TABLES

LIST OF FIGURES

CHAPTER ONE
INTRODUCTION

1.1 Research Background

Bonded concrete overlays (BCOs) have been used to rehabilitate concrete pavements, bridge decks, and slabs. When a new layer of concrete is placed on the horizontal surface of existing concrete in a bridge deck or a pavement, the construction joint between the two concrete layers does not often develop as much bond strength as monolithically cast concrete. The contact surface between the two concrete layers, often called the interface, presents challenges to structural engineers seeking a complete shear transfer across the interface for composite action to occur in the BCO.

(1) Interface Shear Transfer The transfer of shear forces across a plane is generally termed "interface shear transfer." The term is used to distinguish this type of the shearing action from that associated with diagonal shear cracking which occurs in other reinforced concrete members such as reinforced concrete beams. Good bond is necessary to achieve the full shear transfer across the interface. Several techniques are currently used to improve the bond and shear transfer. Adequate preparation of the top surface of existing concrete receiving the overlay is required. Methods used to clean or increase the texture of the contact surface include cold milling, shotblasting, water blasting, and sandblasting. An average texture of 1.2 mm (0.045 in.) is often specified for bonded concrete overlays (King

1992). A potential for creating microcracks between the paste and aggregates exists in case of excessive surface preparation (Silfwerbrand 1990). Bond-enhancing adhesives are often specified by design engineers in addition to the preparation of the contact surface. The most frequently used bonding agents are epoxy or cement mortar grout. Mechanical fastening devices such as epoxy-bonded dowel bars are sometimes used to improve transfer of the shear forces across the interface. Mechanical fasteners have been rarely used because their installation is typically labor intensive and can increase construction costs significantly.

(2) Powder-Driven Nails In 1990, the Hilti Corporation began research on a mechanical fastening device for shear transfer between two concrete layers (Breuss and Gassmann 1992). The result was a large nail, called a "Jumbo nail," shown in Fig. 1.1. The nail is installed into a predrilled hole with a special Hilti powder-driven actuator which makes use of an explosive charge. An actuator, explosive charges, and a special drill bit are shown in Fig. 1.2. It was expected that substantial savings in installation time could be achieved by driving a nail rather than installing an epoxy-bonded dowel bar. Even faster nail installation would be possible if the simple two-step nail installation process, drilling and nail shooting, could be automated. Jumbo nails are fabricated from high strength steel with a minimum yield strength of 600 MPa (90 ksi). The working principle of the jumbo nail in pull-out after driving is illustrated in Fig. 1.3 which shows the profile of a nail and a "stepped" drill hole. The diameter of the lower part of the drill hole is smaller than the nail shank by 0.3 mm (0.01 in.). The nail is installed into the drill hole using a powder-driven actuator so that as the nail is driven into the hole the lower part of the nail is clamped in the smaller drill hole. The tip of the nail penetrates into the existing concrete. The high compression and heat generated by

Figure 1.1 Jumbo Nail

Figure 1.2 Actuator, Explosive Charges, and Drill Bit

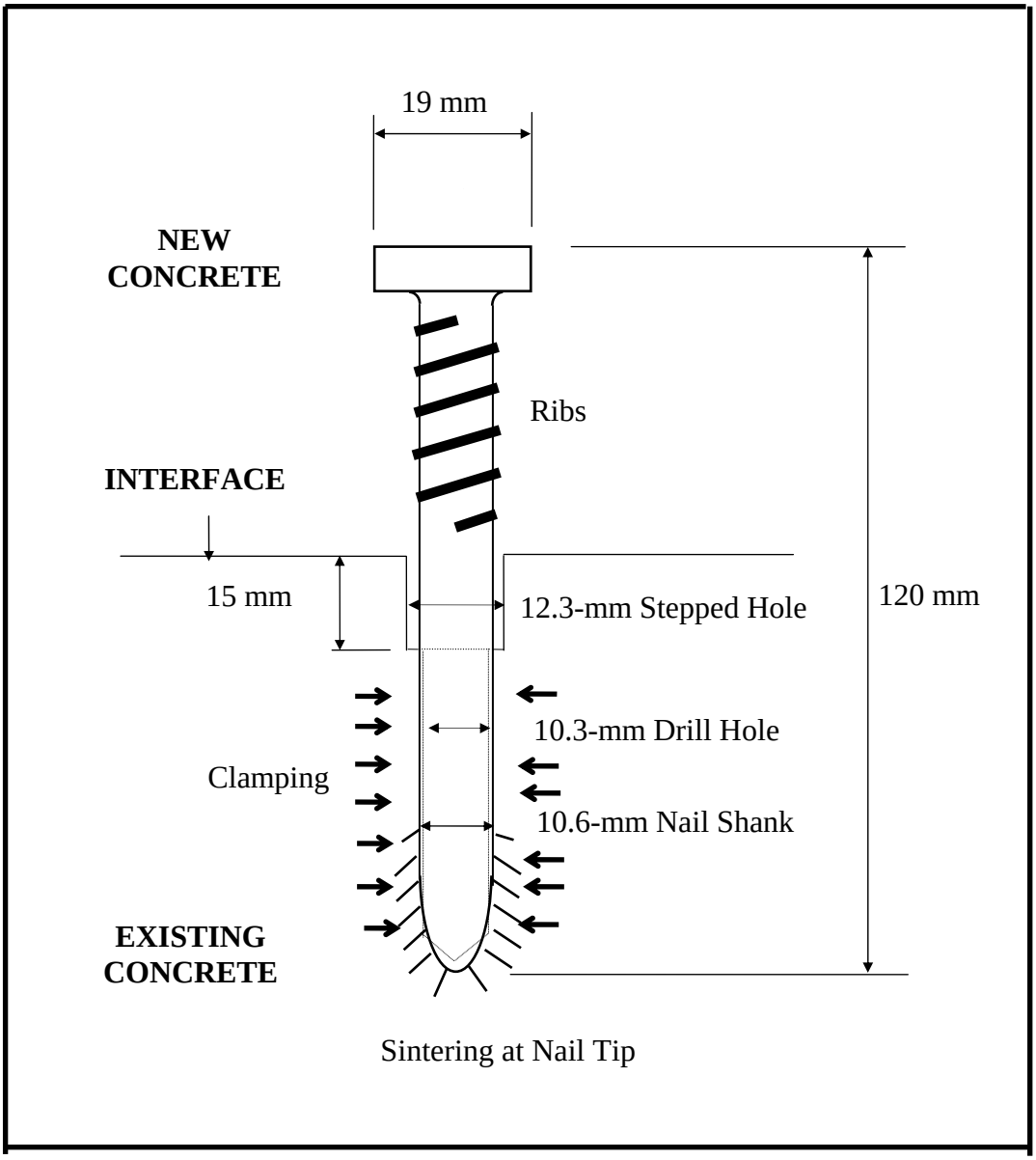

Figure 1.3 Nail and Stepped Drill Hole

driving the nail alters the surrounding concrete especially near the tip of the nail and produces a "sintering" effect. Sintering can also be found on the nail shank. The clamping force of the surrounding concrete on the nail and the sintering provide the nail pull-out strength. The top part of the nail in the overlay is anchored by the nail head. The contribution of the spiral ribs on the upper part of the nail shank (Fig. 1.3) to the pull-out resistance is not significant with the nail geometry although the role of the spiral ribs could become more important if the diameter of the nail head is decreased. The pull-out strength of the bottom half approximately matches that of the top half of the nail (Breuss and Gassmann 1992).

(3) Potential Structural Applications The primary application of jumbo nails in this study was for pavements with bonded concrete overlays. Jumbo nails, however, can be used for many other structural applications where shear transfer between two concrete elements cast at different times needs to be enhanced, such as, bridge deck overlays, interfaces between precast and cast-in-place elements, and interfaces between old and new concretes in columns repaired or strengthened by means of reinforced concrete jackets. Another potential application is infill wall construction, a seismic retrofitting technique for existing structures, where the shear transfer between existing frames and infill walls is required (Bass, Carrasquillo, and Jirsa 1989).

1.2 Concrete Overlays

The attention of many transportation agencies and pavement engineers in the U.S. has recently shifted from construction of new highways to maintaining, repairing, and rehabilitating existing highways. Approximately 35 percent of the 73,000 km (45,500 miles) of interstate highways in the U.S. at the end of fiscal year 1992 are paved with portland cement concrete (PCC) according to one survey of

the Federal Interstate Highway System (Slater 1993). Substantial portions are in need of immediate repairs as the majority of the federal interstate highways were constructed between 1960 and 1970 with a design service life of 20 years. In addition to the Interstate Highway System, some state highways in the U.S. are PCC pavements. Many state highways have reached the stage where rehabilitation is required since the majority of the state highways in the U.S. were constructed in a 50-year span beginning in 1921 (Lundy 1990). Resurfacing deteriorating PCC pavements with asphalt concrete (AC) overlays has been frequently used in the U.S. to extend the service life and improve the riding quality. Studies on the performance of AC resurfacing, however, reveal that AC overlays have a much shorter service life than PCC overlays (Hutchinson 1982). The primary benefit of AC resurfacing is the relatively low initial cost. The frequent need for additional resurfacing due to excessive bleeding, rutting, and premature delamination of AC overlays from the existing substrate significantly increases the life cycle cost of concrete highways. Another advantage of AC resurfacing is the rapid reopening of lanes to traffic with a minimal construction down time. The advantage of AC is diminishing with recent developments in concrete technology such as expedited construction of PCC overlays using high early-strength concrete (Whiting et al. 1993). A recent study on case histories of overlays by the U.S. Army Corps of Engineers (Campbell 1994) suggested that both bonded and unbonded PCC overlays can be successfully used to resurface existing concrete highways. A service life of 10 to 20 years is expected from PCC bridge deck overlays and 15 years or more for PCC pavement overlays according to the study. Unbonded concrete overlays are usually used to rehabilitate an extensively deteriorated AC or PCC pavements since only a minimal amount of repair of the existing pavement is required. Relatively thick (150- to 300-mm or 6- to 12-in.) overlays are placed while a bond breaker or a separation layer is placed between the two concrete layers. Relatively thin bonded concrete overlays (75 to 150 mm or 3 to 6 in.) can

be used when the deterioration of existing pavement is not severe. Bonded concrete overlays are a relatively new technique in pavement engineering introduced in the 1970s (Hutchinson 1982).

Problems which have to be addressed for BCOs include (1) delamination of overlays from the existing concrete, (2) reflection cracking in the overlay, and (3) plastic and drying shrinkage cracking in the overlay. The BCO requires repair of the existing pavement if it has significantly deteriorated before full-depth composite section can be developed. The amount of reflective cracking in the overlay is related to distress in the existing concrete and can be reduced by careful preoverlay repair although it can be costly to repair defects in a severely deteriorated base. The development of shrinkage cracks in the overlay resulting from restrained contraction of the overlay is investigated in this study. Causes of the delamination of overlays from the existing base are still a subject of speculation. Previous studies suggest drying shrinkage of the overlay, thermal effects due to differential temperature distribution across the depth of the pavement section (Lundy 1990), and repeated traffic loading (Metzinger 1990) as possible causes.

1.3 Problem Statement

Delamination of overlays from the base concrete has been observed in some bonded concrete overlays. Delaminations typically occurred near the edge of a pavement or in the vicinity of pavement cracks especially at early ages (Neal 1983, Lundy 1990). The interface shear stress concentration due to shrinkage-related contraction or temperature change-induced contraction or expansion of one layer with respect to the other layer is the likely cause of the delamination. “Jumbo

nails" are investigated as a potential solution to improve bond and force transfer between the two concrete layers.

1.4 Research Scope and Objectives

A comprehensive four-part experimental study was conducted to determine the performance of jumbo nails used as shear connectors between a new layer of concrete cast against an existing concrete layer. The primary application of nails investigated was in bonded concrete overlays. The research objectives were the following:

1. Investigate the behavior of jumbo nails in pull-out, shear, and fatigue shear load,
2. Determine the interface shear strength and the shear transfer mechanism across the interface with and without the use of nails, and
3. Study the performance of nails in bonded concrete overlays.

The experimental program was divided into four parts: pull-out tests of nails, interface shear transfer tests (push-off tests), beam tests for static and fatigue interface shear strength, and a full-scale experimental BCO. All experiments were conducted in the laboratory except the full-scale experimental BCO which was constructed in El Paso, Texas.

Chapter Three describes the preparation and results of the nail pull-out tests. Pull-out tests were conducted first since the pull-out capacity of jumbo nails needed to be established before other tests could be designed. A total of 366 pull-out tests was completed in the Ferguson Structural Engineering Laboratory at the University of Texas at Austin. Eight base slabs with four different combinations of

concrete compressive strength and aggregate type were constructed. Four slabs were used for the pull-out tests. Four replicate slabs were used for the shear transfer tests. The pull-out behavior of nails installed in different slabs was determined. Test variables included the presence of cracks and the nail installation distance from the edge of the slabs. Chapters Four and Five describe the test preparation and the results of the push-off tests which were conducted to investigate the interface strength and the fundamental mechanism of interface shear transfer with and without the use of nails. A total of 116 specimens was tested. A special push-off test setup was devised. Eighty-four tests were performed after overlays were at least 28 days old or when the compressive strength of the overlay approximately matched that of the base slab. Thirty-two additional specimens were tested to determine the development of the interface shear strength at early ages of the concrete overlay (Chapter Six). Chapter Seven describes the beam tests which were conducted for static and fatigue interface shear strength using twelve composite and one monolithically cast beam. Five beams were tested statically. Test results were compared to those from push-off tests. Eight beams were subjected to high cycle fatigue loading in shear. Most beams received between 2,000,000 and 3,000,000 cycles of repeated loads. The performance of the interface with and without the use of nails under repeated loading in shear was examined from beam fatigue tests. Chapter Eight describes the construction and test results of a full-scale experimental BCO built in El Paso, Texas, to test the feasibility of the expedited overlaying technique using high early-strength concrete and shear connectors. Overlays were constructed with a high early-strength concrete mix which developed over 50 MPa (7,250 psi) compressive strength in seven days. Eight test sections were constructed. Jumbo nails were installed in two test sections. All sections were constructed between April and June 1995 when the local environmental conditions were considered most favorable for overlay delamination. Field coring and several nondestructive test methods were used to

detect overlay delamination. The performance of the experimental BCO was closely monitored over a six-month period following the overlay construction.

The results of the studies were used to make design recommendations regarding the use of the powder-driven nails in a future BCO project which is to be constructed on IH-10 in downtown El Paso, Texas, in 1996 (Allison, McCullough, and Fowler 1993).

CHAPTER TWO
REVIEW OF STUDIES ON INTERFACE SHEAR TRANSFER AND BONDED CONCRETE OVERLAYS

2.1 Interface Shear Transfer between Old and New Concretes

Early research on interface shear transfer concentrated on determining the shear strength of the connection between precast beams and cast-in-place slabs for highway bridges. Hanson (1960), for example, investigated the interface strength between precast beams and cast-in-place slabs with the use of vertical dowels or shear keys. In other early research, attempts were made to establish the interaction between the shear and the tensile stresses acting simultaneously along the interface (Mattock et al. 1972, 1975). Birkland and Birkland (1966) and Mast (1968) proposed a shear-friction theory for estimating the ultimate shear force across the interface. The results of the early experimental and theoretical works including those by Hanson, Anderson (1960), Mattock et al. (1969, 1972, 1975), Birkland and Birkland, and Mast are incorporated in the current American Concrete Institute Building Code (ACI 1989).

2.1.1 Push-Off Test

Push-off tests have been used extensively to determine the interface strength between two concrete elements cast at different times. Many different push-off test setups have been used to determine the interface strength and the

shear transfer mechanism. The interface strength determined using the different push-off test methods led to different results although the results were generally consistent for those using similar test methods.

Felt (1956, 1960) first studied the feasibility of using thin resurfacing or patching of old concrete pavements with bonded concrete. Various methods for preparing the surface of existing pavements were explored to determine those that provided the best bond. The strength and the integrity of base concrete and the cleanliness of the old surface were determined to be important. The best bond was obtained when a cement grout bonding agent was used on a dry interface. Good compaction and adequate curing of the fresh concrete were also cited as being important for a strong bond. The laboratory data and the field work indicated that the bond strength in shear may frequently be 2,800 kPa (400 psi) or more although a shear strength of 1,400 kPa (200 psi) or even less was found in existing overlays performing satisfactorily.

Hanson (1960) tested 62 push-off specimens to explore various means of improving horizontal shear transfer at connections between precast beams and cast-in-place slabs for highway bridges. The push-off test setup used by Hanson is shown in Fig. 2.1. Interface roughness, keys, and stirrups or ties crossing the interface were included as test variables. The concrete compressive strength ranged between 21 MPa (3,000 psi) and 42 MPa (6,000 psi). The interface shear reinforcement ratio, area of stirrups or ties divided by the interface area, was 0.4 percent for specimens with stirrups. Maximum shearing stresses of 3,450 kPa (500 psi) for a rough bonded surface and 2,100 kPa (300 psi) for a smooth bonded

Figure 2.1 Push-Off Test Setup by Hanson (1960)

surface were measured.

Mattock et al. investigated the transfer of the shear forces across the interface between precast beams and cast-in-place slabs. Concrete was cast monolithically and a relatively high percentage of shear reinforcement (up to 1.3 percent) was used. It was determined in one study (Hofbeck, Ibrahim, and Mattock 1969) that the ultimate shear transfer strength was a function of the amount of the shear reinforcement in that the change in strength, size, and spacing of the shear reinforcement affected the shear strength. The effect of the tensile or the compressive stresses acting on the shear plane along with the shear stress on the interface strength was studied by Mattock and Hawkins (1972). Test setups used by Mattock et al. are shown in Figs. 2.2 (a), (b), and (c). The “standard” push-off test setup is shown in Fig. 2.2 (a). A setup shown in Fig. 2.2 (b) or pull-off test was used to study the effect of tensile stress acting on the shear plane along with shear.

Figure 2.2 Test Setups by Mattock et al. (1969, 1972)

The comparison of test results determined using the push-off and the pull-off setups is shown in Fig. 2.3. The term “uncracked” was used to describe specimens where the interface was not intentionally damaged (cracked) by a pretest shear loading, while the term “cracked” was used to describe specimens where the interface was intentionally precracked to determine the influence of the shear reinforcement on the interface shear strength. The interface strengths of the “uncracked” specimens determined using the pull-off setup are lower than those determined using the push-off setup while it was estimated that the average intensity of the tensile stresses acting along the interface is about half the intensity of the applied shear stresses in pull-off tests. No differences in the shear strength were noted for initially

Figure 2.3 Comparison between Push-Off and Pull-Off Test Results (Mattock et al. 1969, 1972)

Figure 2.4 Modified Push-Off Test Results (Mattock and Hawkins 1972)

"cracked" specimens tested using the pull-off and the push-off setups, respectively, in Fig. 2.3. The effect of compressive stress acting simultaneously on the shear plane with shear stress was investigated using a modified push-off setup shown in Fig. 2.2 (c). The presence of the compressive stresses increased the interface shear strength as shown in Fig. 2.4.

Paulay, Park, and Phillips (1974) investigated the principal mechanism of shear resistance along horizontal construction joints crossed by reinforcement in cast-in-place concrete construction, such as shear walls. The contribution of dowel action, surface preparation, and reinforcing content on the shear strength of the horizontal construction joints was determined. The test setup and test results are shown in Figs. 2.5 (a) and (b), respectively. The construction joint strength in shear was between 3,450 kPa (500 psi) and 4,800 kPa (700 psi) in specimens with bonded-rough surfaces. It was suggested that the dowels with a 0.7 percent joint reinforcement ratio contributed approximately 16 percent of the strength at the peak.

Seible and Latham (1990) carried out experimental and analytical studies of the interface design and the horizontal construction joint preparation between an old bridge deck and the overlay in bridge deck rehabilitation. The experimental program consisted of push-off tests, tests of overlaid transverse deck slab panels, and a full-scale test on a T-girder bridge section. Test results showed that a minimum interface reinforcement ratio as required by the American Association of State Highway and Transportation Officials (AASHTO) standard specifications was ineffective once delaminations occurred. A minimum dowel reinforcement required for a composite concrete flexural member determined by Eq. 2.1 (AASHTO 1989) is 0.08 percent in case of the Grade 400 MPa (60 ksi) dowel bars:

(a) Test Setup

(b) Test Results

Figure 2.5 Push-Off Test Setup and Test Results by Paulay et al. (1974)

$$A_d = \frac{50 b_v s}{f_y} \qquad (2.1)$$

where A_d = the reinforcement area crossing the interface: b_v = the width of the interface investigated for horizontal shear; and s and f_y = the spacing and strength of dowel reinforcement, respectively, in pounds and inches.

2.1.2 Composite Beam Static Test

Hanson (1960) conducted tests on ten T-shaped girders in addition to the push-off specimens described previously. It was concluded that the push-off tests provided a good representation of the stress-slip curves for the girders tested.

Saemann and Washa (1964) tested 42 composite beams. Test variables included joint roughness, length of the shear span, reinforcement ratio, and position of the joint with respect to the neutral axis. Three different beam span lengths were used: 2.4 m (8 ft.), 3.4 m (11 ft.), and 6.1 m (20 ft.). The percentage of stirrups across the joint ranged between 0 percent and 1.1 percent. Test results for beams with a short and an intermediate span length showed that shear strength increased as surface roughness and reinforcement ratio increased. Little change in shear strength was observed for all beams with a 6.1-m span as contact surface roughness and amount of reinforcement increased. Additional beam tests were completed by Grossfield and Birnstiel (1962). Difficulties in measuring the actual slip between precast beams and slabs were reported due to severe web cracking in beams.

It must be noted that the equation for shear in an elastic section (Eq. 2.2) was used to estimate the interface shear stresses in all beam tests. Although the

stresses calculated using Eq. 2.2 provided a common base for comparison, the equation, which is based on linear elastic behavior of an uncracked beam section, does not represent the actual stress condition after the development of flexural and web shear cracks and slip between precast beams and slabs.

$$\tau = \frac{VQ}{Ib} \tag{2.2}$$

More recently, in slab panel tests by Seible and Latham (1990) which simulated a transverse strip of bridge deck, the midspan load versus deflection plots as well as the crack pattern development were used to compare the performance of different slab panel specimens. Tests on specimens with lubricated (unbonded) interfaces and with 0.07 percent dowel reinforcement showed that the behavior of the unbonded slabs was distinctively different from the other surface preparations (lightly sandblasted or scarified), which all showed monolithic action beyond yield of the flexural deck reinforcement.

2.1.3 Fatigue Test

Badoux and Hulsbos (1967) studied the behavior of the horizontal shear connection in composite concrete beams under repeated loads. Deterioration of the interface shear strength of 29 composite beams was investigated. Principal variables included amount of interface reinforcement, roughness of interface, and ratio of shear span to effective depth of the beam. The test setup is shown in Fig. 2.6. The load was cycled 2,000,000 times. Slip values for the initial loading and after the completion of the repeated loading were compared. The conclusions of the study were the following:

(a) Section Details

(b) Loading Scheme

Figure 2.6 Beam Fatigue Test by Badoux and Hulsbos (1967)

1. Interface cracking with the resulting loss of composite action was initiated by diagonal tension cracking of the precast beam.
2. Interface cracking started for most beams at a section located about two-thirds of the shear span from the support. The crack progressed toward the load point but new cracks appeared closer to the support.
3. Interface slip readings consistently confirmed the cracking observations and gave the most accurate method for judging the interface damage.
4. Roughening the contact surface was beneficial for fatigue strength. Rough surfaces were much stronger than intermediate surfaces.
5. Interface strength in fatigue was found to be related to the amount of interface reinforcement.
6. Shear span-to-depth ratio (a/d ratio) had a relatively small influence on fatigue strength. Beams with a higher a/d ratio had a weaker interface strength due to difference of cracking in the precast beam.

Seible and Latham (1990) performed a full-scale fatigue test of a section cut from an existing bridge. One-half of the bridge span was scarified and the other half was sandblasted. Dowel reinforcement was provided around the perimeter of the bridge deck to prevent debonding and early age curling due to differential shrinkage along free edges. A 15-cm (6-in.) reinforced concrete overlay was placed. The specimen was subjected to 200,000 cycles of sinusoidal loading. No interlayer delamination was recorded after cycling.

2.1.4 Shear-Friction Theory

Birkland and Birkland (1966) and Mast (1968) proposed a shear-friction theory with which the ultimate shear strength across an interface can be determined. The shear-friction hypothesis is illustrated in Fig. 2.7. It is first

assumed that a crack will form along the interface subjected to shear. When the shear force, ***V***, acts along a cracked interface, one crack face slips relative to the other as shown in Fig. 2.7. Slip is accompanied by the separation of the crack faces for a rough and irregular interface. The separation is assumed to be sufficient to yield the reinforcement crossing the interface. The reinforcement provides a compressive force, ***T***, across the interface, which is equal to the area of the reinforcement multiplied by the yield strength. The applied shear force is then resisted by friction between the two cracked faces which are subjected to a compressive force equal to the tensile forces in reinforcement and by the dowel action provided by the shear reinforcement. A hypothetical friction angle, $\tan\varphi$, is used for the force, ***N***, the horizontal component of which resists the applied shear force. Section 11.7 of the ACI Building Code defines the shear-friction equation (Eq. 2.3). When shear-friction reinforcement is perpendicular to the shear plane, the ultimate shear strength, V_n, can be determined using Eq. 2.3 (ACI 1989):

$$V_n = A_{vf} F_y \mu \qquad (2.3)$$

where the coefficient of friction, μ, is

1.4λ for concrete placed monolithically,

1.0λ for intentionally roughened concrete-to-concrete interface,

0.6λ for not intentionally roughened concrete-to-concrete interface, and

0.7λ for concrete anchored to as-rolled structural steel by headed studs or by reinforcing bars,

Figure 2.7 Shear-Friction Hypothesis (Birkland and Birkland 1966)

and λ is 1.0 for normal weight concrete, 0.85 for “sand-lightweight” concrete, and 0.75 for “all lightweight” concrete.

2.1.5 Dowel Action

Previous research (Paulay, Park, and Phillips 1974, Gambarova and Prisco 1991) suggested three different dowel mechanisms: flexure of the reinforcing bars across the interface, shear across the bars, and kinking of the reinforcing bars as shown in Fig. 2.8. Dowel action is also related to local bearing forces in the concrete close to the contact area with the dowel. When the dowels are large, the strength of the surrounding concrete in bearing rather than the yield strength of the reinforcement will limit the shear capacity of a dowel.

Figure 2.8 Mechanisms of Dowel Action (Gambarova and Prisco 1991)

2.2 Bonded Concrete Overlays

Felt (1956, 1960) and Gillette (1963) investigated the performance of bonded concrete overlays (BCOs) constructed as early as 1913 and 1954, respectively. The delamination of overlays from base concrete was found in many early BCO projects in condition surveys. The extent of overlay delamination varied from one project to another and was typically limited to local areas at edges or corners and near cracks. However, delamination was considered to result from improper surface preparation or construction techniques. It was concluded in both studies that relatively thin concrete overlays would perform adequately if proper surface preparation techniques and construction procedures were followed.

The modern day BCO is regarded as a relatively new technique in pavement engineering which saw increased use beginning in the 1970s (Hutchinson 1982). Improvements in paving technology, such as slip-form paving machines and improved shotblasting equipment, and the trend toward selection of resurfacing type on the basis of life-cycle costs, rather than initial costs, has led to increased usage of BCO (Whiting et al. 1993). Debonding failures of overlays have been reported in some recent BCO projects although many successful projects have also been reported. Research results suggest that the shear stress concentration near the edge of a pavement or in the vicinity of pavement cracks is the likely cause of the delamination of overlays from the existing concrete (Lundy 1990). Repeated traffic wheel loading has also been investigated as the possible cause of overlay delamination (Metzinger 1990).

2.2.1 End Effect

The problem of the concentration of the high shear and tensile stresses in a narrow region near the end of the bonded composite structural member has been known to structural engineers as the "End effect." The stress at the end is caused by shrinkage-related contraction or temperature change-induced contraction or expansion of one layer with respect to the other layer. Many analytical and experimental studies (Timoshenko 1926, Hess 1969, Grimado 1978, Al-Negheimish 1988) have determined that the relatively high shear and tensile stresses developed in the end region decay quickly to zero inside the composite member at a distance from the end approximately equal to the total thickness of the composite member. Axial forces induced by restrained contraction or expansion of one layer with respect to the other can be analytically determined in a relatively simple manner (Timoshenko 1926). The distribution of stresses concentrated near the end, or the end stresses, has been investigated in many studies. Chen, Cheng,

and Gerhardt (1982), assumed an isothermal condition and linear elastic material behavior and derived a governing differential equation which led to an exact plane stress solution of the end stresses in closed form. The equation was derived for an elastic three-layered composite beam in which the third layer was a very thin adhesive layer. The work of Chen, Cheng, and Gerhardt was expanded to yield the plane strain solution by Choi, Fowler, and Wheat (1996). The analytical procedure proposed by Chen et al. was used to determine the end stress distribution in very thin polymer concrete (PC) overlays. The typical thickness of PC overlays is less than 25 mm (1 in.). Figure 2.9 shows the composite beam model used in the analyses. The distribution of axial, shear, and interface normal stresses in the end region of a PC-PCC composite beam caused by restrained thermal contraction of the PC was determined using the procedure suggested by Chen et al. and is shown in Figs. 2.10 (a) and (b), respectively. Choi et al. also performed a parametric study on the end stress development. The effect of the various modular and the thickness ratios between the top and the bottom layers on the end stress development was studied for very thin concrete overlays. It was determined that the interface stresses increase as the modular ratio and the thickness ratio of the top layer to the bottom layer increase.

2.2.2 End Effect in Bonded Concrete Overlays

Lundy (1990), using a finite element program, studied the development of the stress concentration near the edge of a BCO or in the vicinity of pavement interior cracks at early ages of the overlay. Analyses were performed for the period ranging between 12 and 48 hours after the overlay placement. The maximum

Figure 2.9 Composite Beam Model Used for Thermal Stress Analyses (Choi et al. 1996)

(a)

(b)

Figure 2.10 End Effect: Distribution of Interface Stresses (Choi et al. 1996)

temperature difference between the overlay and existing concrete was taken as 18 °C (33 °F). The temperature distribution across the depth of the BCO was determined based on field test data. The shrinkage of the overlay was taken into account through the use of 17 °C (30 °F) temperature differential between the overlay and existing pavement. The analytical results indicated maximum interface stresses after 24 hours of 170 kPa (24 psi) in shear and 120 kPa (17 psi) in tension on pavement edges and 210 kPa (30 psi) in shear and 150 kPa (22 psi) in tension near interior cracks for a BCO with a 100-mm- (4-in.-) thick overlay cast on top of 200-mm- (8-in.-) thick existing concrete. Lau, Fwa, and Paramasivam (1994) performed an elastic finite element study of interface stresses. The effect of vertical wheel loads, temperature loading and wheel breaking forces was studied. The computed shear stresses at the pavement-overlay interface for typical values of pavement and overlay thickness, created by wheel loads and thermal gradients were compared to reported values of the interface shear strength. The shear stresses at the interface in each loading case were found to be small in relation to the interface bond strength of laboratory-prepared overlaid specimens (approximately 5 percent of the shear strength). It was concluded that debonding in overlay construction in the field was likely to be caused by stress concentrations due to local defects.

2.2.3 Recent Bonded Concrete Overlay Projects in U.S.

Many organized efforts to document recent developments in construction procedures and the performances of the bonded concrete overlays have been made by state Departments of Transportation (DOT) in the U.S. Many states including California (Neal 1983), Iowa (Calvert 1990, Marks 1990, Harris 1992), Louisiana (Temple and Cumbaa 1985, King 1992), and Texas (Bagate et al. 1985, Teo, Fowler, and McCullough 1989) have published such data. Varying degrees of success of the bonded concrete overlays have been reported. Delamination failures

of the overlays are rather common in BCO projects although the extent of the delamination is typically localized. Two projects, however, experienced rather severe delamination problems. The debonding failure of one project necessitated overlaying the pavement using asphalt concrete. Failure in the other project convinced transportation officials that BCO was not a viable method of resurfacing.

A severe overlay delamination problem was reported in a BCO constructed by the California Department of Transportation, CALTRANS, in June 1981 (Neal 1983). The 75-mm (3-in.) BCO was placed on a 2.4-km (1.5-mile) section of Interstate 80. This section, which is at a high elevation, was subjected to relatively large temperature fluctuations during and after the construction. Debonding of the overlay was noted shortly after the overlay placement. Approximately one-third of the overlay separated from the underlying slab in some sections. The entire project was overlaid with asphalt concrete in October 1981. Subsequent laboratory studies were undertaken to investigate the cause of the delamination. Repeated thermal loading was determined to be the cause.

A bonded concrete overlay was constructed in Wisconsin (McGhee 1994) on a 16-year-old PCC pavement which had been given a “critical” distress rating prior to overlaying in 1988. State reports do not mention repairs to the underlying pavement in preparation for the overlay. Due to excessive debonding, the overlay had returned to a nearly critical level after only two years of service. At the end of five years, the DOT reported extensive surface cracking and apparent debonding. On the basis of this project, the Wisconsin DOT recommended “... that thin bonded concrete overlays should not be considered as a means of extending the service life of a continuously reinforced concrete pavement structure.”

2.2.4 Bonded Concrete Overlays in Texas

Three bonded concrete overlays were constructed in Texas beginning in 1983. The construction process and the performance of the overlays were closely monitored by the Center for Transportation Research at the University of Texas at Austin.

2.2.4.1 Experimental BCO, Houston South Loop An approximately 300-m- (1,000-ft.-) long experimental BCO section was first constructed on Loop IH-610 South in Houston, Texas, during the summer of 1983 (Bagate et al. 1985). Prior to this experimental BCO, asphalt concrete was typically used to resurface existing PCC pavements in Texas. The existing pavement was 200 mm (8 in.) thick. Surface preparation of the existing surface consisted of cold milling to a nominal depth of 6 mm (1/4 in.) followed by sandblasting. Immediately prior to overlaying, a cement grout was uniformly broomed onto the prepared surface. The overlay thichnesses were 50 mm (2 in.) and 75 mm (3 in.). Three 50-mm overlays had three types of reinforcement: (1) none, (2) welded wire fabric, and (3) steel fibers. Two 75-mm overlays were reinforced with welded wire fabric and steel fibers, respectively. The performance of this experimental BCO after five years in service was rated excellent (Teo, Fowler, and McCullough 1989). The fiber reinforced sections exhibited very little cracking. The first rebar-sounding survey performed in February 1990, however, showed that some overlay delaminations had occurred. The majority of the delamination was found near a longitudinal construction joint at the center of the 14.5-m- (48-ft.-) wide pavement. The extent of the delamination was found to be less than one percent of the area in each test section (Lundy 1990).

2.2.4.2 IH-610 North BCO, Houston, Texas The Texas DOT constructed a large-scale second BCO in Houston consisting of approximately 40-lane-km (25-

lane-miles) on Loop IH-610 North during the winter of 1985. Figure 2.11 shows the location of the experimental BCO and IH-610 North BCO sites. The depths of the overlay and the base concrete were 100 mm (4 in.) and 200 mm (8 in.), respectively. Surface preparation consisted of shotblasting followed by air blasting immediately before the overlay placement. The majority of the overlay was constructed using siliceous river gravel and welded-wire-fabric reinforcement. A cement grout bonding agent was used for most sections. Three different condition surveys were completed on test sections in March 1987, August 1987, and March 1988. The rebar-sounding survey determined about one percent overlay delaminations. All delaminated areas were found adjacent to longitudinal and transverse pavement cracks or joints. Figure 2.12 shows the average delamination on test sections. The test variables and the result of two condition surveys are shown in Tables 2.1 and 2.2, respectively (Teo, Fowler, and McCullough 1989).

2.2.4.3 IH-610 South BCO, Houston, Texas In 1989, the Texas DOT undertook the construction of the third BCO of an existing 200-mm- (8-in.-) thick PCC pavement on Loop IH-610 South. This project consisted of approximately 64-lane-km (40-lane-miles) of 100-mm (4-in.) bonded overlays. The overall construction process was similar to the IH-610 North BCO project. Several different bonding agents were used including cement grout, epoxy, and latex-modified grout. Overlay delamination was found within 18 hours following the overlay placement in two test sections where latex-modified grout was used as the

Figure 2.11 Map of Houston Area Showing Two Bonded Concrete Overlay Sites

bonding agent. The delaminated area continued to expand during the six-week monitoring period and about 30 percent of the total area had delaminated one month after the overlay was placed in two test sections with latex-modified grout (Fig. 2.13). It was believed that the latex-modified grout had been permitted to dry before the overlay concrete was placed which created a bond breaker. The overlays on these test sections were later removed and replaced with bonded concrete overlays using cement grout (Lundy 1990).

2.2.5 Use of Mechanical Fasteners in Bonded Concrete Overlays

A recent BCO project in Louisiana reported the use of mechanical fastening devices for positive bonding (King 1992). The existing 16-year-old 200-mm- (8-

(a) West Bound Lanes

(b) East Bound Lanes

Figure 2.12 Percent Delamination: IH-610 North BCO (Teo et al. 1989)

Table 2.1 Variables and Length (m) of Test Sections: IH-610 North BCO

Bonding Agent	Overlay Reinforcement Type			
	Fibrous Concrete		Welded Wire Fabric	
	River Gravel	Limestone	River Gravel	Limestone
Cement Grout	--	670	300	4,100
No Grout	--	--	--	120

Table 2.2 Percent Delamination of Overlays: IH-610 North BCO

Location	Condition	Survey Date	
		Mar. 1987	Mar. 1988
West Bound Lane 1	Overall	0.3	0.3
	No Grout	2.2	1.8
West Bound Lane 2	Overall	0.3	0.3
	No Grout	3.4	4.5
East Bound Lane 1	Overall	1.4	1.4
	Limestone	0.0	0.1
	River Gravel	1.8	1.8
East Bound Lane 2	Overall	2.0	2.1
	Limestone	0.0	0.1
	River Gravel	2.6	2.6

Figure 2.13 Delamination of Overlays: IH-610 South BCO

in.-) thick PCC pavement was overlaid with 100-mm- (4-in.-) thick steel fibrous concrete in order to provide an additional 20-year service life. The project objective was to provide an overlay with a high probability for long term success by using a concrete mix with high cement content, internal reinforcement, and with good bonding characteristics. Steel fibers were used in anticipation of reflective cracking in the overlay. Reinforcement bars (fabricated in U shape) were epoxied into the existing slab to provide positive bonding at the slab edges where thin overlays have a tendency to debond due to curling and/or warping. Tests on overlaid pavements revealed excellent bond strength and reduced edge deflections.

CHAPTER THREE
PULL-OUT TESTS: EXPERIMENTAL PROGRAM AND TEST RESULTS

3.1 Introduction

Preparation for the pull-out tests and test results are described in this chapter. Colecchia (1994) also reported jumbo nail pull-out test results. Shear reinforcement installed across the unbonded-smooth interface between two concrete layers subjected to shear forces will provide shear resistance primarily by dowel action. When the interface is rough and irregular, as is the case for bonded concrete overlays, the overlay has to displace vertically in relation to the base concrete as it displaces horizontally as the interface is subjected to shear forces. The vertical displacement mobilizes a tensile force in the reinforcement. The applied shear force is then resisted by the shear-friction, in which the friction between the two cracked faces and the dowel action together resist the applied shear force. Adequate pull-out resistance of nails required for shear-friction was examined by the pull-out tests. The pull-out resistance of nails was also investigated to ensure the development of tensile forces in the nail when the overlay attempts to separate from the base layer in bonded concrete overlays.

Table 3.1 Slab Index, Compressive Strength, and Aggregate Type

Slab Index	Aggregate Type	Compressive Strength (MPa)	Remarks
1	River gravel	32 [a]	Normal strength
2	Soft limestone	19 [b]	Low strength
3	Hard limestone	28 [b]	Normal strength
4	Soft limestone	51 [c]	High strength

Note: a, b, c: 97-day, 56-day, and 74-day compressive strengths, respectively.

3.2 Preparation for Pull-Out Tests

3.2.1 Test Slabs

Eight concrete test slabs, 4 meter (13 ft.) long, 1.4 meter (4.5 ft.) wide, and 0.2 meter (8.0 in.) deep, were fabricated. Reinforcement at the slab mid depth consisted of U.S. # 6 bars (diameter = 20 mm or 0.75 in.) placed at 250 mm (10 in.) on center in both directions, which provided a 0.5 percent reinforcement ratio typical of highway construction. Slabs were cast in pairs on four separate dates. The concrete mixes used for casting on different dates varied in compressive strength (f'c) and aggregate types. All slabs were cured under wet burlap and plastic sheets for seven days. For each concrete mix, a pair of slabs was cast. The first of each set of slabs was used for the pull-out tests. The second of each set was reserved for the shear transfer tests. Table 3.1 summarizes the compressive strength and aggregate type used in each pair of slabs. The maximum size of the

aggregates was 25 mm (1 in.). The slabs in Table 3.1 will be labeled as follows: slab 1, normal strength slab with river gravel, slab 2, low strength slab, slab 3, normal strength slab with hard limestone aggregate, and slab 4, high strength slab.

3.2.2 Test Setup and Test Procedure

Testing began after the ages of the slabs were at least 56 days. The drill hole was made using the special Hilti drill bit in a rotary hammer drill. The specified drill hole depth was 60 mm (2.4 in.). A hand pump was first used to remove dust from the hole. Compressed air and a vacuum cleaner were used later for dust removal. Drill hole cleaning is required because the presence of excessive dust may interfere with the sintering. Nails were driven into the drill holes. Figures 3.1 and 3.2 show the drilling and the nail driving operations, respectively. One purpose of the "stepped" drill hole (Fig. 1.3) is to eliminate concrete surface cracks generated during driving of the nail (Breuss and Gassmann 1992). It was often observed, however, that some hair line cracks developed on the concrete surface during nail driving. The cracks were very small in width (less than 0.03 mm or 0.001 in.) and developed in the radial direction. The cumulative length of the cracks was recorded.

The pull-out load was applied using a hydraulic cylinder resting on a reaction ring. The diameter and the height of the steel tube used as the reaction ring were 250 mm (10 in.) and 500 mm (20 in.), respectively. Access to the nail inside the reaction ring was provided by openings cut in the tube wall. A loading assembly shown in Fig. 3.3 was fabricated. A circular opening with a diameter slightly larger than the nail head diameter was cut in the bottom steel of the loading

Figure 3.1 Stepped-Hole Drilling

Figure 3.2 Nail Driving

Figure 3.3 Pull-Out Test Loading Assembly

Figure 3.4 Pull-Out Test Setup

Figure 3.5 Instrumentation for Nail Displacement Readings

assembly. A set of split collars was fabricated to fit below the nail head. Tension on the nail was applied through a threaded steel bar connecting the hydraulic cylinder and the nail loading assembly. The pull-out test setup including reaction ring, hydraulic cylinder, and hand pump is shown in Fig. 3.4. The nail displacement readings were taken on top of the nail head as shown in Fig. 3.5. Displacement readings were taken using a linear potentiometer with 0.025-mm (0.001-in.) accuracy. The applied load was monitored using a pressure transducer. Signals from the pressure transducer and the linear potentiometer were recorded during testing. The rate of sampling was approximately 20 data sets per second. Load was applied slowly for 60 seconds in all tests with the nail pull-out failure typically occurring at approximately 30 to 40 seconds.

3.2.3 Test Variables

The pull-out test program was developed primarily to simulate field conditions for bonded concrete overlays as closely as possible. The influence of concrete strength and aggregate types and various installation positions of the nails on the test slabs was investigated. The effect of the cumulative length of the hair line cracks which often developed on top surface of the concrete receiving the nail was investigated. The Hilti powder-driven actuator (Fig. 3.2) was equipped with a dial that allowed the operator to adjust the amount of charge that was directed toward driving the nail. The lowest and the highest dial readings (power levels) were one and four, respectively. Tests were performed at power levels 1, 2, 3, and 4 in order to study the effect of the charge.

3.2.3.1 Concrete Strength and Aggregate Type The effect of the concrete strength and aggregate type on the pull-out behavior of the nails was investigated by testing nails installed on four different test slabs. The nail pull-out strength is provided by the clamping action of the surrounding concrete and the sintering while the clamping action provides approximately 70 percent of the nail pull-out strength when nails are used in the normal strength concrete (Breuss and Gassmann 1992). It was theorized that the magnitude of the clamping force would be dependent on the concrete elastic modulus and compressive strength. The sintering may also be influenced by the concrete strength and aggregate types. The normal strength slab with river gravel and the low strength slab had compressive strengths of 32 MPa (4,650 psi) and 19 MPa (2,750 psi), respectively, at the time of testing. The normal strength slab with hard limestone aggregate and the high strength slab had compressive strengths of 28 MPa (4,100 psi) and 51 MPa (7,400 psi), respectively, at the time of testing.

3.2.3.2 Nail Installation Position The nail installation position on a slab was grouped into three categories: installation near the slab edge (edge), installation near an existing crack (cracked concrete), and installation where the nail is not driven near a crack or an edge (standard). Nails were installed at a distance larger than 300 mm (12 in.) away from a crack or slab edge for the "standard" pull-out tests. Figure 3.6 shows one test slab where the layout of 16 nail positions is shown before nails are driven for the standard pull-out tests.

Nails were installed closer to the slab edges in the "edge" pull-out tests. It is likely that jumbo nails will be installed near pavement edges due to the fact that overlay delaminations typically occur along the edges in bonded concrete overlays. Preliminary tests showed that the powder-driven nail installation can cause a cone of concrete to spall off when a nail is installed too close to the edge. Nails were driven at distances between 100 mm (4 in.) and 150 mm (6 in.) away from the edge of slabs in 12.5-mm (0.5-in.) or 25-mm (1-in.) increments. Nails were driven and then immediately pulled out for the standard and the edge tests. Four different actuator power levels were used in the standard and the edge pull-out tests.

Several different pull-out schemes were used for the "cracked-concrete" pull-out tests. Flexural cracks were created on one side of all test slabs using a setup shown in Fig. 3.7. Cracks were created by loading the slab in flexure in series "A." Nails were driven into a crack after the slab was unloaded and then the slab was reloaded so that the crack began to widen in series "A." Nails were pulled out when the slab was reloaded. Series "B" was the simplest, where nails were driven into an existing crack and then immediately pulled out. Figure 3.8 shows

Figure 3.6 Slab Layout before Standard Pull-Out Tests

Figure 3.7 Loading Frame Used to Create Flexural Cracks on Test Slabs

Figure 3.8 Cracked Face of Slab: Cracked-Concrete Pull-Out Tests

Figure 3.9 Nail Installed Close to a Crack

the cracked face of one test slab. The width of the crack before and after nail driving was different. The change in the crack width was recorded by measuring the crack width before and after nail installation using a crack comparator in all cracked-concrete pull-out tests. Series "C" was similar to series "A" but nails were pulled out when the slab was reloaded to approximately half the loading level as in series "A." Nails were driven close to a crack rather than into a crack in series "D." Nail installation distances were 25 mm (1 in.), 50 mm (2 in.), and 75 mm (3 in.) away from cracks. Figure 3.9 shows a nail installed 25 mm away from a crack. The next two test series, "F" and "G", involved driving a line of nails across the width of the slab at 200-mm (8-in.) intervals and then loading the slab in flexure. This produced a line of cracks of approximately 0.05 mm (0.002 in.) in width following the line of the nails. Slabs were further loaded until the cracks began to widen and nails were pulled out in series "F." Slabs were unloaded and nails were pulled out in series "G." Only one actuator power level (power level 2) was used for all "cracked-concrete" pull-out tests.

3.2.4 Test Series

A total of 366 pull-out tests was completed. Tests were divided almost equally between standard, edge, and cracked-concrete pull-out tests. Table 3.2 summarizes the number of nails tested in standard, edge, and cracked-concrete pull-out tests. Many replicate standard and edge nails were tested as shown. The cracked-concrete pull-out tests were further divided into six different test series, "A" through "G", as shown in Table 3.3. The number of replicates ranged between three and twelve in each test series.

Table 3.2 Number of Nails Tested by Pull-Out Test Types

Slab Index	Test Types			Total
	Standard	Edge	Cracked Concrete	
1	32	36	38	106
2	32	36	33	101
3	24	24	29	77
4	24	24	34	82
Total	112	120	134	366

Table 3.3 Number of Nails Tested in Cracked-Concrete Pull-Out Tests

Slab Index	Test Series						Total
	A	B	C	D	F	G	
1	4	12	4	9	6	3	38
2	4	8	4	9	4	4	33
3	--	10	--	9	6	4	29
4	3	9	3	9	6	4	34
Total	11	39	11	36	22	15	134

3.3 Pull-Out Test Results

3.3.1 Typical Nail Pull-Out Behavior

The typical pull-out load versus nail displacement plots determined from two standard pull-out tests, ***R4S.2*** and ***R4S.7***, are shown in Fig. 3.10. Specimen notation was based on the slab (R = normal strength slab with river gravel), actuator power level (4 = power level 4), test type (S = standard test), and replicate number (2 = replicate number 2). The peak loads of 43 kN (10 kips) and 41 kN (9 kips) are determined in ***R4S.2*** and ***R4S.7***, respectively, with displacements of approximately 0.4 mm (0.02 in.) at the peak. The pull-out load quickly decays to zero after the peak while the nail pulls out a cone of concrete in ***R4S.2***, which is called a cone-type failure in this study. Different load-displacement behavior is shown in the other specimen. The nail displacement rapidly increases while the pull-out load quickly drops after the peak. The rapid change in the load-displacement plot could not be accurately measured due to relatively slow rate of sampling which was approximately 20 data sets per second. At some point after the peak, the nail resists further displacement and a post peak load plateau forms at approximately 70 percent of the peak load in ***R4S.7***. The nail was pulled out cleanly from concrete. The vast majority of the nail failure modes were similar to that of ***R4S.7***. Figure 3.11 shows four cone-type failures and twelve nail pull-out failures in 16 standard pull-out tests on the normal strength slab with river gravel.

3.3.2 Cone-Type Failure and Sintering

Of the total of 366 nails tested, 22 nails failed by pulling out a cone of concrete: 18 on slab one, none on slab two, one on slab three, and three on slab

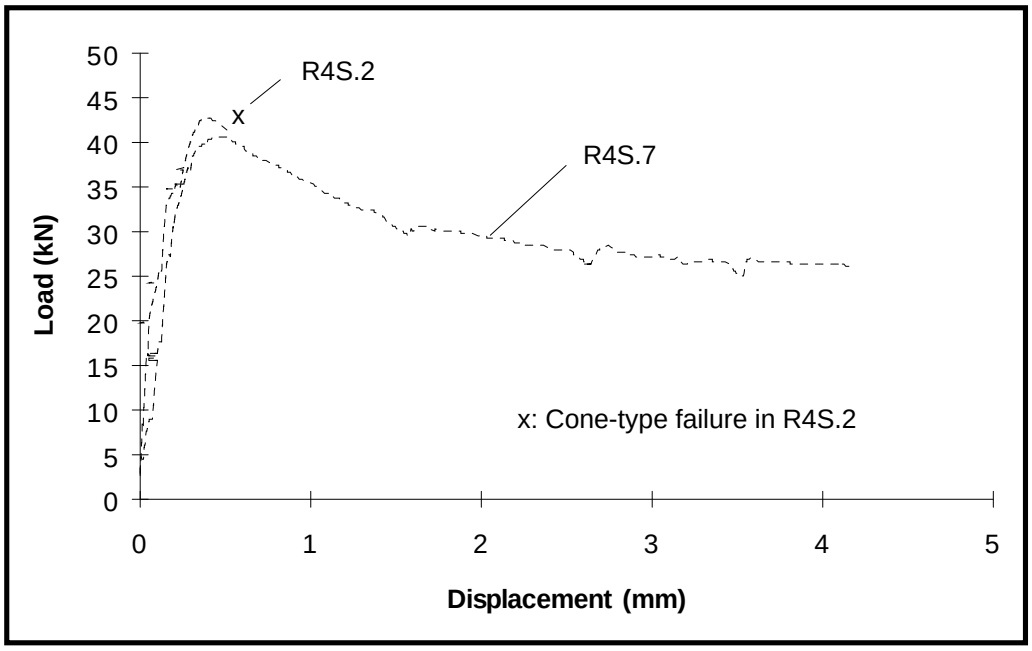

Figure 3.10 Load vs. Nail Displacement: Standard Pull-Out Tests

Figure 3.11 Test Slab after Standard Pull-Out Tests

four. One aspect of the nail behavior which correlated well with the occurrence of the cone-type failures was the degree of sintering. The high compression and heat generated by driving the nail alter the surrounding concrete and produce sintering. In most cases, sintering was found on the tip of the nails. Sintering sometimes extended along the nail shank. The sintering usually consisted of a thin layer of concrete paste with thicker patches of mortar and small pieces of aggregate fused to the nail at times. Figures 3.12 and 3.13 show a cone-type failure and different degrees of the sintering.

3.3.3 Standard Test Results

A total of 112 standard pull-out tests was completed. The peak loads of all nails were determined from load-displacement plots similar to those shown in Fig. 3.10. The nail pull-out strength of all standard tests is summarized in Table 3.4. Each entry in Table 3.4 typically represents the results of six or eight tests. An average pull-out strength of 34 kN (7.5 kips) was determined from all standard pull-out tests on four different slabs. The nail displacements at the peak load typically ranged between 0.25 mm (0.01 in.) and 0.5 mm (0.02 in.). Test results reveal that the nail pull-out strength is strongly influenced by the concrete strength since nails installed in the higher strength concrete show significantly higher pull-out strength. The average pull-out strength of all nails installed in high strength concrete was 44 kN (10 kips). The average pull-out strength of all nails installed on the low strength concrete was 20 kN (4.5 kips). The average pull-out strengths were 38 kN (8.5 kips) and 36 kN (8 kips) in normal strength concrete with river gravel and normal strength concrete with hard limestone aggregate, respectively. Test results on two normal strength concretes with the two different types of aggregate suggest that the effect of the aggregate types on the nail pull-out

(a)

(b)

Figure 3.12 Cone-Type Failure

Figure 3.13 Different Degrees of Sintering

strength is not significant. The effect of the actuator power levels on the nail pull-out strength can be determined in Table 3.4. The pull-out strengths of nails driven at higher power levels are higher than those of nails driven at lower power levels in Table 3.4. The difference in the pull-out strength, however, is not large. On the other hand, the cumulative length of the surface cracks which often form by driving the nail increases with increasing power levels as shown in Table 3.5. The overall average of the cumulative length of the surface cracks in nails driven using power level 1 is 45 mm (1.8 in.) and that in nails driven using power level of 4 is 84 mm (3.3 in.). It was decided to use power level 2 for further nail driving since the gain in the nail pull-out strength by using higher power level is not large while longer cracks tend to form at higher power levels.

Table 3.4 Summary of Pull-Out Strength (kN): Standard Pull-Out Tests

Slab Index	Concrete Strength (MPa)	Power Level				Average
		1	2	3	4	
1	32	***36***	***37***	***39***	***40***	***38***
2	19	***17***	***20***	***19***	***22***	***20***
3	28	***34***	***36***	***38***	***36***	***36***
4	51	***45***	***41***	***43***	***46***	***44***
Average	--	***32***	***33***	***34***	***35***	***34***

Table 3.5 Cumulative Length (mm) of Surface Cracks after Nail Driving

Slab Index	Concrete Strength (MPa)	Power Level				Average
		1	2	3	4	
1	32	***5***	***0***	***25***	***35***	***16***
2	19	***13***	***17***	***2***	***49***	***20***
3	28	***16***	***25***	***39***	***30***	***28***
4	51	***150***	***178***	***195***	***220***	***186***
Average	--	***45***	***55***	***65***	***84***	***62***

The standard pull-out test results are shown in Fig. 3.14. The nail pull-out strengths are plotted against the square root (SQRT) of the concrete compressive strength in Fig. 3.14. A linear relationship between the nail pull-out strength and the square root of the concrete compressive strength represents a reasonable estimate of pull-out strength.

3.3.4 Edge Test Results

Jumbo nails are likely to be installed close to pavement edges because overlay delaminations typically occur along edges. High interface shear stresses which form by effects of restrained contraction or expansion of one layer with respect to the other layer decay quickly to zero inside the pavement at a distance approximately equal to the total thickness of the pavement from the end (Fig. 2.10). Nails were installed at distances between 100 mm (4 in.) and 150 mm (6 in.) away from the edge of all slabs in the edge pull-out tests to determine the performance of the nails driven close to the slab edges. A total of 120 edge pull-out tests was completed. Table 3.6 is a summary of the pull-out strength of all nails installed close to the slab edges. Each entry in Table 3.6 typically represents the results of eight tests. Test results reveal that the nail pull-out strength is influenced by the distance between the installed nail and the slab edge. Pull-out strength decreases with decreasing edge distance. The average pull-out strength of all nails installed at a distance 100 mm (4 in.) away from the edge is 27 kN (6 kips) or 80 percent of the standard-test pull-out strength in Table 3.6. Edge distances smaller than 100 mm were not tested because driving the nail closer to the edge will likely cause concrete to spall. The average pull-out strengths of all nails installed at a distance 125 mm (5 in.) and 150 mm (6 in.) away from the edge are 29 kN (6.5 kips) and 32 kN (7 kips), which are approximately 85 percent and 95 percent of the standard-test

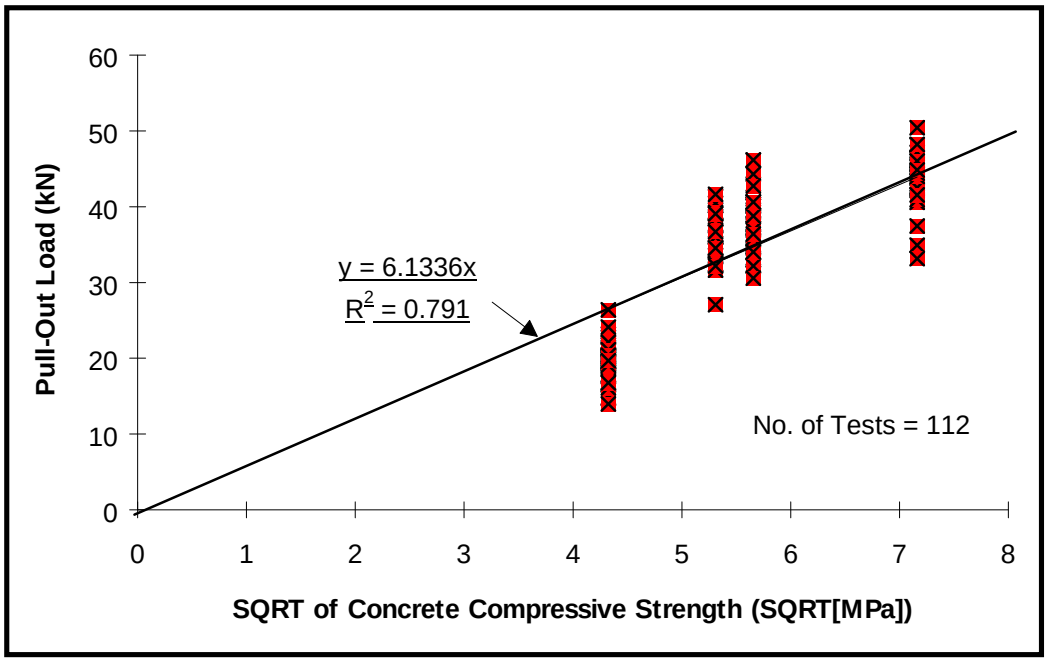

Figure 3.14 Standard Pull-Out Test Results

Table 3.6 Summary of Edge Pull-Out Tests

Slab Index	Edge Distance (mm)				
	100	113	125	138	150
1	***35*** [a] (91) [b]	***37*** (98)	***35*** (92)	***39*** (102)	***39*** (102)
2	***21*** (105)	***19*** (95)	***22*** (110)	***22*** (110)	***22*** (110)
3	***28*** (78)	--	***33*** (92)	--	***31*** (85)
4	***24*** (56)	--	***26*** (60)	--	***36*** (82)
Average	***27*** (80)	***28*** (82)	***29*** (85)	***30*** (90)	***32*** (94)

Note a: Pull-out strength in kN,
b: Percentage of standard-test pull-out strength.

pull-out strength, respectively. Test results suggest that clamping action of surrounding concrete on nails is reduced by a loss of confinement as the nail is driven close to the slab edge while the sintering is not affected as the nail driving positions vary. The pull-out strength reduction is most severe with high strength concrete (Table 3.6) while there is no strength reduction with low strength concrete. Test results reveal that the pull-out strength reduction becomes more severe with increasing concrete strength. The nail pull-out strength is approximately 80 percent of the standard-test pull-out strength when the edge distance is 150 mm (6 in.) in the high strength concrete. The nail pull-out strengths are approximately 100 percent and 85 percent of the standard-test pull-out strength in two normal strength concretes with river gravel and hard limestone aggregate, respectively, when the edge distance is 150 mm (6 in.).

3.3.5 Cracked-Concrete Test Results

The pull-out strength and the behavior of jumbo nails driven into an existing crack or close to a crack must be determined since nails will be installed in cracked highway pavements. Structural and shrinkage cracks are common in existing highways. A total of 134 cracked-concrete pull-out tests was completed. Table 3.7 summarizes the test results in terms of the nail pull-out strength and percentages of the standard-test pull-out strength.

3.3.5.1 Series-B Test Results Nails were driven into cracks and then immediately pulled out in series B. The width of the flexural cracks before nail installation ranged between 0.05 mm (0.002 in.) and 0.75 mm (0.03 in.). The width of existing cracks increased about 0.3 mm (0.01 in.) after nails were driven. Reductions in the nail pull-out strength when nails are driven into cracks are shown in Table 3.7. The average pull-out strength of all series-B nails is 24 kN (5.5 kips) which corresponds to approximately 70 percent of the standard-test pull-out strength. Each entry in Table 3.7 represents the results of eight tests or more. The reduction in pull-out strength is most severe in normal strength concrete with hard limestone aggregate, probably due to the fact that the wider flexural cracks were created in the slab.

3.3.5.2 Series-D Test Results Nails were driven close to cracks rather than into a crack in series D. Nails were driven at distances of 25 mm (1 in.), 50 mm (2 in.), and 75 mm (3 in.) away from existing cracks. Test results are shown in Table

3.7 with each entry representing an average of three tests. There are reductions in the nail pull-out strength when a nail is installed close to a crack. The average pull-out strengths of nails installed at 25 mm, 50 mm, and 75 mm away from cracks are 18 kN (4 kips), 21 kN (4.7 kips), and 26 kN (5.8 kips), respectively, in all four slabs which correspond to approximately 50 percent, 62 percent, and 75 percent of the standard-test pull-out strength. It must be noted that strength reductions were even more severe in series-D tests, when the distances between the nail and the crack were 25 mm and 50 mm, than those in series-B pull-out tests where nails were driven directly into cracks. Test results suggest that driving a nail close to an existing crack is similar to driving a nail close to an edge, probably because cracks represent the end of a continuous elastic media when nails are near the crack. Test data of cracked-concrete pull-out tests and the edge pull-out tests were combined and are shown in Fig. 3.15. Figure 3.15 shows continuously increasing pull-out strength with increasing distances away from edges or cracks.

3.3.5.3 Other Cracked-Concrete Pull-Out Tests Other cracked-concrete pull-out tests all show the detrimental effect of cracks on nail pull-out behavior. Series-A and series-C nails were driven into cracks, but were tested when the slabs were reloaded. Average pull-out strengths of 9 kN (2 kips) and 18 kN (4 kips) were determined in series A and C, which correspond to approximately 25 percent and 50 percent of the standard-test pull-out strength, respectively. Nails were installed at 200-mm (8-in.) spacing across the width of the slab in series F and G. Slabs were loaded in flexure so that cracks could form along the line of nails. Nails were pulled out while slabs were loaded in series F and nails were pulled out after slabs were unloaded in series G. The average pull-out strengths of 14 kN (3 kips) and 20 kN (4.5 kips) were determined in series F and G, which correspond to approximately 40 percent and 60 percent of the standard-test pull-out strength.

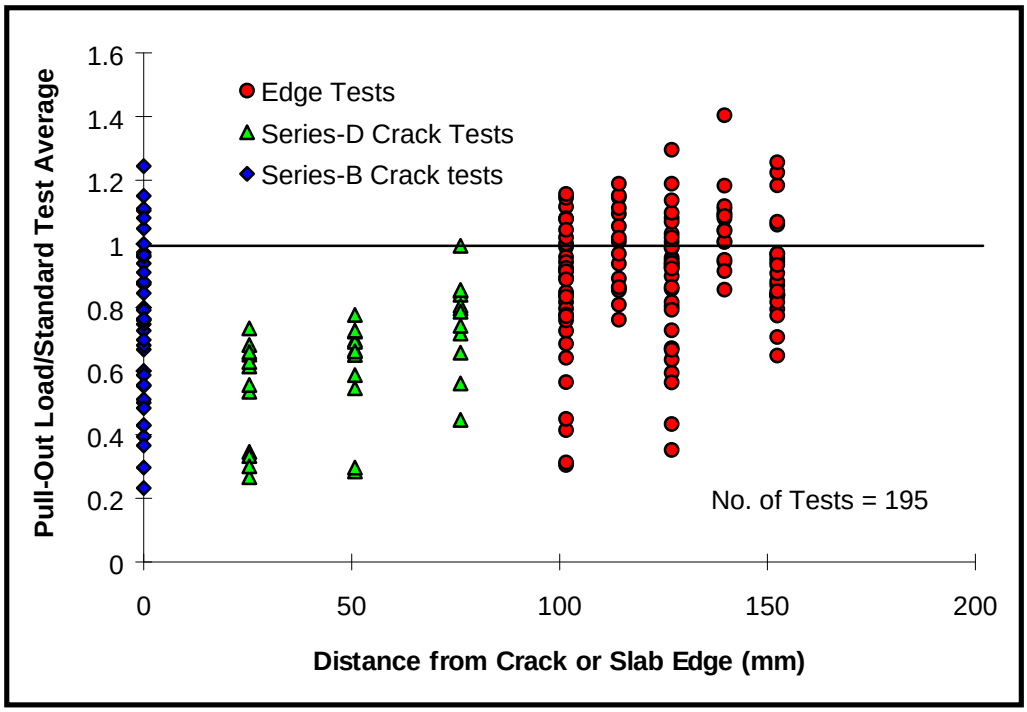

Figure 3.15 Edge and Cracked-Concrete Pull-Out Test Results

3.4 Pull-Out Test Summary and Conclusions

The pull-out capacity of the jumbo nails was established to determined their performance in tension when used as interface reinforcement in bonded concrete overlays. The pull-out test data are essential for implementation in other situations as well. The pull-out test program was primarily developed to simulate field conditions for bonded concrete overlays. The influence of concrete strength and nail installation positions on four different test slabs was investigated. The effect of existing cracks on nail pull-out behavior was also studied. The influence of other variables, such as actuator power levels and cumulative length of the hair line cracks, on the nail pull-out strength, was investigated. All pull-out test results are summarized in Appendix A.

Two different nail pull-out failure modes occurred: cone-type failure and nail pull-out. The majority of nails were pulled out of the concrete at failure but there were no significant differences in pull-out strengths between the two different pull-out failure modes. The average pull-out strength of all standard nails tested was 34 kN (7.5 kips). Nail displacement at the peak typically ranged between 0.25 mm (0.01 in.) and 0.5 mm (0.02 in.). The standard pull-out test results revealed that nail pull-out strength was strongly influenced by concrete strength since nails installed in higher strength concrete showed significantly higher pull-out strength. The average pull-out strength of nails installed in low strength concrete was 20 kN (4.5 kips), while it was 38 kN (8.5 kips) and 36 kN (8 kips) in two normal strength concretes with river gravel and hard limestone aggregate, respectively. The average pull-out strength of nails installed in high strength concrete was 44 kN (10 kips). The distance between a nail and an existing crack or the slab edge influenced pull-out strength. The pull-out strength decreased with decreasing edge or crack distances. The average pull-out strength of all nails installed at a distance

100 mm (4 in.) from the edge was 80 percent of the standard-test pull-out strength. The average pull-out strengths of all nails installed at a distance 125 mm (5 in.) and 150 mm (6 in.) from the edge were approximately 85 percent and 95 percent of the standard-test pull-out strength, respectively. Pull-out strength reduction was not observed in the low strength concrete. Test results also revealed that driving a nail close to an existing crack was similar to driving a nail close to an edge. The combined test data from cracked-concrete pull-out tests and edge pull-out tests show increasing nail pull-out strength with increasing distances from the edge or cracks. Nails were driven into cracks and then immediately pulled out in series B. Pull-out strength was also reduced when nails were driven directly into existing cracks. The average pull-out strength of all series-B nails was 24 kN (5.5 kips) which corresponded to 70 percent of the standard-test pull-out strength. Other cracked-concrete pull-out tests also showed the detrimental effect of cracks on nail pull-out performance.

CHAPTER FOUR
DIRECT SHEAR TRANSFER TESTS - EXPERIMENTAL PROGRAM

4.1 Introduction

Interface strength and mechanism of shear transfer between two concrete layers cast at different times, such as bonded concrete overlays, were determined by direct shear transfer tests (push-off tests). Bond and interface shear force transfer between old and new concrete layers were investigated to determine the shear behavior of jumbo nails installed as "shear connectors" in the bonded concrete overlays. Eighty-four push-off tests were completed. The fabrication and results of push-off tests are described in Chapters Four and Five, respectively.

4.2 In-Situ Push-Off Test Setup

It was necessary to devise a new shear transfer test rather than using a "standard" push-off test such as one used by Mattock et al. (1972) shown in Fig. 2.2. The pull-out test results showed that an edge distance of approximately 200 mm (8 in.) is necessary for a jumbo nail driven into a normal strength concrete to develop full pull-out strength. Accordingly, a jumbo nail push-off specimen requires overall dimensions considerably larger than those of a standard push-off test. A special in-situ push-off test was devised to use four slabs readily available from the pull-out test program.

The in-situ push-off test setup is shown in Figs. 4.1 through 4.3. Up to sixteen overlays were cast on a base slab as shown in Fig. 4.2. Two 25-mm (1-in.) inside diameter PVC pipes were embedded in each overlay. The vertical distance between the center of the PVC pipes and the interface was 20 mm (3/4 in.) in Fig. 4.3. A 16-mm (5/8-in.) nominal diameter high strength (F_y = 1,050 MPa or 150 ksi) threaded steel bar was inserted through each PVC pipe. One end of the threaded bar was tightened against the back of the 13-mm- (0.5-in.-) thick mild steel back plate with a nut. The other end of the threaded bar was connected to a front loading head by another nut. Two hydraulic cylinders (180-kN or 40-kips capacity each) were placed horizontally between a loading head and two reaction blocks. The cylinders were aligned so that their centerline coincided with the interface. As the hydraulic cylinders extended, the loads were applied to the back side of the overlay through the steel back plate so that the interface was subjected to shear force. Loading was continued until an interface shear failure was observed or until the horizontal displacement of the overlay relative to the base slab was excessive. It must be noted that, because the centerline of the bars is not right at the interface, the eccentricity of the load will produce a small moment on the interface. The magnitude of the stresses on the interface due to the eccentric loading was considered to be negligible. The eccentricity was the same in all tests so the loading condition is unchanged when comparing test results.

Advantages of the in-situ push-off test method are that a multiple number of specimens can be made using one set of forms and the push-off test can be performed in place as soon as the overlay concrete gains the desired compressive strength.

Figure 4.1 In-Situ Push-Off Test

Figure 4.2 Placement of Overlay Specimens

4.3 Preparation of Push-Off Test Specimens

Replicates of the four pull-out test slabs were used as base slabs in the push-off tests. Both sides of the slabs were used. When surface preparation was necessary, shotblasting or sandblasting was used to clean or roughen the contact surface. A portable BLASTRAC shotblasting machine shown in Fig. 4.4 was used for shotblasting. Varying degrees of contact surface roughness were created by varying shot sizes and shotblasting time. The shotblasting process involved a spinning drum that throws steel shot against the surface of the concrete. A vacuum unit on the machine picks up the debris and shot are collected with a magnet unit. Sandblasting was used for the surface preparation in one push-off test series. The equipment shown in Fig. 4.5 was used to sandblast the surface. The prepared interface was similar to the medium shotblasting based on visual inspection. The contact surface roughness was measured using the Mini Texture Meter (MTM). The texture was determined from an average of two readings. Figures 4.6 and 4.7 show the MTM and the working principle of the non-contacting laser transducer used in the MTM, respectively. The light projected by the laser is collected by the receiving lens shown in Fig. 4.7. As the surface texture varies so does the spot of light projected by the laser which is received by the collecting lens focused on different diodes. Each time the laser is pulsed, diode readings are stored and used for the texture calculation. One of the more conventional methods which can be used to determine the surface roughness is the sand patch method (ASTM 1990) which can be easily used in the field. It was desired that the average texture determined by the MTM be the same as the one determined by the sand patch method. All MTM average textures presented have been calibrated to be equivalent to those determined by the sand patch method (Hassan, Meyer, and Fowler 1991).

Figure 4.4 Portable BLASTRAC Shotblasting Machine

Figure 4.5 Sandblasting Equipment

Figure 4.6 Mini Texture Meter

Figure 4.7 Working Principle of Mini Texture Meter

The interface contact area was controlled by using a template made of a 5-mm- (3/16-in.-) thick foamcore board shown in Fig. 4.8. The interface shear reinforcement ratio was defined as the ratio of the nail cross-sectional area over the interface area. The interface reinforcement ratio ranged between 0.13 percent and 0.38 percent for all test specimens with nails. All overlays were cast against the dry top surface of the base slab. Bond-enhancing agents, such as cement grout or epoxy, were not used in this study. Felt (1956) suggested that the best bond was achieved when the interface was dry and grouted. Two Army Corps of Engineers studies, however, reported that there are no significant differences between specimens which received cement grout and those which did not (Whitney et al. 1992). It was decided to keep all interfaces dry to eliminate the effect of moisture from the test results. The overlays were placed following surface preparation and nail installation. All overlays were moist cured for three days under a plastic sheet and then air dried. Several different concrete mixes were used for the overlays as summarized in Appendix C. The 28-day compressive strength (f'c) of the overlays ranged between 20 MPa (2,900 psi) and 38 MPa (5,500 psi). The compressive strengths of the overlays approximately matched those of the base at the time of testing in most tests.

4.4 Push-Off Test Series

Table 4.1 is a summary of test variables of all push-off tests. Of sixty-four test specimens with bonded interfaces, one or two jumbo nails were used across the interface in 48 specimens and no nails were used in 16 specimens. Twenty specimens had unbonded interfaces as shown in Table 4.1. Push-off tests were divided into five different test series.

(a) Smooth Troweled Surface

(b) Shotblasted Surface: Medium Roughness

Figure 4.8 Interface Layout before Overlay Placement

4.4.1 Direct Shear, Series I: DS-I

Sixteen overlays were cast on top of the normal strength slab with river gravel (Table 3.1). The contact surfaces of specimens in this test series were shotblasted to varying degrees of roughness to determine the influence of the interface roughness on the interface shear strength. The interface roughness was grouped as light (L), medium (M), and heavy (H). An average texture smaller than 0.4 mm (0.02 in.) was defined as light shotblasting while a texture depth between 0.4 mm and 0.6 mm (0.025 in.) was defined as medium shotblasting. An average texture larger than 0.6 mm was defined as heavy shotblasting. Figures 4.9 (a) and (b) show different degrees of surface roughness created by shotblasting. Table 4.2 is a summary of the test variables of DS-I. Fourteen specimens were tested monotonically, and two specimens were subjected to several cycles of loading and unloading as shown in Table 4.2. One or two nails were used for ten specimens. No nails were used in the remaining six specimens. The contact area was 230 cm^2 (36 $in.^2$) or 465 cm^2 (72 $in.^2$). The interface shear reinforcement ratio was 0.38 percent for all specimens with nails.

4.4.2 Direct Shear, Series II: DS-II

Sixteen overlays were cast on top of the low strength slab (Table 3.1). The primary test variable of DS-II was the average tributary contact area per nail. The interfaces of all specimens were heavily shotblasted before the overlay was placed. The interface reinforcement ratio was changed from 0 to 0.38 percent by varying the contact area and using 0, 1, or 2 jumbo nails. The contact area was 230 cm^2 (36 $in.^2$), 465 cm^2 (72 $in.^2$), or 700 cm^2 (108 $in.^2$). Table 4.3 is a summary of the test variables of DS-II. Thirteen specimens were tested monotonically, and three

(a) Light Shotblasting

(b) Heavy Shotblasting

Figure 4.9 Contact Surface Roughness Created by Shotblasting

Table 4.2 Summary of Push-Off Test Program: DS-I

Specimen Index	Number of Nails	Contact Area (cm^2)	Average Texture (mm)	Reinforcing Ratio (%)	Shear Load Type
1-L-1.1	1	230	0.3	0.38	M[1]
1-L-1.2	1	230	0.3	0.38	M
1-L-2.1	2	465	0.3	0.38	M
1-L-2.2	2	465	0.3	0.38	C[2]
1-L-0.1	0	465	0.3	--	M
1-L-0.2	0	465	0.3	--	C
1-M-1.1	1	230	0.5	0.38	M
1-M-1.2	1	230	0.5	0.38	M
1-M-0.1	0	465	0.5	--	M
1-M-0.2	0	465	0.5	--	M
1-H-1.1	1	230	0.8	0.38	M
1-H-1.2	1	230	0.7	0.38	M

Note 1: M = Monotonic loading, Cont'd.
2: C = Several cycles of loading and unloading.

Table 4.2 Summary of Push-Off Test Program: DS-I (Cont'd.)

Specimen Index	Number of Nails	Contact Area (cm^2)	Average Texture (mm)	Reinforcing Ratio (%)	Shear Load Type
1-H-2.1	2	465	0.7	0.38	M[1]
1-H-2.2	2	465	0.8	0.38	M
1-H-0.1	0	465	0.7	--	M
1-H-0.2	0	465	0.7	--	M

Note 1: M = Monotonic loading,
2: Specimen Notation-

First number: Base slab 1: Normal strength slab with river gravel,
Second letter: Interface roughness,
L: Light shotblasting,
M: Medium shotblasting,
H: Heavy shotblasting,
Third number: Number of nails used across the interface (0, 1, or 2),
Fourth number: Replicate designation.

Table 4.3 Summary of Push-Off Test Program: DS-II

Specimen Index	Number of Nails	Contact Area (cm^2)	Average Texture (mm)	Reinforcing Ratio (%)	Shear Load Type
2-1-36.1	1	230	0.8	0.38	M[1]
2-1-36.2	1	230	0.8	0.38	M
2-0-36.1	0	230	0.7	--	M
2-0-36.2	0	230	0.7	--	M
2-1-72.1	1	465	0.8	0.19	M
2-1-72.2	1	465	0.9	0.19	M
2-2-72.1	2	465	0.7	0.38	M
2-2-72.2	2	465	0.9	0.38	M
2-0-72.1	0	465	0.7	--	M
2-0-72.2	0	465	0.7	--	M
2-1-108.1	1	700	0.7	0.13	M
2-1-108.2	1	700	0.9	0.13	C[2]

Note 1: M = Monotonic loading, Cont'd.
2: C = Several cycles of loading and unloading.

Table 4.3 Summary of Push-Off Test Program: DS-II (Cont'd.)

Specimen Index	Number of Nails	Contact Area (cm^2)	Average Texture (mm)	Reinforcing Ratio (%)	Shear Load Type
2-2-108.1	2	700	0.8	0.25	M[1]
2-2-108.2	2	700	0.8	0.25	C[2]
2-0-108.1	0	700	0.8	--	M
2-0-108.2	0	700	0.7	--	C

Note 1: M = Monotonic loading,
2: C = Several cycles of loading and unloading,
3: Specimen Notation-

First number: Base slab 2: Low strength slab,
Second number: Number of nails across the interface (0, 1, or 2),
Third number: Interface contact area (36, 72, or 108 $in.^2$),
Final number: Replicate designation.

specimens were subjected to several cycles of loading and unloading as shown.

4.4.3 Direct Shear, Series III: DS-III

Under field conditions, the interface of a bonded concrete overlay may not develop adequate bond strength for a variety of reasons. A weak concrete interface can result from premature loading or from poor construction quality control such as inadequate surface preparation, inattention to cleanliness of the surface, or low quality concrete. The behavior of an unbonded interface with nails subjected to shear forces was studied in this test series. Table 4.4 is a summary of the test variables of DS-III. The specimens were overlaid on two normal strength slabs with river gravel and hard limestone aggregates (six specimens on each slab). The contact area was heavily shotblasted for specimens with rough interfaces. The adhesion between the base concrete and the overlay was intentionally prevented using a bond breaker. Two thin layers of multi-purpose grease were applied uniformly over the interface to break the bond. Four severely shotblasted interfaces and two relatively smooth trowel finished interfaces were used, respectively, on each slab. The contact area was 465 cm^2 (72 $in.^2$) for all test specimens.

4.4.4 Direct Shear, Series IV: DS-IV

The effect of the stepped drill hole (Fig. 1.3) on the shear behavior of jumbo nails was studied. Two different drill hole types were created for these tests: an "exaggerated stepped" drill hole and a "straight" drill hole. Figure 4.10 shows the two different types of drill holes tested. The diameter of the upper portion of the drill hole was made larger than the nail diameter by approximately 5 mm (0.2 in.)

Table 4.4 Summary of Push-Off Test Program: DS-III (Unbonded)

Specimen Index	Number of Nails	Contact Area (cm^2)	Average Texture (mm)	Reinforcing Ratio (%)	Remarks
1-H-1U.1	1	465	1.0	0.19	
1-H-1U.2	1	465	1.0	0.19	
1-H-2U.1	2	465	1.1	0.38	
1-H-2U.2	2	465	0.8	0.38	
1-N-1U.1	1	465	--	0.19	T.F.[1]
1-N-1U.2	1	465	--	0.19	T.F.
3-H-1U.1	1	465	1.2	0.19	
3-H-1U.2	1	465	1.2	0.19	
3-H-2U.1	2	465	1.2	0.38	
3-H-2U.2	2	465	1.2	0.38	
3-N-1U.1	1	465	--	0.19	T.F.
3-N-1U.2	1	465	--	0.19	T.F.

Note 1: Specimens with unbonded-smooth (trowel-finished) interface,
2: Specimen notation is similar to DS-I while the fourth letter “U” denotes unbonded interface.

Figure 4.10 Two Different Drill Hole Types

for four specimens. This was accomplished in two steps. The supplied special Hilti drill bit was first used for the initial drilling to create a “stepped” drill hole. Later, the stepped portion was redrilled with a drill bit of a large diameter (16 mm or 5/8 in.). After the nails were driven, the extra space between the base concrete and the nail shank was completely filled with grease so that fresh concrete would not enter the gap. This type of drill hole was called the “exaggerated stepped” drill hole. “Standard” stepped drill holes were made and the space between the base concrete and the nail shank was filled with quick setting epoxies for the other four specimens. This type of drill hole was called the “straight” drill hole. Table 4.5 is a summary of the test variables of DS-IV. Eight overlays were cast on the high strength slab (Table 3.1). The adhesion was prevented using the same bond breaker described previously. Four heavily shotblasted interfaces and four relatively smooth trowel finished interfaces were used, respectively, for tests.

Table 4.5 Summary of Push-Off Test Program: DS-IV (Unbonded)

Specimen Index	Number of Nails	Contact Area (cm^2)	Average Texture (mm)	Reinforcing Ratio (%)	Remarks
4H1STR.1	1	230	1.1	0.38	
4H1STR.2	1	230	1.2	0.38	
4H1STP.1	1	230	1.1	0.38	
4H1STP.2	1	230	1.1	0.38	
4N1STR.1	1	230	--	0.38	
4N1STR.2	1	230	--	0.38	
4N1STP.1	1	230	--	0.38	
4N1STP.2	1	230	--	0.38	

Note Specimen notation-

First number: Base slab 4: High strength slab,
Second letter: Interface preparation,
H: Heavy shotblasting,
N: Smooth trowel finish,
Third number: Number of nails across the interface (1),
Fourth through sixth letter: Drill-hole type,
STR: Straight hole,
STP: Exaggerated stepped hole,
Final number: Replicate designation.

4.4.5 Direct Shear, Series V: DS-V

One objective of the DS-V test series was to investigate the shear behavior of jumbo nails driven into an existing crack or very close to a crack. The other objective was to determine the effect of base concrete compressive strength on interface shear strength. The interfaces of specimens in this test series were prepared with sandblasting whenever surface treatment was necessary. Figure 4.11 shows the sandblasted interface of specimens with and without cracks. Table 4.6 is a summary of the test variables of DS-V. Thirty-two overlays were cast on four base slabs (eight specimens on each slab). The 28-day compressive strength of the overlays was approximately 29 MPa (4,200 psi). The test variables included compressive strength of the base concrete, roughness of the interface, and presence of existing cracks. A number of flexural cracks was created on one face of the base slabs. The width of these flexural cracks ranged between 0.2 mm and 0.3 mm (0.008 in. and 0.012 in.). One or two nails were driven into the crack or very close to the crack for twelve specimens.

4.5 Instrumentation and Test Procedures

The applied shear load and displacement of the overlay were continuously monitored. The horizontal and the vertical displacements of the overlay, the peak shear load, and the post peak behavior in shear were recorded. The applied shear load was monitored using a pressure transducer. The horizontal and vertical movements of the overlay were monitored using linear potentiometers. The accuracy of the linear potentiometer was 0.025 mm (0.001 in.). The horizontal and vertical displacements were measured on top of the overlay as shown in Fig. 4.12.

(a) Cracked Interface

(b) Crack-Free Interface

Figure 4.11 Sandblasted Contact Surface

Table 4.6 Summary of Push-Off Test Program: DS-V

Specimen Index	Number of Nails	Contact Area (cm^2)	Reinforcing Ratio (%)	Width of Crack (mm)	Crack Distance (mm)	Interface Preparation
1M1NC.1	1	230	0.38	--	--	Sandblast
1M1SC.1	1	230	0.38	0.3	30	Sandblast
1M1CR.1	1	230	0.38	0.2	--	Sandblast
1N1NC.1	1	230	0.38	--	--	T.F. [1]
1M2NC.1	2	465	0.38	--	--	Sandblast
1M2NC.2	2	465	0.38	--	--	Sandblast
1M2SC.1	2	465	0.38	0.2	60	Sandblast
1M0NC.1	0	465	--	--	--	Sandblast
2M1NC.1	1	230	0.38	--	--	Sandblast
2M1NC.2	1	230	0.38	--	--	Sandblast
2M1CR.1	1	230	0.38	0.3	--	Sandblast
2N1NC.1	1	230	0.38	--	--	T.F.
2M2NC.1	2	465	0.38	--	--	Sandblast

Note 1: T.F. = Trowel finish

Cont'd.

Table 4.6 Summary of Push-Off Test Program: DS-V (Cont'd.)

Specimen Index	Number of Nails	Contact Area (cm^2)	Reinforcing Ratio (%)	Width of Crack (mm)	Crack Distance (mm)	Interface Preparation
2M2SC.1	2	465	0.38	0.3	60	Sandblast
2M2CR.1	2	465	0.38	0.2	--	Sandblast
2M0NC.1	0	465	--	--	--	Sandblast
3M1NC.1	1	230	0.38	--	--	Sandblast
3M1SC.1	1	230	0.38	0.2	15	Sandblast
3M1CR.1	1	230	0.38	0.3	--	Sandblast
3N1NC.1	1	230	0.38	--	--	T.F. [1]
3M2NC.1	2	465	0.38	--	--	Sandblast
3M2SC.1	2	465	0.38	0.3	60	Sandblast
3M2CR.1	2	465	0.38	0.3	--	Sandblast
3M0NC.1	0	465	--	--	--	Sandblast
4M1NC.1	1	230	0.38	--	--	Sandblast
4M1NC.2	1	230	0.38	--	--	Sandblast

Note 1: T.F. = Trowel finish

Cont'd.

Table 4.6 Summary of Push-Off Test Program: DS-V (Cont'd.)

Specimen Index	Number of Nails	Contact Area (cm^2)	Reinforcing Ratio (%)	Width of Crack (mm)	Crack Distance (mm)	Interface Preparation
4M1CR.1	1	230	0.38	0.2	--	Sandblast
4N1NC.1	1	230	0.38	--	--	T.F. [1]
4M2NC.1	2	465	0.38	--	--	Sandblast
4M2NC.2	2	465	0.38	--	--	Sandblast
4M2CR.1	2	465	0.38	0.2	--	Sandblast
4M0NC.1	0	465	--	--	--	Sandblast

Note 1: T.F. = Trowel finish,
2: Specimen notation-

First number: Base slab
1: Normal strength with river gravel,
2: Low strength slab,
3: Normal strength with hard limestone aggregate,
4: High strength slab,

Second letter: Interface preparation,
M: Sandblasting,
N: Smooth trowel finish,

Third number: Number of nails across the interface (0, 1, or 2),

Fourth & fifth letter: Presence of crack,
NC: No crack,
CR: Nail driven in the crack,
SC: Nail driven close to crack,

Final number: Replicate designation.

Figure 4.12 Instrumentation for Overlay Displacement Measurement

The shear load was applied at a rate of approximately 9 kN (2 kips) per minute. For specimens with nails, a sudden drop in shear load and a corresponding large increase in the horizontal and vertical displacement values were observed after the peak shear load was reached. Slip reached immediately after the peak could not be accurately recorded with a sampling rate of five data sets per second. The test continued until an overlay horizontal displacement of approximately 10 mm (0.4 in.) was reached for all specimens with nails. For specimens without nails, complete interface shear failure was observed after the peak shear load was reached and the test was stopped immediately.

CHAPTER FIVE
DIRECT SHEAR TRANSFER TESTS - TEST RESULTS

5.1 General

The push-off test results using Hilti jumbo nails as shear connectors are presented in terms of load-displacement response and tabulations of peak shear and shear at large increments of displacement. Conclusions are drawn from the results.

5.2 Interface Roughness: DS-I

The effect of contact surface roughness, or interface roughness, on shear behavior of sixteen specimens with and without jumbo nails was determined in the DS-I test series. The base was the normal strength slab with river gravel (Table 3.1). The compressive strength of the overlay approximately matched that of the base concrete at the time of testing. The test results are summarized in Table 5.1.

5.2.1 Specimens with Nails

The shear loads versus the horizontal displacements of the overlays determined from replicate tests in which the contact surface was lightly shotblasted are shown in Fig. 5.1. The contact area layout before the overlay was placed is

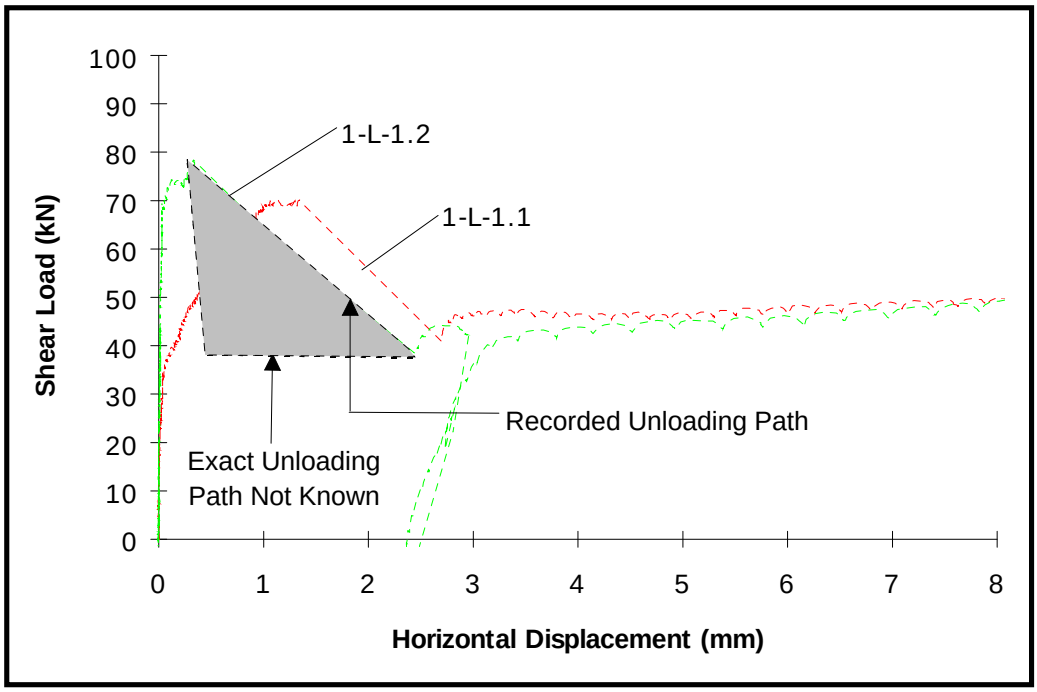

Figure 5.1 Load vs. Displacement: Specimens with Lightly Shotblasted Interface, Contact Area = 230 cm^2, 1 Nail

Figure 5.2 Interface Layout before Overlay Placement: 1 Nail

shown in Fig. 5.2. The interface shear reinforcement ratio (ρ) was 0.38 percent. As the shear loads increased, the initial overlay horizontal displacements were very small for both specimens. The overlay began to slip, however, in ***1-L-1.1***, when approximately half of the peak shear load was applied. The peak load of 70 kN (16 kips) was reached at a displacement of 1.1 mm (0.04 in.). Interface shear suddenly dropped after the peak load was reached. This instant slip after the peak could not be accurately recorded due to the interval of sampling (five data sets per second). Dotted lines indicate extrapolated data and are probably not correct. It is likely that the actual response was a nearly vertical drop in the curves as indicated for ***1-L-1.2***. The dashed lines could be constructed anywhere in the shaded area. A flat shear load plateau (approximately 45 kN or 10 kips) occurred following the sudden drop. The load-displacement plot of ***1-L-1.2*** in Fig. 5.1 shows a different load-displacement behavior. The peak shear load of 78 kN (18 kips) was reached at a vary small horizontal displacement of 0.3 mm (0.01 in.). The specimen was unloaded and then reloaded after the drop in shear load. The difference in the two curves in Fig. 5.1 can be attributed to the load at which adhesion between the two surfaces began to fail. The adhesion was lost approximately at 35 kN (7.8 kips) and at 70 kN (15.7 kips) in ***1-L-1.1*** and ***1-L-1.2***, respectively. However, the peak loads were within 10 percent of one another indicating that the role of the nails in interface shear transfer was nearly the same in the replicate specimens after adhesion was lost and after peak load was reached. The total slip exceeded 10 mm (0.4 in.) when the nail was pulled out of the base concrete in both tests. At peak load, shear-friction is fully developed. In the flat plateau the action is a combination of shear-friction and dowel action, however, dowel action is likely to predominate. The profiles of the base concrete and the overlay after testing of ***1-L-1.1*** are shown in Fig. 5.3.

(a) Base Concrete

(b) Overlay

Figure 5.3 Pull-Out Failure of Nail from Base Concrete: Light Shotblasting

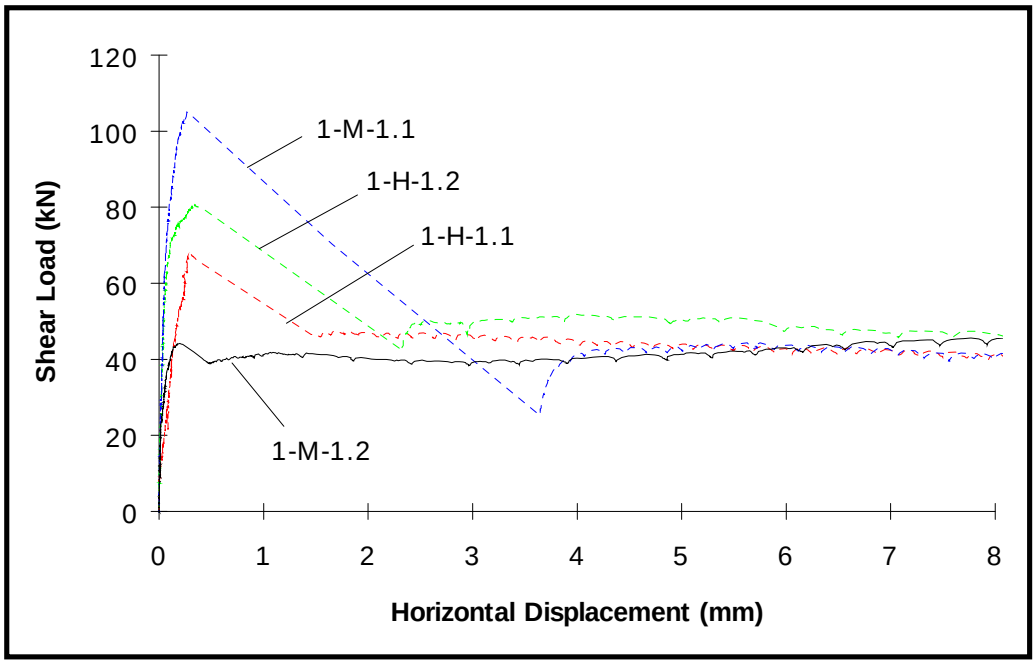

Figure 5.4 Load vs. Displacement: Specimens with Medium and Heavily Shotblasted Interface, Contact Area = 230 cm^2, 1 Nail

Shear load versus horizontal overlay displacement plots for four specimens which had heavy and medium contact surface roughness are shown in Fig. 5.4. All four specimens had the same contact area and interface reinforcement ratio (ρ = 0.38 %). The displacements increased slowly with applied shear loads for all specimens. Note that at peak load, the displacements for all specimens are between 0.2 mm (0.008 in.) and 0.3 mm (0.012 in.). No significant overlay slip occurred before the peak load was reached. After the peak, there was again a sudden drop in load and a corresponding large increase in slip in three of the specimens. The relatively flat load plateaus due to dowel action at large displacements were similar in all specimens. It is interesting to note that in test ***1-M-1.1*** the load dropped below the flat plateau and increased, probably an indication that full dowel action

was not immediately mobilized and required additional slip to develop. When the test ended, the base concrete and the overlay were inspected. The failure surfaces are shown in Fig. 5.5 for ***1-H-1.1***. The results of three tests in which two nails were used are shown in Fig. 5.6. The contact area of 465 cm^2 (72 $in.^2$) was twice as large as those of specimens with one nail to keep the interface reinforcement ratio the same (ρ = 0.38 %). The contact area before the overlay placement is shown in Fig. 5.7. The distance between two nails was 150 mm (6 in.). The contact surfaces of specimens ***1-H-2.1*** and ***1-H-2.2*** were heavily shotblasted while that of ***1-L-2.1*** was only lightly shotblasted. The peak loads and peak displacements of the two specimens with heavy surface preparation were both less than values for ***1-L-2.1***. A sudden bond failure was again observed at the peak, and the overlay slipped instantly while the applied load quickly dropped to a flat shear plateau. Figure 5.8 shows that both nails failed by pulling out of the overlay in ***1-H-2.1***. The load-displacement plot of ***1-L-2.1*** shows the "early slip" of the overlay due to the relatively light interface preparation. The base concrete and the overlay were inspected after testing, and one nail pulled a cone out of the base concrete while the other nail was pulled out of the base concrete as shown in Fig. 5.9. This difference in failure modes of two nails explains the dual plateaus following the peak load; one at about 120 kN (27 kips) and one at about 40 kN (9 kips) at 8 mm (0.3 in.) displacement.

Vertical separation of the contact surfaces between two concrete layers was observed in all tests, especially as the applied shear loads approached peak strength. No premature failure of the nails in pull-out was noticed in the DS-I tests. Tensile forces developed in the nails as the contact surfaces separated vertically. The compressive force over the interface provided by the nails increased the interface shear strength (shear-friction). The overlay displacements in the vertical

direction

(a) Base Concrete

(b) Overlay

Figure 5.5 Pull-Out Failure of Nail from Base Concrete: Heavy Shotblasting

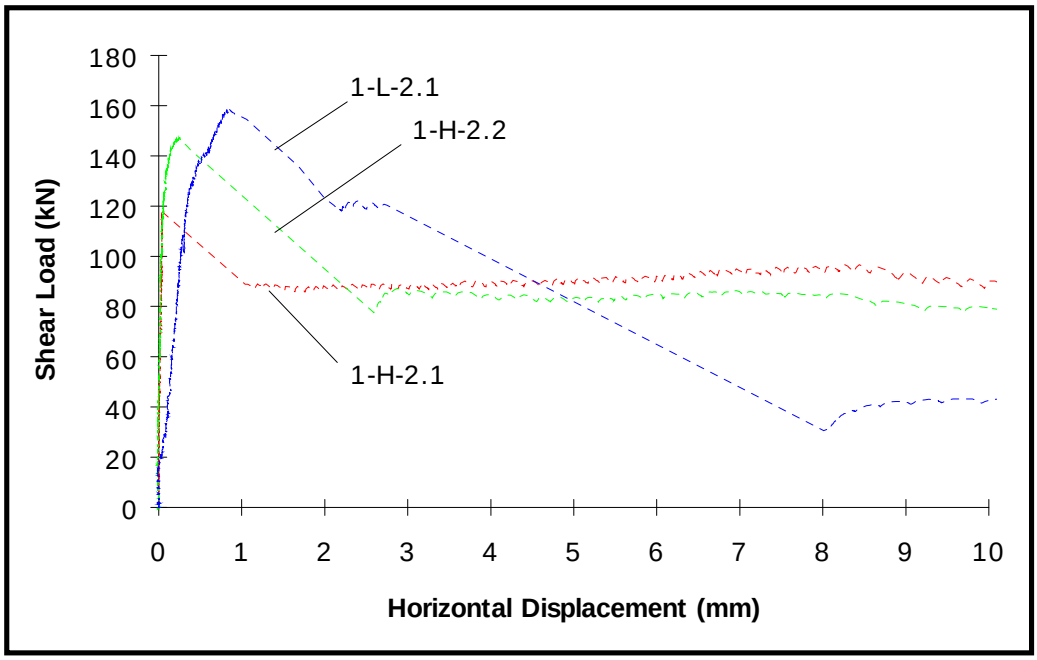

Figure 5.6 Load vs. Displacement: Specimens with Light and Heavily Shotblasted Interface, Contact Area = 465 cm^2, 2 Nails

Figure 5.7 Interface Layout before Overlay Placement: 2 Nails

(a) Base Concrete

(b) Overlay

Figure 5.8 Pull-Out Failure of Nails from Overlay

(a) Base Concrete

(b) Overlay

Figure 5.9 Nail Pull-Out Including Cone Failure in Base Concrete

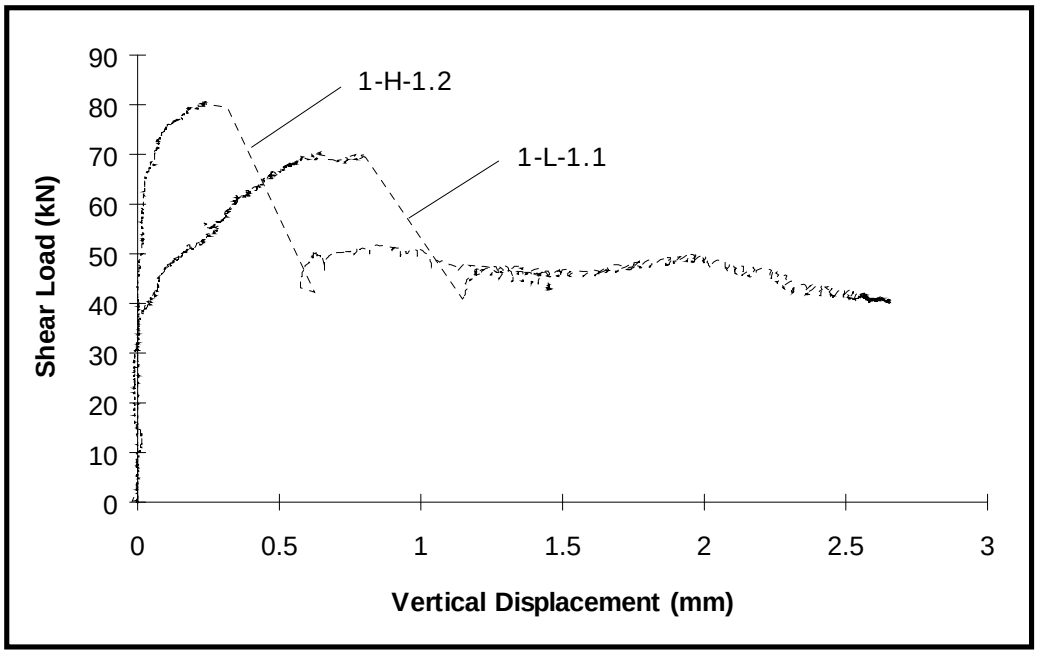

Figure 5.10 Load vs. Vertical Displacement: Specimens with Light and Heavily Shotblasted Interface, Contact Area = 230 cm^2, 1 Nail

were typically equal to or less than those in the horizontal direction. The shear load versus the overlay vertical displacement plots are shown for two specimens with light and heavy shotblasted interface, respectively, in Fig. 5.10 and can be compared with the horizontal displacements for the same specimens in Figs. 5.1 and 5.4.

5.2.2 Control Specimens: Specimens without Nails

No nails were used in the six control specimens which had a contact area of 465 cm^2 (72 $in.^2$). Test results are summarized in Table 5.1. Test results of the control specimens show that the peak load was reached at very small horizontal and

vertical displacements of the overlay. The interface failed suddenly and completely in shear along the contact area. The typical profiles of the base concrete and the overlay after test are shown in Fig. 5.11 for one specimen. The maximum and minimum peaks for the six control specimens were 145 kN (33 kips) and 100 kN (22 kips) with a mean of 121 kN (27 kips). The mean horizontal displacement of the overlay at the peak shear load was 0.1 mm (0.004 in.). The peak load and displacement in specimens without nails were lower than the values for specimens with two nails.

5.2.3 Effect of Several Loading and Unloading Cycles

Two specimens were subjected to several cycles of loading and unloading in DS-I as was noted in Table 4.2. The specimens were loaded until the horizontal displacement reached a predetermined value and were unloaded. The same procedure was repeated until the peak load was reached. The peak shear loads of two specimens, ***1-L-2.2*** and ***1-L-0.2***, subjected to several cycles of loading and unloading, were lower than those of their companion specimens shown in Table 5.1, which suggests possible cumulative interface damage during the loading and unloading cycles.

5.2.4 Summary: Effect of Interface Roughness on Strength

The influence of surface roughness on interface shear strength is summarized in Table 5.2. Values shown in Table 5.2 represent an average of two tests. The average shear stress was calculated by dividing the applied shear force by the interface area. The mean of the ultimate interface shear strength of all DS-I specimens was 2,930 kPa (425 psi). There were no significant differences in the

(a) Base Concrete

(b) Overlay

Figure 5.11 Interface Shear Failure: No Nails

Table 5.2 Effect of Surface Roughness on Interface Shear Strength: DS-I

No. of Nails	Contact Area (cm^2)	Roughness of Contact Area			Average Strength (kPa)
		Light (kPa)	Medium (kPa)	Heavy (kPa)	
0	465	2,590 [a]	2,810 [a]	2,400 [a]	2,600
1	230	3,200	3,220	3,200	3,210
2	465	3,170	--	2,860	3,020
Average	--	2,990	3,020	2,820	2,930

Note a: Interface shear strength = shear load / contact area

Table 5.3 Horizontal Displacement at Peak Shear Load: DS-I

No. of Nails	Contact Area (cm^2)	Roughness of Contact Area			Average Displ. (mm)
		Light (mm)	Medium (mm)	Heavy (mm)	
0	465	--	0.1 [a]	0.1 [a]	0.1
1	230	0.7	0.2	0.3	0.4
2	465	0.9	--	0.1	0.4
Average	--	0.8	0.2	0.2	0.3

Note a: Horizontal displacement of overlay at peak shear load

peak shear loads determined between companion specimens which received different levels of surface preparation. Results from tests with two nails and those with no nails can be compared directly because the contact areas are the same (465 cm^2 or 72 $in.^2$). Specimens with two nails had 16 percent higher average shear stresses (3,020 kPa or 440 psi) at the peak than those without nails (2,600 kPa or 380 psi). The average shear stresses determined from tests with one nail which had a smaller contact area of 230 cm^2 (36 $in.^2$) were higher than in those with a larger contact area in Table 5.2. An elastic finite element analysis was performed to examine the interface shear stress distribution. Analysis results revealed that the distribution of shear stresses across the contact area was not uniform but was highly concentrated toward the side receiving the applied load and that shear stresses were more evenly distributed with a smaller contact area. Horizontal displacement of the overlay at peak shear load in specimens with light interface preparation are considerably higher than those in specimens with medium and heavy interface preparation as indicated in Table 5.3. Test results reveal that slip was necessary to mobilize the strength especially after adhesion was lost in cases where the interface was not sufficiently roughened. The overlay horizontal displacements at the peak are higher in specimens with nails than in those with no nails. Nails permit some redistribution of stresses across the interface when adhesion is lost. Without nails, there is no redistribution once the contact surface adhesion is lost.

5.3 Contact Area vs. Number of Nails Used: DS-II

The objective of the DS-II test series was to investigate the effect of the tributary area of nails. Three different contact areas were used: 230 cm^2 (36 $in.^2$), 465 cm^2 (72 $in.^2$), or 700 cm^2 (108 $in.^2$). Each specimen had 0, 1, or 2 nails. The

base was the low strength slab (Table 3.1). The compressive strength of the overlay approximately matched that of the base concrete at the time of testing. Test results are summarized in Table 5.4.

5.3.1 Average Shear Stress vs. Horizontal Displacement

The average shear stresses versus horizontal displacements of overlay for two specimens with the same 230 cm^2 (36 $in.^2$) contact area are plotted in Fig. 5.12. One nail was used in specimens ***2-1-36.1*** and ***2-1-36.2***. Specimens ***2-0-36.1*** and ***2-0-36.2*** had the same 230 cm^2 (36 $in.^2$) contact area and no nails were used. No significant differences in the interface strength were found between specimens with one nail and no nails as indicated in Table 5.4. Figure 5.13 shows the shear stress versus displacement plots for three specimens which had the same contact area (465 cm^2 or 72 $in.^2$). Two nails were used for one specimen and one nail was used for the other two specimens. It should be noted that a test, ***2-2-72.2***, did not fail in shear due to a testing error. The alignment of the hydraulic cylinders changed during testing as higher loads were applied, and the overlay failed in an undesirable mode. Again, no significant differences in the peak stresses were found between specimens with one nail and no nail as indicated in Table 5.4 and the peak stress in one specimen with two nails, ***2-2-72.1***, was approximately 10 percent higher. Several specimens which had a relatively large contact area of 700 cm^2 (108 $in.^2$) failed in the base concrete or in the overlay due to the low strength of concrete. The results of three tests which had the same 700 cm^2 (108 $in.^2$) contact area are shown in Fig. 5.14. The peak shear stresses in all three specimens were nearly the same but displacements at the peak were quite different in Fig. 5.14. It must be noted that a specimen with no nails, ***2-0-108.1***, completely failed once the peak

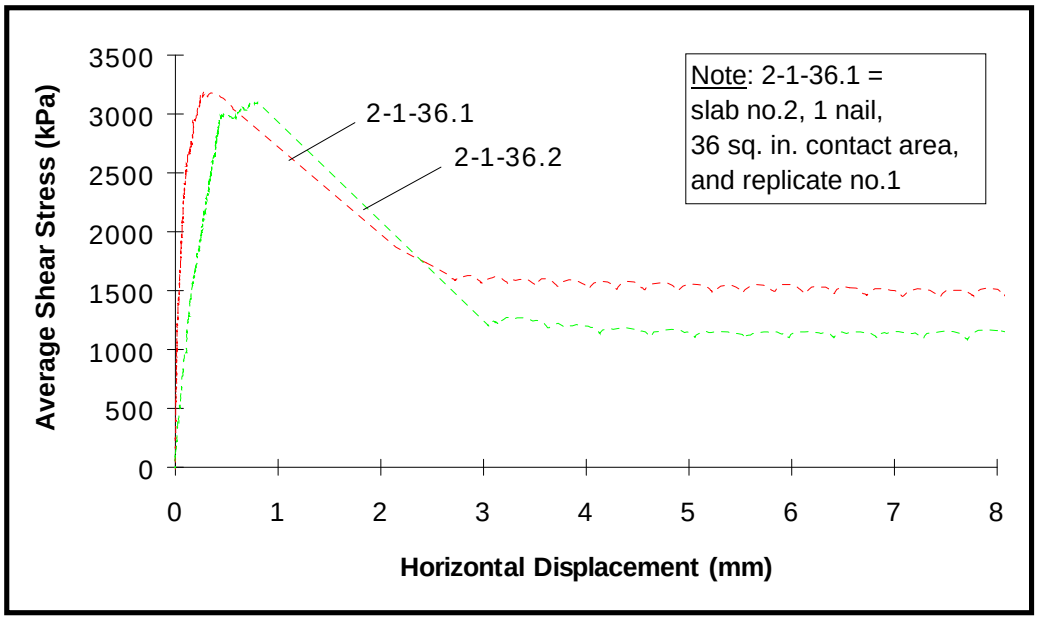

Figure 5.12 Average Shear Stress vs. Displacement: Contact Area = 230 cm^2, 1 Nail

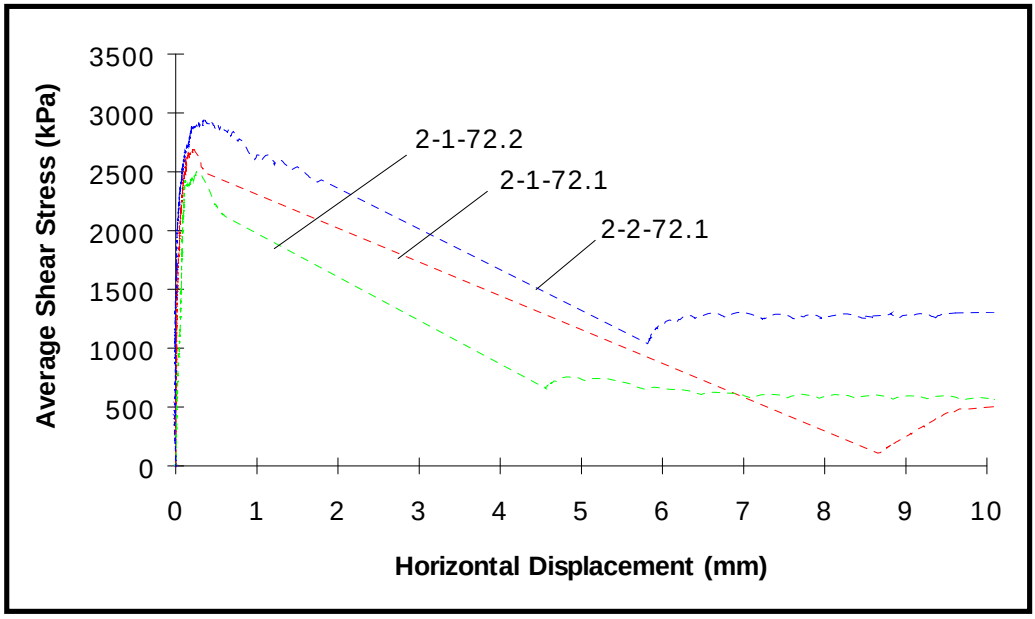

Figure 5.13 Average Shear Stress vs. Displacement: Contact Area = 465 cm^2, 1 or 2 Nails

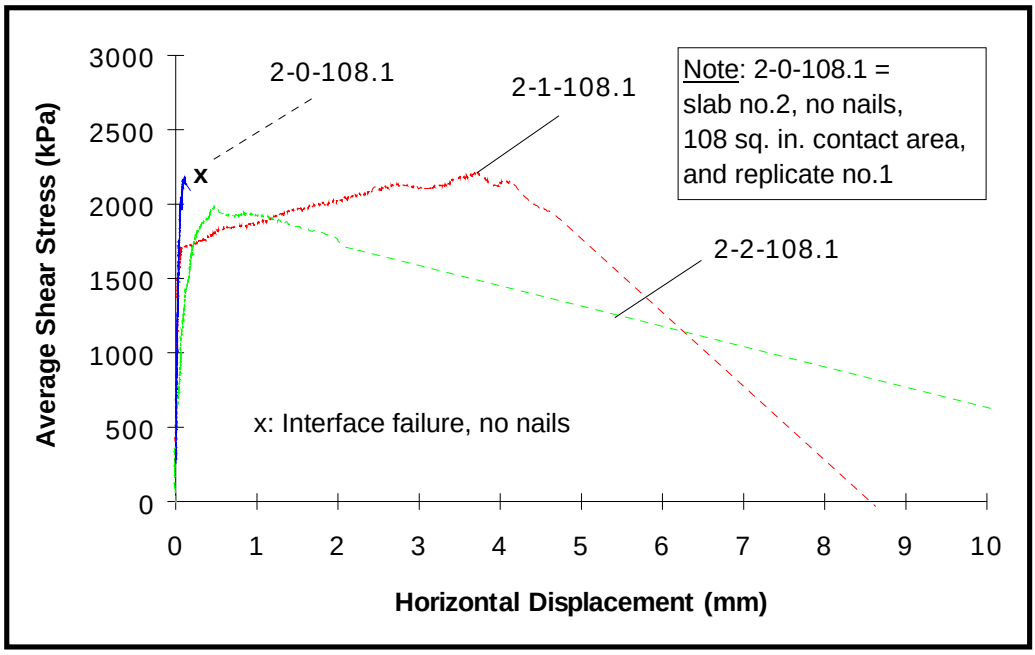

Figure 5.14 Average Shear Stress vs. Displacement: Contact Area = 700 cm^2, 0, 1 or 2 Nails

shear stress was reached. Figure 5.15 shows that the failure occurred partly in the low strength overlay in ***2-1-108.1***. The peak stress determined from a specimen with two nails, ***2-2-108.1***, was low because failure occurred in the base concrete before the interface failed as can be seen in Fig. 5.16.

5.3.2 Specimens Subjected to Loading and Unloading Cycles

Companion specimens for three tests with large contact area (Fig. 5.14) were subjected to several cycles of loading and unloading. A complete loading and unloading curve is shown in Fig. 5.17 for ***2-1-108.2***. A peak shear stress of 1,660 kPa (240 psi) was reached at a displacement of 0.5 mm (0.02 in.) at failure. The

(a) Base Concrete

(b) Overlay

Figure 5.15 Failure in Low Strength Concrete

(a) Base Concrete

(b) Overlay

Figure 5.16 Failure in Low Strength Base Concrete

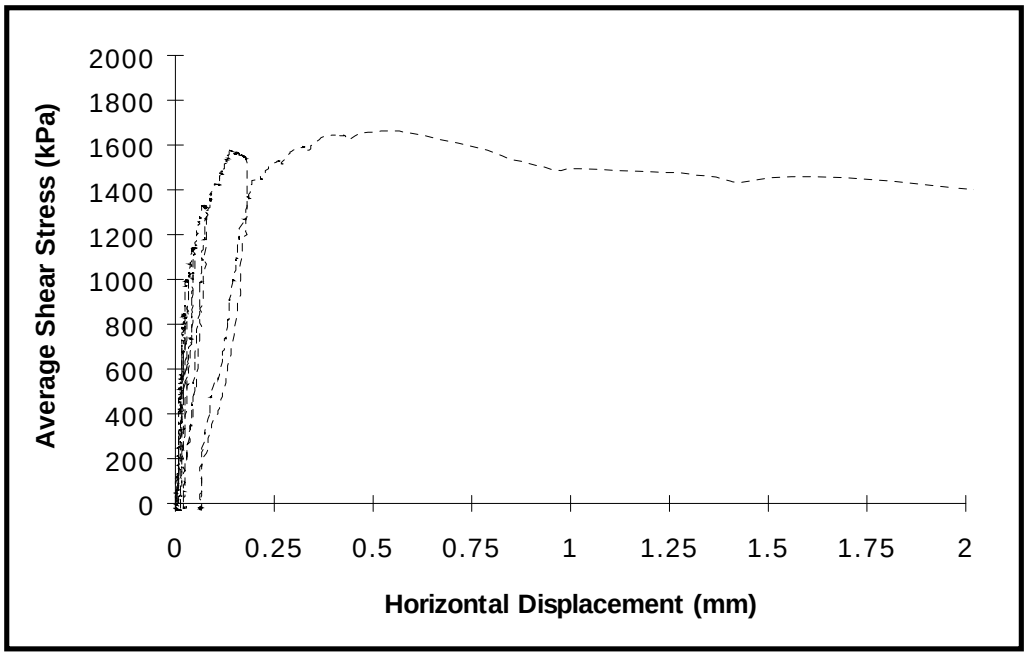

Figure 5.17 Average Shear Stress vs. Displacement: ***2-1-108.2***, Contact Area = 700 cm^2, 1 Nail

reduction in peak stress from a value of 2,210 kPa (320 psi) for ***2-1-108.1*** was probably due to the cyclic loading. The test results are summarized in Table 5.4.

5.3.3 Summary: Contact Area vs. Number of Nails Used

The mean of the ultimate interface shear strength of all DS-II specimens was 2,570 kPa (375 psi). The low strength base concrete and overlays were used for DS-II test series. The mean interface strength of all DS-II specimens was 88 percent of that of DS-I (2,930 kPa or 425 psi) due to the low strength base concrete and the overlay. The average shear stress and the horizontal displacement of the overlay at the peak shear load is summarized in Table 5.5. The values shown in

Table 5.5 Interface Shear Strength and Displacement at Peak Load: DS-II

No. of Nails	Contact Area (cm^2)								
	230			465			700		
	Reinf. Ratio (%)	Stress (kPa)	Displ. (mm)	Reinf. Ratio (%)	Stress (kPa)	Displ. (mm)	Reinf. Ratio (%)	Stress (kPa)	Displ. (mm)
0	--	3,250	0.3	--	2,650	0.2	--	2,170	0.1
1	0.38	3,150	0.5	0.19	2,600	0.2	0.13	1,940	3.7
2	--	--	--	0.38	2,940	0.4	0.25	2,050	0.5
Avrg.	--	3,200	0.4	--	2,730	0.2	--	2,050	1.4

Table 5.5 generally represent an average of two tests. Test results reveal that there were no significant differences in the interface strength as the number of nails was increased for all contact areas investigated.

5.4 Unbonded Interface: DS-III

The behavior of the unbonded interfaces with nails was determined in DS-III test series. Concrete adhesion was intentionally eliminated by using bond breaker. Two normal strength slabs with river gravel and hard limestone aggregates (Table 3.1) were used. The compressive strength of the overlay approximately matched that of the base slab at the time of testing. The contact areas were kept the same (465 cm^2 or 72 $in.^2$) for all specimens. A total of twelve tests was conducted. Two specimens with one nail (ρ = 0.19 %) and two

specimens with two nails (ρ = 0.38 %) had heavy shotblasted contact surfaces. Two other specimens with one nail (ρ = 0.19 %) had relatively smooth trowel-finished contact surfaces. The same combination of nails and the contact surface was used for the normal strength base slabs with river gravel and hard limestone aggregate, respectively. Test results are summarized in Table 5.6.

5.4.1 Unbonded-Rough Interface

Figure 5.18 shows push-off test results of four specimens with an unbonded-rough interface. The base concrete is the normal strength slab with river gravel. Two specimens, ***1-H-1U.1*** and ***1-H-1U.2***, had one nail and two other specimens, ***1-H-2U.1*** and ***1-H-2U.2***, had two nails. Horizontal displacements were about the same in all cases when maximum shear load was reached. The average of the maximum shear loads was 80 kN (18 kips) and the average horizontal displacement was 1.1 mm (0.04 in.) for two specimens with two nails. The average maximum shear loads for two specimens with one nail was 55 kN (12 kips) and the average horizontal displacement was 1.9 mm (0.07 in.). The extra nail contributed an additional capacity of about 25 kN (5.6 kips) or 45 percent of the strength with one nail. Figure 5.19 shows the test results of four unbonded-rough specimens with a normal strength base slab with hard limestone aggregate. The load-displacement plots in Fig. 5.19 are similar to those shown in Fig. 5.18. The average maximum shear load was 89 kN (20 kips) at an average horizontal displacement of 2.5 mm (0.1 in.) for the two specimens with two nails. The values for the two specimens with one nail were 52 kN (12 kips) and 1.8 mm (0.07 in.). In this case, the extra nail contributed an additional capacity of about 37 kN (8.3 kips).

Table 5.6 Summary of Push-Off Test Results: DS-III (Unbonded)

Specimen Index	Values at Peak Shear Load			Shear Load at Horiz. Displ.			Nails Failure Mode	Re-marks
	Shear Load (kN)	Horiz. Displ. (mm)	Vert. Displ. (mm)	3 mm (kN)	6 mm (kN)	9 mm (kN)		
1-H-1U.1	58	1.4	0.5	53	44	39	PO/B [2]	
1-H-1U.2	51	2.3	0.8	51	47	43	PO/B	
1-H-2U.1	78	1.1	0.5	77	76	73	PO/B	
1-H-2U.2	82	1.2	0.6	76	77	76	PO/B	
1-N-1U.1 [1]	28	1.0	0.2	31	36	43	PO/B	T.F. [4]
1-N-1U.2 [1]	31	1.0	0.1	35	43	41	PO/B	T.F.
3-H-1U.1	54	1.3	0.4	48	43	43	PO/OL [3]	
3-H-1U.2	49	2.2	0.5	48	45	41	PO/B	
3-H-2U.1	84	2.0	0.8	82	76	72	PO/OL	
3-H-2U.2	95	2.9	0.5	94	87	84	PO/OL	
3-N-1U.1 [1]	32	1.0	0.1	35	37	40	PO/B	T.F.
3-N-1U.2 [1]	24	1.0	0.1	27	33	39	PO/OL	T.F.

Note 1: Shear load and vertical displacement values correspond to horizontal displacement of 1 mm, 2: PO/B = Pulled-out from base concrete, 3: PO/OL = Pulled-out from overlay, 4: T.F. = Trowel finish.

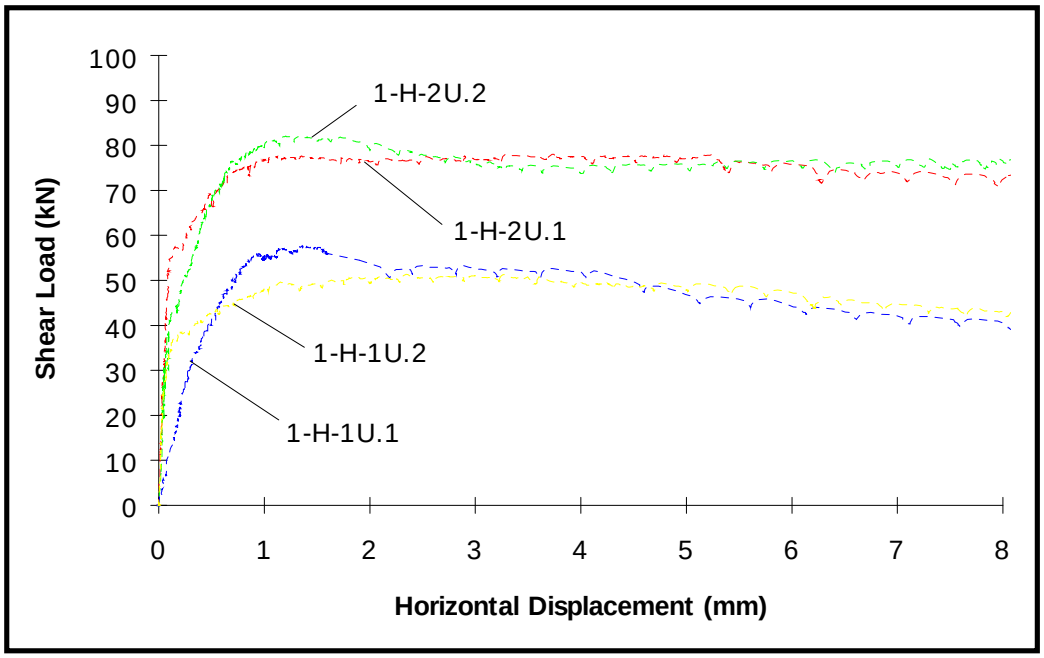

Figure 5.18 Load vs. Displacement: Specimens with Unbonded-Rough Interface, Normal Strength Slab with River Gravel, Contact Area = 465 cm^2, 1 or 2 Nails

5.4.2 Unbonded-Smooth Interface

Figure 5.20 shows test results for two unbonded specimens with smooth interface and a normal strength base slab with river gravel. One nail (ρ = 0.19 %) was used with a contact area of 465 cm^2 (72 $in.^2$) for both tests. The load-slip behavior of the unbonded-smooth specimens was distinctively different from that of the unbonded-rough specimens. The relatively high initial stiffness in the load-displacement plots decreased rapidly with increasing shear loads in both tests. Peak shear loads were reached at very large displacements. The theoretical strength of the nail in direct shear using F_y/SQRT(3) is also plotted in Fig. 5.20

where F_y is nail

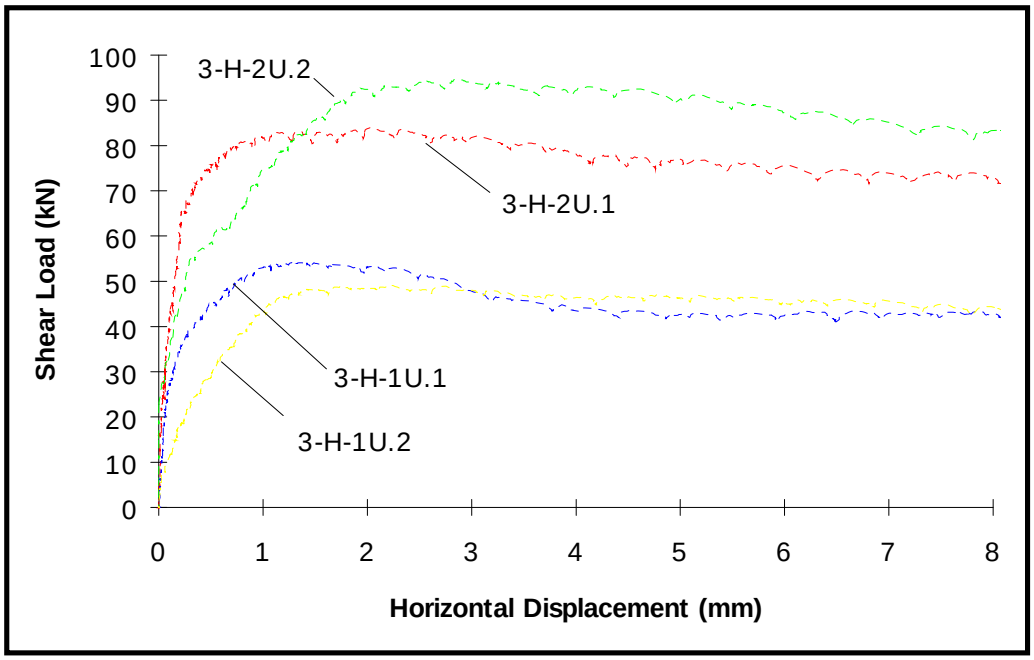

Figure 5.19 Load vs. Displacement: Unbonded-Rough Interface, Normal Strength Slab with Hard Limestone Aggregate, Contact Area = 465 cm^2, 1 or 2 Nails

yield strength (600 MPa or 87 ksi). Approximately 30 kN (6.7 kips) dowel strength developed at displacements between 1.5 mm (0.06 in.) and 3.0 mm (0.12 in.). The fact that shear increased at larger displacements suggests that other shear resisting mechanisms are involved at larger displacements. The nail developed tension as the displacement increased and some shear-friction capacity was mobilized even though the surface was smooth. Similar test results are shown in Fig. 5.21 for a normal strength slab with hard limestone aggregate. Test results clearly indicate that an effective shear transfer across the interface could not be achieved when the contact surface was smooth and unbonded. The contribution of shear

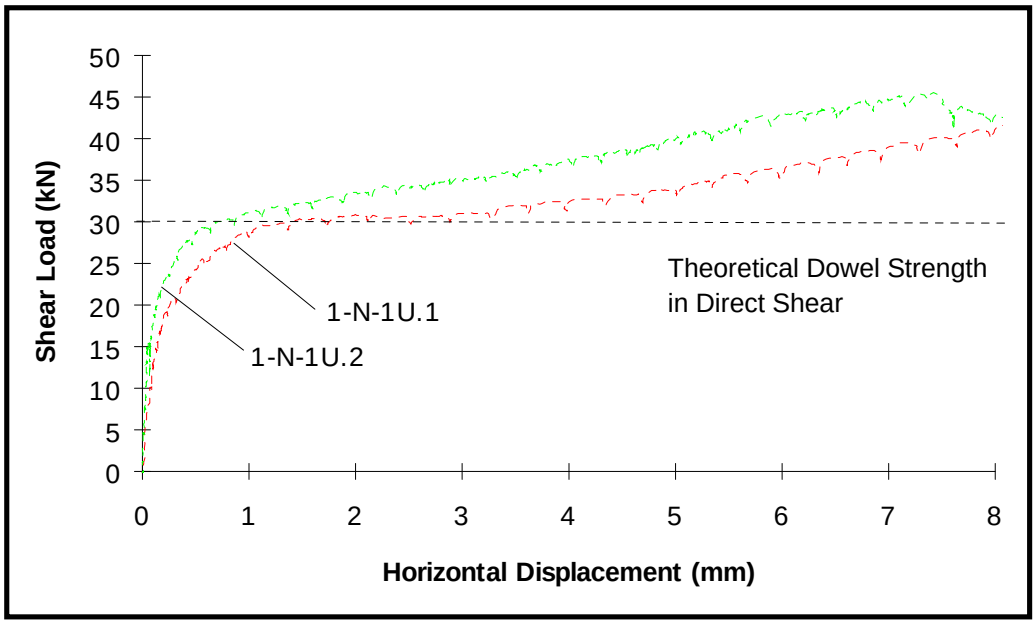

Figure 5.20 Load vs. Displacement: Specimens with Unbonded-Smooth Interface, Normal Strength Slab with River Gravel, Contact Area = 465 cm^2, 1 Nail

reinforcement, in this case jumbo nails, across the interface became significant only after large slip occurred.

5.4.3 Summary: Unbonded Interface

A total of 12 push-off tests was completed in series DS-III to investigate the shear behavior of unbonded interfaces with nails. Test results reveal that a specimen with an unbonded-rough contact surface can effectively resist shear and limit the horizontal slip to acceptable values. This was not possible with an unbonded-smooth contact surface. Test results of three specimens with bonded-

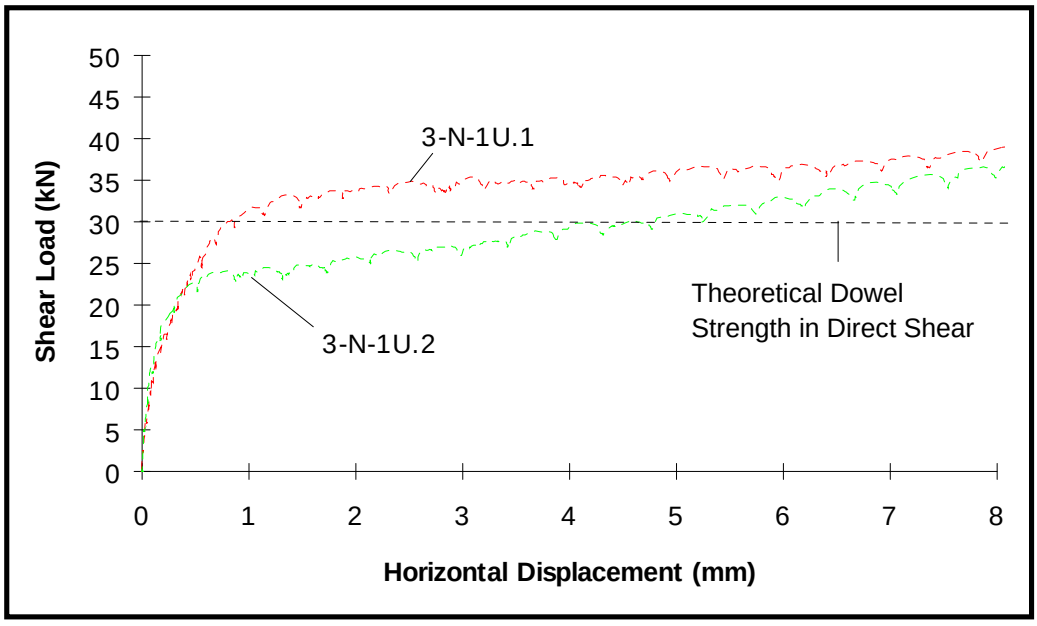

Figure 5.21 Load vs. Displacement: Unbonded-Smooth Interface, Normal Strength Slab with Hard Limestone Aggregate, Contact Area = 465 cm^2, 1 Nail

rough, unbonded-rough, and unbonded-smooth interface, respectively, are plotted for comparison in Fig. 5.22. In all three specimens, there was one nail across the interface. The load-displacement plots of the unbonded specimens did not show the sharp peak of the bonded-rough specimens. An unbonded-rough specimen with one nail effectively resisted the shear force and limited the overlay displacement to small values when the applied maximum shear load was approximately half of the peak load of a bonded-rough specimen. The magnitude of shear loads in the relatively flat plateaus in a bonded-rough and an unbonded-rough specimens was similar at large displacements.

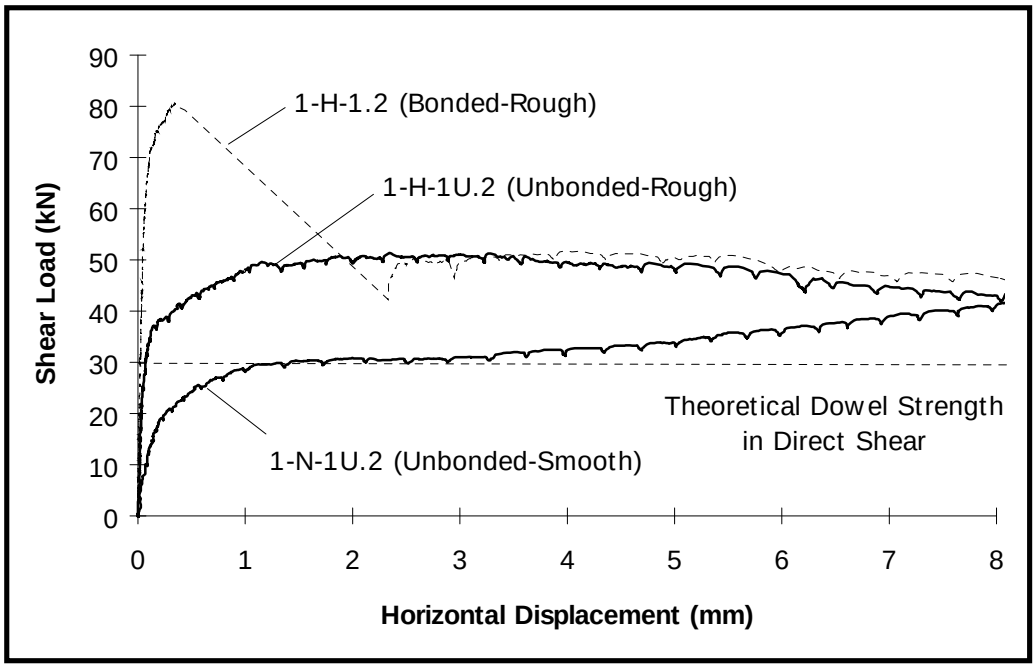

Figure 5.22 Different Load vs. Displacement Behaviors in Specimens with Bonded-Rough, Unbonded-Rough, and Unbonded-Smooth Interfaces

5.5 Effect of "Stepped" Drill Hole: DS-IV

The effect of the stepped drill hole (Fig. 1.3) on shear behavior of jumbo nails was studied in DS-IV test series. The initial shear stiffness of the nail can be affected by the presence of the gap between the nail shank and the stepped hole. The diameter of the stepped hole is 1.7 mm (0.07 in.) larger than the nail shank diameter in Fig. 1.3. Figure 5.23 shows the DS-IV test results. Each load-displacement plot in Fig. 5.23 represents an average of two test results. The initial displacement values corresponding to the same shear loads did not differ significantly until a shear load of approximately 17 kN (4 kips) and a horizontal displacement of approximately 0.3 mm (0.01 in.) were reached for specimens with rough contact areas. Displacements at higher loads for nails with an "exaggerated stepped" hole were larger than those with a "straight" drill hole. Differences in displacement values increased rapidly as higher loads were applied. Similar observations were made for specimens with a smooth contact surface. Initial displacement values corresponding to the same shear loads did not differ significantly until the shear load reached approximately 6 kN (1.3 kips) for specimens with smooth contact areas. The horizontal displacements corresponding to the higher loads for specimens with an "exaggerated stepped" hole were larger than those with a "straight" drill hole. The results showed that specimens with a stepped drill hole were not as effective in resisting shear as those with a straight drill hole.

5.6 Existing Crack Effects in Base Concrete: DS-V

The push-off test results of 32 bonded specimens in series DS-V are described. All four base slabs (Table 3.1) were used for these tests with eight tests

on each slab. Sandblasting was used to roughen the contact surface whenever surface preparation was necessary. One objective of the DS-V test series was to investigate the shear behavior of jumbo nails driven into an existing crack or very close to a crack. Such cracks can be expected to develop in the portland cement concrete (PCC) pavements during service life. The terms “cracked” and “crack-free” are used in this study. A “cracked” specimen is one which has existing cracks in the base concrete while a “crack-free” specimen is one which does not have any existing cracks in the base concrete. An existing crack represents a discontinuity in the otherwise continuous base concrete. Pull-out tests of nails near a crack indicated that a crack was nearly the same as an edge in terms of its effect on pull-out capacity. Flexural cracks were created in the base slabs to represent structural cracks in PCC pavements. Nails were driven into or very close to a crack. The shear loads were applied in a direction approximately parallel to the crack direction. Test results determined in the cracked specimens were compared with those in the crack-free specimens. The other objective was to determine the effect of the base concrete compressive strength on the interface shear strength.

It must be noted that nails from the shipment that were used in the pull-out tests were also used in series DS-V. The push-off tests revealed that these nails had limited ductility, and brittle nail fractures were observed in many DS-V specimens.

5.6.1 Low Strength vs. Normal Strength Slab

Sixteen overlays were placed on the normal strength slab with river gravel and on the low strength slab (eight overlays on each slab). Test results are summarized in Tables 5.7 and 5.8. Of eight overlays, seven were placed against a rough sandblasted contact surface. One overlay was placed against a relatively

smooth troweled surface. The contact area was either 230 cm^2 (36 $in.^2$) or 465 cm^2 (72 $in.^2$) while the interface reinforcement ratio was the same 0.38 percent for all specimens with nails. No nails were used for the one control specimen.

5.6.1.1 Normal Strength Slab with River Gravel Figure 5.24 shows the test results of three specimens with one nail in the normal strength base slab with river gravel. The contact areas of all three specimens were sandblasted. A nail was driven very close to a crack in ***1M1SC.1*** and into a crack in ***1M1CR.1***. The third specimen, ***1M1NC.1***, was free of any cracks. The peak stress in a cracked specimen was lower than that in a crack-free specimen. Nails fractured in two tests before pulling out of the base concrete or the overlay. A brittle nail failure was observed in ***1M1CR.1*** at a large horizontal displacement of 6 mm (0.25 in.). A similar nail failure was also observed in ***1M1SC.1*** at a displacement larger than 10 mm (0.4 in.). The test results of three specimens with two nails across the interface are shown in Fig. 5.25. Nails were driven close to a crack in ***1M2SC.1***. Two other specimens, ***1M2NC.1*** and ***1M2NC.2***, were free of cracks. The peak shear stress of the cracked specimen was only slightly lower than the peak stresses in two crack-free specimens. Brittle nail failures were again observed. Some nails fractured into two and some into three parts. The profiles of the fractured surface in two specimens are shown in Figs. 5.26 and 5.27. The front nail was pulled out from the base concrete while the rear nail failed in shear ***1M2NC.1*** in Fig. 5.26. The front nail failed in a shear while the rear nail was pulled out from the overlay in ***1M2SC.1*** in Fig. 5.27.

5.6.1.2 Low Strength Slab A nail was driven into a crack in ***2M1CR.1*** while two other specimens, ***2M1NC.1*** and ***2M1NC.2***, were free of any cracks. The test results are shown in Fig. 5.28. Only the peak portion of the plot is shown for

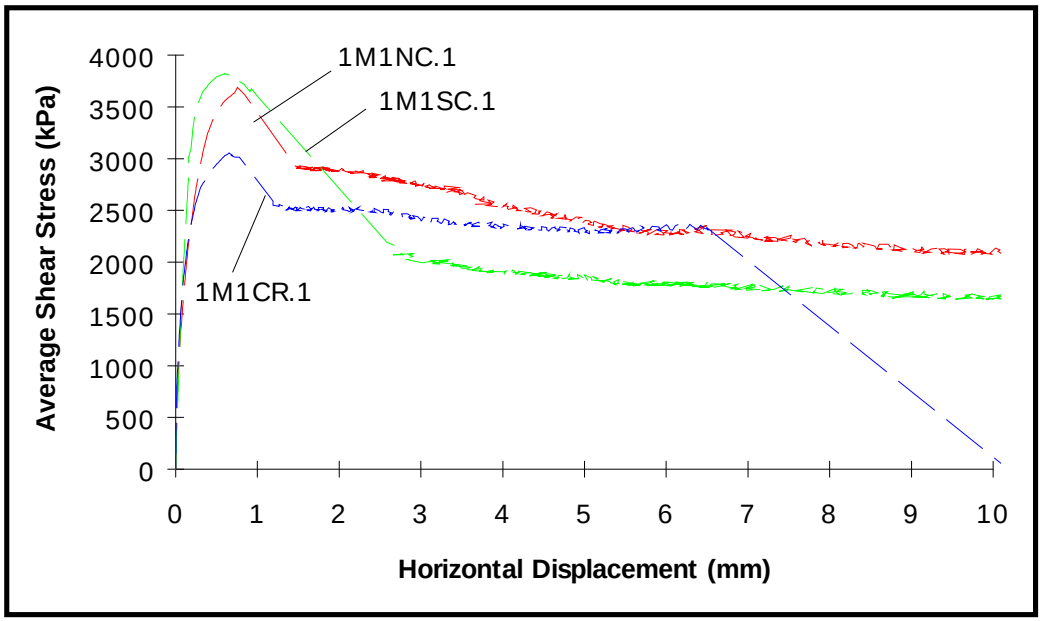

Figure 5.24 Average Shear Stress vs. Displacement: Normal Strength Slab with River Gravel, Contact Area = 230 cm^2, 1 Nail

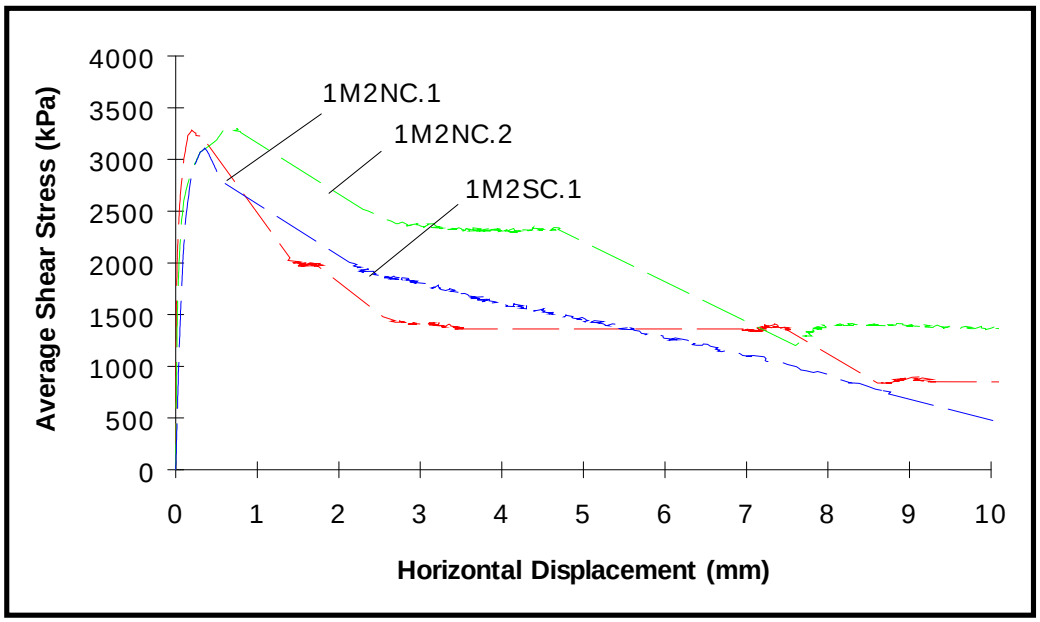

Figure 5.25 Average Shear Stress vs. Displacement: Normal Strength Slab with River Gravel, Contact Area = 465 cm^2, 2 Nails

(a) Base Concrete

(b) Overlay

Figure 5.26 Nail Pull-Out and Shear Fracture

(a) Base Concrete

(b) Overlay

Figure 5.27 Nail Shear Fracture and Pull-Out Failure

2M1NC.1 because the displacement data were not accurately measured due to a testing error. The peak shear stresses were nearly the same as shown in Fig. 5.28. Two nails were driven close to a crack in ***2M2SC.1*** and into a crack in ***2M2CR.1***. The third specimen, ***2M2NC.1***, was free of any cracks. The test results are shown in Fig. 5.29. Only the peak portion is again shown for ***2M2NC.1*** due to an incorrect displacement measurement. The peak shear stresses in all three tests are similar.

5.6.1.3 Specimens with Smooth Troweled Interface One overlay was placed against the smooth troweled surface of the base concrete on each slab. The peak interface strength was lower in ***1N1NC.1*** with the smooth troweled interface than with sandblasted interface (Table 5.7). The initial interface bond was weak and the horizontal displacements increased rapidly at relatively low shear stresses in ***2N1NC.1*** as noted in Table 5.8. The test results reveal that an interface treatment before the placement of the overlay, such as sandblasting, significantly improved the interface bond development.

5.6.1.4 Control Specimens One control test specimen without nails was tested on each slab. A direct comparison of the test results is possible between tests which used two nails and no nails because the contact area was the same 465 cm^2 (72 $in.^2$). The interface strength of the control specimens was lower than that in specimens with nails as shown in Tables 5.7 and 5.8.

5.6.2 Normal Strength vs. High Strength Slab

Sixteen overlays were placed on the normal strength slab with hard limestone aggregate and the high strength slab. Test results are summarized in

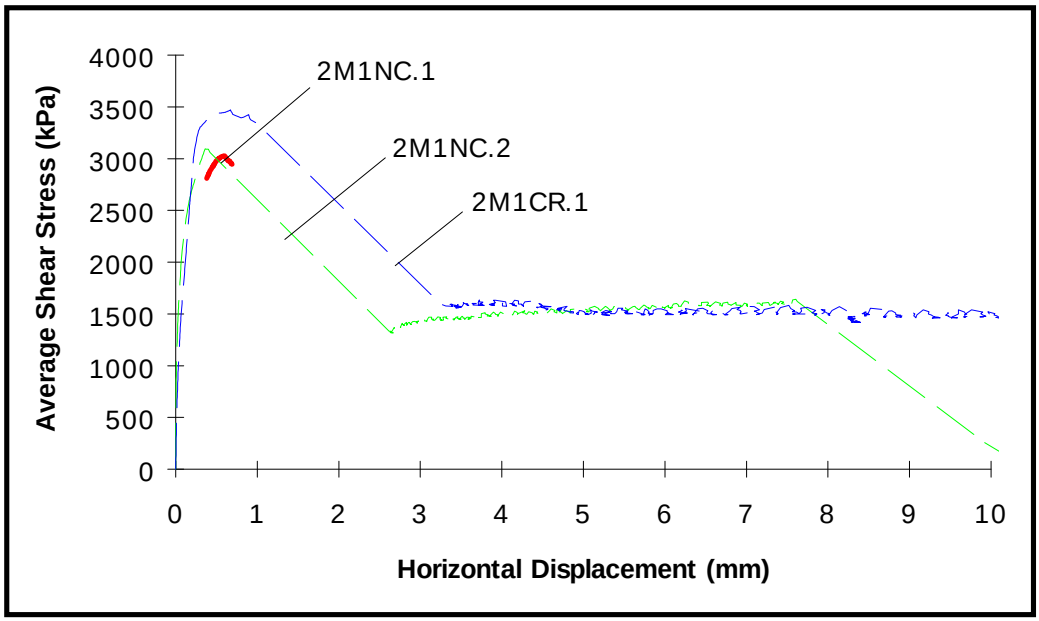

Figure 5.28 Average Shear Stress vs. Displacement: Low Strength Slab, Contact Area = 230 cm^2, 1 Nail

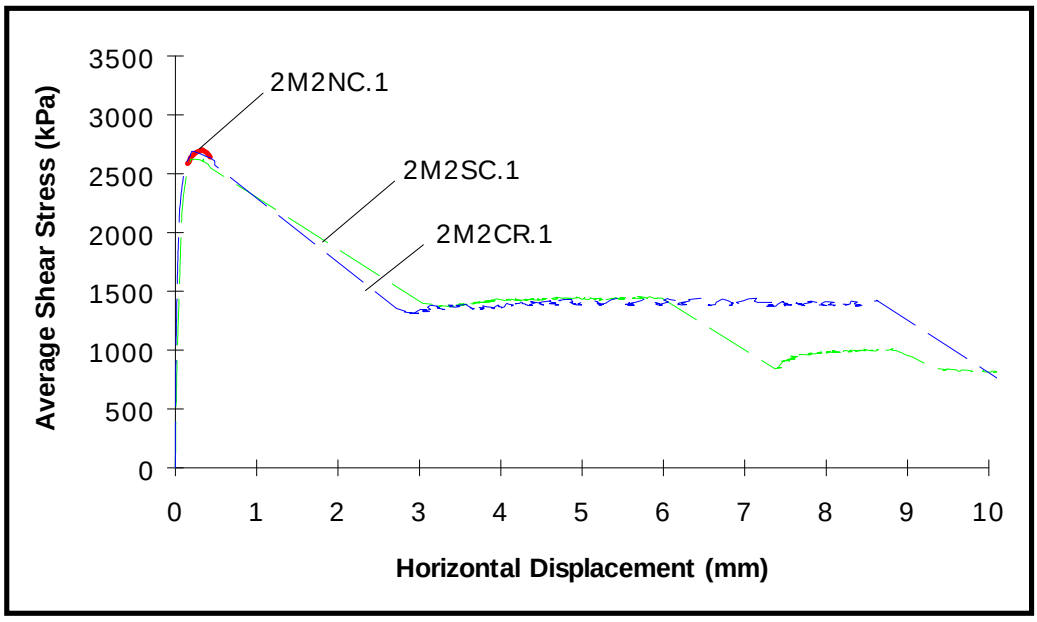

Figure 5.29 Average Shear Stress vs. Displacement: Low Strength Slab, Contact Area = 465 cm^2, 2 Nails

Tables 5.9 and 5.10. Test results of three specimens, 3M0NC.1, 3M2SC.1, and 4N1NC.1, are not reported due to the malfunction of a hydraulic cylinder in one test and the change in the alignment of the hydraulic cylinders during testing in two other tests.

5.6.2.1 Normal Strength Slab with Hard Limestone Aggregate Figure 5.30 shows the results of four tests with one nail in the normal strength base slab with hard limestone aggregate. The contact area was sandblasted for three specimens while a smooth troweled surface was used for one specimen. A nail was driven close to a crack in ***3M1SC.1*** and into a crack in ***3M1CR.1*** while the third specimen, ***3M1NC.1***, was free of any cracks. The peak stresses in two cracked specimens were lower than the peak stress of a crack-free specimen. The shear resistance of nails after the peak in cracked specimens was also lower than that of a crack-free specimen. Test results of a specimen with a smooth troweled surface, ***3N1NC.1***, is also shown in Fig. 5.30. The initial stiffness was similar to that determined in sandblasted specimens but the horizontal displacement began to increase rapidly at low shear stresses. Figure 5.31 shows the results of two tests with a rough interface in which two nails were used in the normal strength base slab with hard limestone aggregate. Two nails were driven into a crack in ***3M2CR.1***, while the other specimen, ***3M2NC.1***, was free of any cracks. The peak shear stresses of the specimens were nearly the same.

5.6.2.2 High Strength Slab Figures 5.32 and 5.33 show the results of three tests with one and two nails in the high strength base slab. It was difficult to properly roughen the contact surface of the high strength concrete by sandblasting. As a result, initial adhesion was relatively low in these tests. The peak shear stresses were reached at relatively large horizontal displacements as shown in Fig.

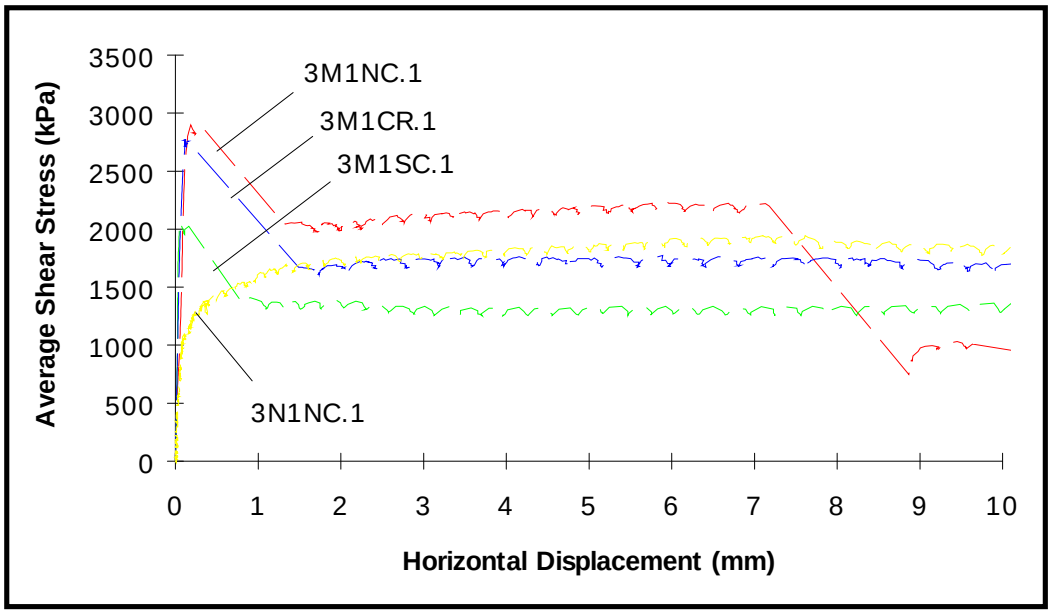

Figure 5.30 Average Shear Stress vs. Displacement: Normal Strength Slab with Hard Limestone Aggregate, Contact Area = 230 cm^2, 1 Nail

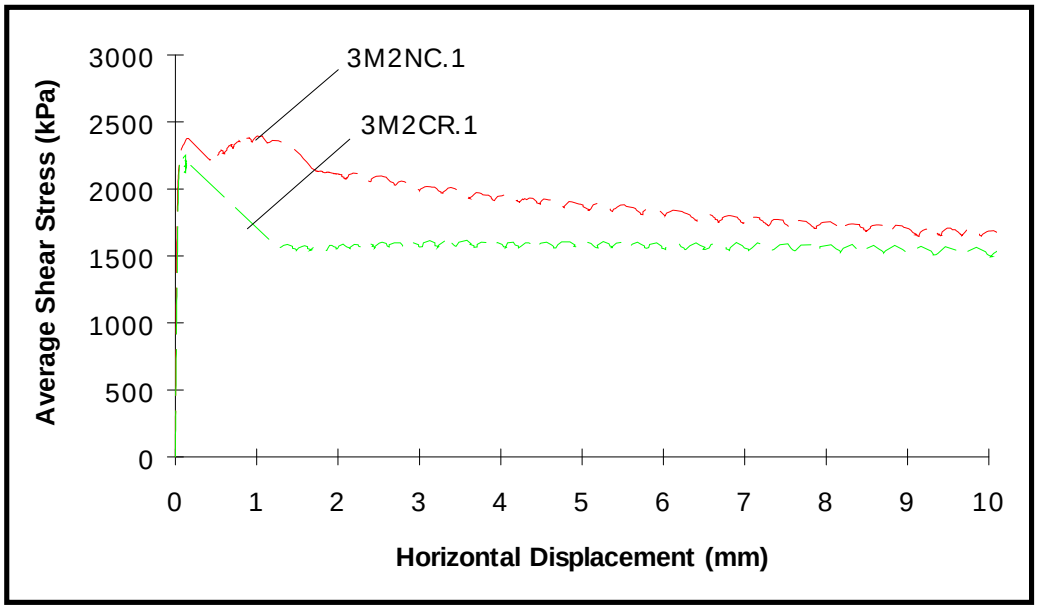

Figure 5.31 Average Shear Stress vs. Displacement: Normal Strength Slab with Hard Limestone Aggregate, Contact Area = 465 cm^2, 2 Nails

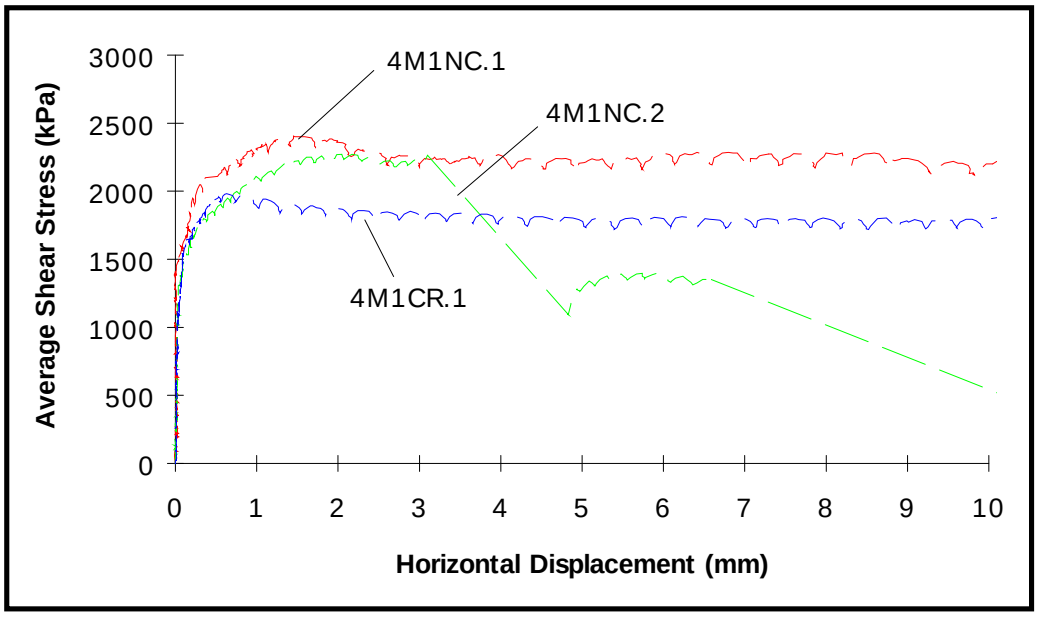

Figure 5.32 Average Shear Stress vs. Displacement: High Strength Slab, Contact Area = 230 cm^2, 1 Nail

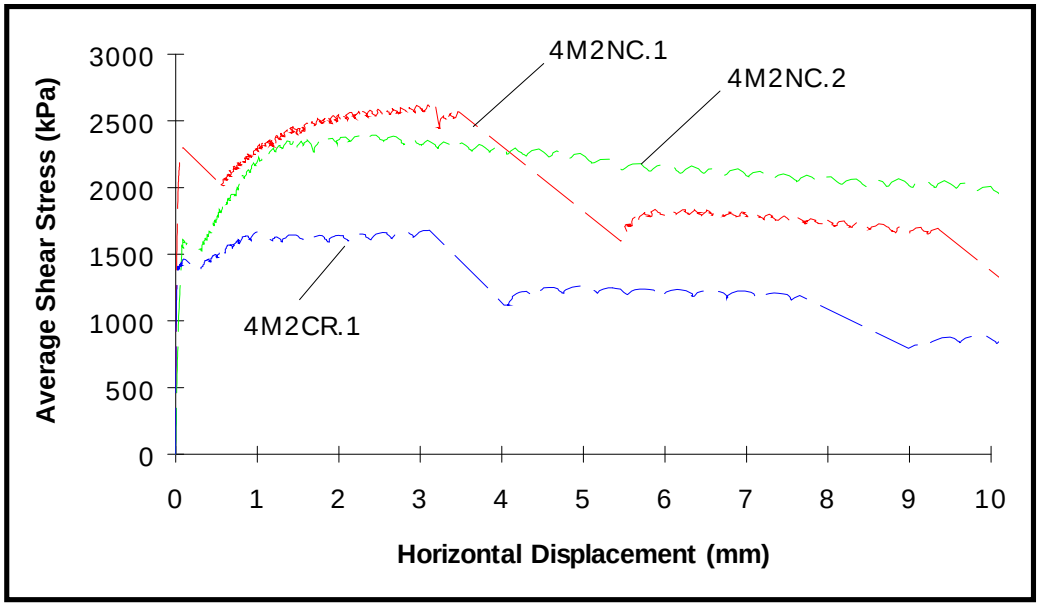

Figure 5.33 Average Shear Stress vs. Displacement: High Strength Slab, Contact Area = 465 cm^2, 2 Nails

5.32 while the absence of the initial sharp peaks characteristics of most bonded-rough surfaces was noted in all three tests. A nail was driven into a crack in ***4M1CR.1*** while two other specimens, ***4M1NC.1*** and ***4M1NC.2***, were free of any cracks. The peak shear stress and the shear resistance provided by a nail after the peak were lower in a cracked specimen than in crack-free specimens. Two nails were driven into a crack in ***4M2CR.1***, and two other specimens, ***4M2NC.1*** and ***4M2NC.2***, were free of cracks. Load-displacement plots in Fig. 5.33 show initial peaks at very small horizontal displacements. A small, but sudden decrease in shear stresses along with increasing horizontal displacements was observed after the initial peak. The highest stresses were reached at substantially larger displacements than those at initial peaks in all tests. The peak stress and the shear resistance of nails after the peak in the cracked specimen were again lower than those in the two crack-free specimens.

5.6.3 Summary: Concrete Strength and Presence of Cracks

5.6.3.1 Effect of Concrete Strength on Interface Strength The interface strength determined from DS-V tests is summarized in Table 5.11. Test results reveal that there are reductions in the interface strength in specimens with the low strength base slab compared with those placed on the normal strength base slab. The average interface strength of overlays on the low strength slab was 87 percent of that on a normal strength slab with river gravel. Interface strengths of overlays on the high strength slab were lower than those on the normal strength slab with hard limestone aggregate due most likely to insufficient interface preparation of the high strength concrete using sandblasting.

Table 5.11 Summary of Interface Strength: DS-V (Bonded-Rough Interface)

Base Slab	Number of Nails	Contact Area (cm^2)	All Tests (kPa)	Crack-free Specimens (kPa)	Cracked Specimens (kPa)
Normal Strength with River Gravel	1	232	3,520 (3) [a]	3,690 (1) [a]	3,440 (2) [a]
	2	465	3,230 (3)	3,300 (2)	3,110 (1)
Low Strength with Soft Limestone Aggregate	1	232	3,200 (3)	3,060 (2)	3,470 (1)
	2	465	2,670 (3)	2,700 (1)	2,660 (2)
Normal Strength with Hard Limestone Aggregate	1	232	2,580 (3)	2,900 (1)	2,420 (2)
	2	465	2,330 (2)	2,400 (1)	2,260 (1)
High Strength with Soft Limestone Aggregate	1	232	2,220 (3)	2,340 (2)	1,980 (1)
	2	465	2,230 (3)	2,510 (2)	1,680 (1)

Note a: Number of tests completed

5.6.3.2 Effect of Existing Cracks on Interface Strength Test results reveal that there were reductions in the interface strength of the cracked specimens when compared to those of the crack-free specimens. Test results were fairly consistent with the exception of the low strength slab. The interface strength of the cracked specimens was approximately 90 percent of that of the crack-free specimens in two normal strength slabs. The mean interface strength of the cracked specimens was between 70 and 85 percent of that of the crack-free specimens in the high strength slab.

5.7 Conclusions

5.7.1 Bonded Interface

The mean of the interface shear strengths of all specimens with a bonded-rough interface was 2,760 kPa (400 psi) with the maximum and minimum of 4,530 kPa (660 psi) and 1,660 kPa (240 psi). The interface strengths of shotblasted and sandblasted specimens were about the same. The interface roughness of sixteen specimens was grouped as light (L), medium (M), and heavy (H) shotblasting in series DS-I. Test results revealed the following:

1. No significant differences in the interface shear strength were found between companion specimens which received different levels of surface preparation.
2. Overlay slip sometimes occurred at fairly low shear stresses when the interface was lightly shotblasted. However, the peak loads were typically within 10 percent of the replicate specimens which experienced no premature slip.
3. The overlay horizontal displacements at the peak were higher in specimens with nails than in those with no nails because nails permitted redistribution of stresses across the interface when adhesion was lost.
4. Specimens with two nails (ρ = 0.38 %) had 16 percent higher average shear stresses (3,020 kPa or 440 psi) at the peak than those without nails (2,600 kPa or 380 psi).

The interface shear reinforcement ratio changed between 0 percent and 0.38 percent in sixteen tests (series DS-II). Test results revealed the following:

1. No significant differences in the interface strength were found as the number of nails was increased for all contact areas investigated.
2. The mean of the interface shear strengths of all specimens was 2,570 kPa (370 psi). The mean interface strength was 88 percent of that of series DS-I (2,930 kPa or 425 psi) due to the low strength base concrete and the overlay.

Thirty-two tests were conducted to investigate the shear behavior of jumbo nails driven into an existing crack or very close to a crack and to determine the effect of the base concrete compressive strength on the interface shear strength (series DS-V). Test results revealed the following:

1. There were reductions in the interface strength and the post peak shear resistance by nails of the cracked specimens when compared to those of the crack-free specimens.
2. Interface strength of the cracked specimens was approximately 90 percent of that of the crack-free specimens in two normal strength slabs. The mean interface strength of the cracked specimens was between 70 and 85 percent of that of the crack-free specimens in the high strength slab.
3. Average interface strength in the low strength slab was 87 percent of that in the normal strength slab.
4. Interface strength in specimens on the high strength slab was lower than that in the normal strength slab probably due to the insufficient interface preparation of the high strength concrete using sandblasting.

5.7.2 Unbonded Interface

The shear behavior of the unbonded-rough and the unbonded-smooth interfaces with nails was investigated in series DS-III. Test results revealed the following:

1. A specimen with an unbonded-rough interface could effectively resist the shear force and limit the interface slip.
2. The load-slip behavior of the unbonded-smooth specimens was distinctively different from that of the unbonded-rough specimens. The contribution of shear reinforcement across the interface became significant only after large slip occurred, and approximately 30 kN (6.7 kips) dowel strength developed at displacements of 1.5 mm (0.06 in.).
3. The shear capacity of an unbonded-rough specimens with one nail was approximately 50 kN (11 kips). Test results of the unbonded-rough specimens with one and two nails were compared. The contribution of an extra nail in resisting shear was approximately 30 kN (6.7 kips).

CHAPTER SIX
INTERFACE STRENGTH DEVELOPMENT AT EARLY AGES

6.1 Introduction

The interface shear strength development for the first several weeks after the placement of the overlay was experimentally studied. It was important to determine the interface strength between the base concrete and the overlay at early ages because delamination failures in bonded concrete overlays (BCOs) are frequently reported at early ages. Debonding of the overlay, for example, was noted shortly after overlay placement in a BCO constructed by the California Department of Transportation (Neal 1983). Subsequent laboratory studies were undertaken to investigate the cause of the delamination, and repeated temperature changes were determined to be the cause. Volume change of the overlay due to drying shrinkage and temperature change was suggested as the cause for early age overlay delamination in BCOs by Lundy (1990). Based on a finite element study, Lundy suggested that maximum interface stresses of 170 kPa (24 psi) and 120 kPa (17 psi) in shear and tension, respectively, can develop at pavement edges by an -18 °C (-33 °F) temperature change and by overlay shrinkage 24 hours after casting. Slightly higher interface stresses near interior cracks were predicted by Lundy. The interface strength development shortly after overlay placement is relatively unknown, and limited experimental data are currently available.

Table 6.1 Overlay Compressive Strength (MPa) during Test Period

Days[1] / Index	0.5	1	1.5	2	3	4	7	14	28	35
ES-I	--	10	13	16	18	21	24	27	29	--
ES-II	6	10	--	15	18	19	22	23	--	25

Note 1: Age of overlays in days, 2: All cylinders were moist cured for three days.

6.2 Preparation of Early Age Push-Off Specimens

Two series of early age push-off tests were carried out using the in-situ push-off test setup. The variable in the first test series (ES-I) was the age of the overlays. Push-off tests were performed when the age of the overlays was between one and 28 days. The variable in the second test series (ES-II) was the overlay curing method. The effect of the two different curing methods on the interface strength development was investigated with push-off tests performed when the age of the overlays was between 12 hours and 35 days. The overlay compressive strength development during the test period was determined by compressive cylinder tests and is shown in Table 6.1.

6.2.1 Interface Strength Development at Early Ages: ES-I

The objective was to determine the rate of the interface shear strength gain at early ages. The high strength slab, which was also used for the push-off tests of the fully-cured specimens, was used as the base concrete (Table 3.1). The interface was heavily shotblasted for all specimens. The average texture of the heavily

shotblasted interface was similar to the typical shotblasted surfaces used in the field for BCOs. The contact area was 465 cm^2 (72 $in.^2$) in all specimens. One Hilti jumbo nail was used across the bonded interface for eight specimens (interface shear reinforcement ratio, ρ = 0.19 %). The contribution of the nail in improving the interface shear strength was not significant at this reinforcement ratio but nails provided a post peak shear resistance as indicated by earlier push-off tests. No nails were used for the other eight specimens. Sixteen overlays were placed. The 28-day compressive strength of the overlay was 29 MPa (4,200 psi) as given in Table 6.1. The overlays were moist cured in the formwork under a plastic sheet for three days. The formwork and the plastic sheet were removed after three days, and the overlays were then air dried. The formwork and the plastic sheet were removed two hours before testing for specimens tested earlier than three days. A set of specimens, one with a nail and one without nails, was tested at the same time. The ages of the overlays were 1, 1 1/2, 2, 3, 4, 7, 14, and 28 days at the time of testing. Compressive cylinder tests were performed on the same day immediately following the push-off tests. Table 6.2 summarizes test preparation. The specimen notation in Table 6.2 was based on slab 4 (high strength base slab), number of nails used across the interface (0 or 1), and age of the overlay at the time of testing (between 1 and 28 days).

6.2.2 Overlay Curing Method: ES-II

The test objective was to evaluate the effect of the two different overlay curing methods on the early age interface shear strength development. The normal strength slab with hard limestone aggregate was used as the base concrete (Table 3.1). The interface was heavily shotblasted and the contact area was 465 cm^2 (72

Table 6.2 Summary of Early Age Test Program: ES-I

Specimen Index	Number of Nails	Contact Area (cm^2)	Average Texture (mm)	Reinforcing Ratio (%)	Age of Overlay (days)
4-1-1D	1	465	0.8	0.19	1
4-1-1DH	1	465	0.8	0.19	1 1/2
4-1-2D	1	465	1.0	0.19	2
4-1-3D	1	465	1.0	0.19	3
4-1-4D	1	465	1.1	0.19	4
4-1-7D	1	465	0.8	0.19	7
4-1-14D	1	465	0.8	0.19	14
4-1-28D	1	465	0.9	0.19	28
4-0-1D	0	465	1.1	--	1
4-0-1DH	0	465	0.9	--	1 1/2
4-0-2D	0	465	0.8	--	2
4-0-3D	0	465	0.9	--	3

Cont'd.

Table 6.2 Summary of Early Age Test Program: ES-I (Cont'd.)

Specimen Index	Number of Nails	Contact Area (cm^2)	Average Texture (mm)	Reinforcing Ratio (%)	Age of Overlay (days)
4-0-4D	0	465	0.9	--	4
4-0-7D	0	465	0.8	--	7
4-0-14D	0	465	1.0	--	14
4-0-28D	0	465	1.0	--	28

Note Specimen notation:

First number: Base slab 4 = high strength slab,
Second number: Number of nails used across the interface (0 or 1),
Third number through fifth letter: Age of overlay in days.

in.^{2}) in all specimens. One nail was always used across the interface. A total of 16 overlays was placed. The 35-day compressive strength of the overlay was 25 MPa (3,600 psi) as shown in Table 6.1. The surface of fresh concrete was covered with white pigmented curing compound at a rate of 3 m^2 per liter (120 sq. ft. per gallon), which is frequently used on BCOs. The compound was sprayed on eight overlays approximately two hours after casting. The curing compound formed a thin continuous film over the overlays which minimized moisture loss. Eight other specimens were continuously moist cured until tested using wet burlap and plastic sheets. One wet-cured (moist cure) and one dry-cured (curing compound) specimens were tested on the same day. Push-off tests were performed when the ages of the overlays were 1/2, 1, 2, 3, 4, 7, 14, and 35 days. Table 6.3 summarizes the tests. The specimen notation in Table 6.3 was based on slab 3 (normal strength slab with hard limestone aggregate), overlay curing method (WT: wet cure, DY: dry cure), and age of overlays at the time of testing (between 12 hours and 35 days).

6.3 Test Results: Interface Strength Development at Early Ages

6.3.1 Effect of Age of Overlays

The bond strength between the base concrete and the overlay is expected to increase with increasing age as the overlay gains strength with time. Test results revealed that good bond developed 24 hours after the overlay placement. The peak shear loads of 62 kN (14 kips) and 66 kN (15 kips) were reached 24 hours after the placement of the overlay in specimens with and without a nail (***4-1-1D*** and ***4-0-1D***). The average of the peak shear loads and the average interface shear stresses at failure of the two specimens were 64 kN (14.5 kips) and 1,370 kPa (200 psi),

Table 6.3 Summary of Early Age Test Program: ES-II

Specimen Index	Number of Nails	Contact Area (cm^2)	Average Texture (mm)	Reinforcing Ratio (%)	Age of Overlay (days)	Overlay Curing Method
3-WT-HD	1	465	0.7	0.19	1/2	M.C. [1]
3-WT-1D	1	465	0.8	0.19	1	M.C.
3-WT-2D	1	465	0.8	0.19	2	M.C.
3-WT-3D	1	465	0.8	0.19	3	M.C.
3-WT-4D	1	465	0.8	0.19	4	M.C.
3-WT-7D	1	465	0.9	0.19	7	M.C.
3-WT-14D	1	465	0.8	0.19	14	M.C.
3-WT-35D	1	465	0.7	0.19	35	M.C.
3-DY-HD	1	465	0.8	0.19	1/2	C.C. [2]
3-DY-1D	1	465	0.8	0.19	1	C.C.
3-DY-2D	1	465	0.8	0.19	2	C.C.
3-DY-3D	1	465	0.8	0.19	3	C.C.

Note 1: M.C. = Moist cure, Cont'd.
2: C.C. = White pigmented curing compound.

Table 6.3 Summary of Early Age Test Program: ES-II (Cont'd.)

Specimen Index	Number of Nails	Contact Area (cm^2)	Average Texture (mm)	Reinforcing Ratio (%)	Age of Overlay (days)	Overlay Curing Method
3-DY-4D	1	465	0.8	0.19	4	C.C. [1]
3-DY-7D	1	465	0.9	0.19	7	C.C.
3-DY-14D	1	465	0.8	0.19	14	C.C.
3-DY-35D	1	465	0.7	0.19	35	C.C.

Note 1: C.C. = White pigmented curing compound,

2: Specimen notation:

First number: Base slab 3 = normal strength slab with hard limestone aggregate,

Second and third letter: Curing method (WT: wet cure, DY: dry cure),

Fourth number through sixth letter: Age of overlay in days.

respectively. Higher interface shear strengths were found in specimens tested later. The peak shear loads of 104 kN (23.5 kips) and 95 kN (21.5 kips) were determined in specimens with and without a nail, respectively, tested three days after overlay placement (***4-1-3D*** and ***4-0-3D***). Test results revealed a rapid initial gain of the interface strength in the first three days.

Moist curing was discontinued three days after casting, and all specimens were then air dried. There was a considerable drop in the interface shear strength in the two specimens tested one day after moist curing stopped. The peak shear load determined in a specimen with a nail (***4-1-4D***) was 81 kN (18 kips) which corresponds to a 22 percent drop in the interface strength when compared to that of a specimen tested on the previous day (***4-1-3D***). The peak shear load determined in a specimen without a nail (***4-0-4D***) was 73 kN (16.5 kips) which again corresponds to a drop of 23 percent when compared to a specimen tested on the previous day (***4-0-3D***). The considerable difference in interface shear strengths between specimens tested three and four days after casting was probably caused by drying shrinkage of overlays.

Interface strengths of the specimens tested four and 14 days after overlay placement were compared. Higher interface strengths were found in specimens tested 14 days after casting. The peak shear loads determined in specimens tested 28 days after casting (***4-1-28D*** and ***4-0-28D***), however, were again considerably lower than those in specimens tested 14 days after casting (***4-1-14D*** and ***4-0-14D***). The peak shear load determined in a specimen with a nail was 61 kN (13.5 kips) after 28 days. There was a drop of 35 percent when compared to a specimen tested after 14 days. The peak shear load of a specimen without a nail was 72 kN (16 kips) after 28 days which corresponded to a drop of 29 percent when compared to a

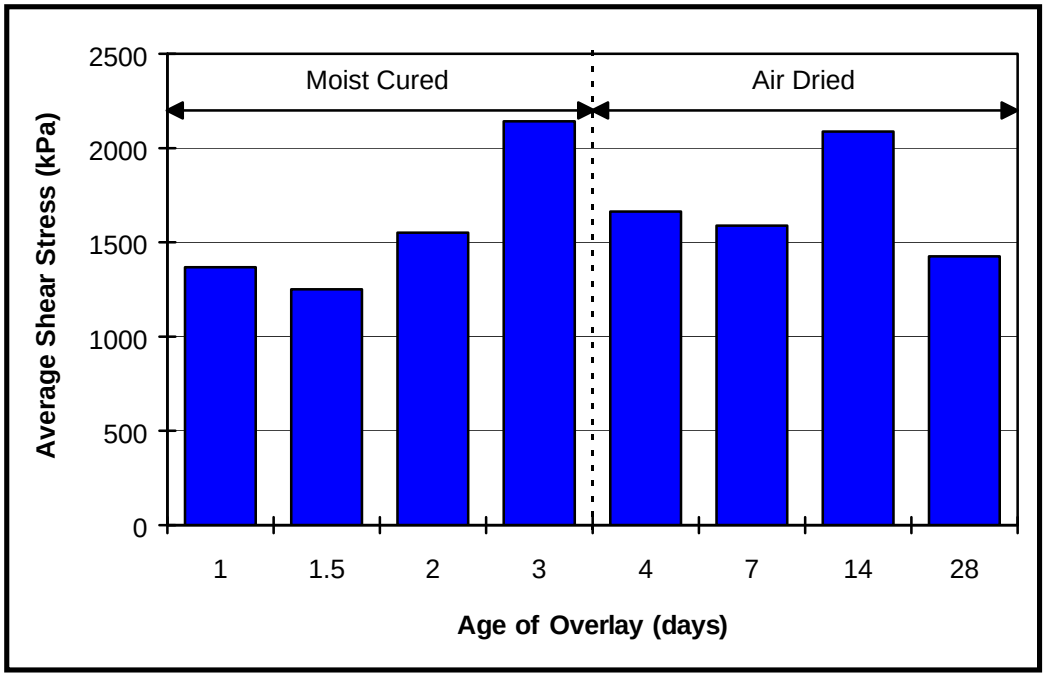

Figure 6.1 Interface Shear Strength Development at Early Ages: ES-I

specimen tested after 14 days. The differences in interface shear strengths between specimens tested 14 and 28 days after the overlay placement are likely caused by drying shrinkage of overlays. Figure 6.1 shows the interface shear strength development at early ages. The bars in Fig. 6.1 represent the results of two tests. The interface strength did not increase with time, but was affected by other factors such as the curing procedure used on the overlays.

6.3.2 Behavior of Specimens with Nail

The shear loads versus overlay displacements of the push-off specimens with a nail tested between one and three days after overlay placement and those of

specimens tested between four and 28 days are shown in Fig. 6.2. The load-displacement plot for a specimen tested 24 hours after casting showed an initial peak (62 kN or 14 kips) at a very small horizontal displacement (0.02 mm or 0.001 in.). The interface shear strength increased in specimens tested later. The highest interface strength (104 kN or 23.5 kips) was reached three days after casting. The interface shear strengths determined in specimens tested later were lower than those after three days as shown in Fig. 6.2 (b). Nails typically pulled-out from the overlay at early ages. A nail pull-out failure from an overlay two days after casting is shown in Fig. 6.3.

6.4 Test Results: Effect of Overlay Curing Method

6.4.1 Interface Strength in Wet-Cured Specimens

The push-off test results of continuously wet-cured specimens and dry-cured specimens are summarized in Tables 6.5 and 6.6. A peak shear load of 27 kN (6 kips) was reached 12 hours after placement of the overlay in a wet-cured specimen (***3-WT-HD***). The average interface shear stress at failure was 580 kPa (85 psi). A considerably higher 75 kN (17 kips) was determined for a specimen tested 24 hours after the overlay placement (***3-WT-1D***). The interface shear stress at failure was 1,610 kPa (235 psi). Test results again indicated the rapid initial interface strength gain for the first three days. The peak shear load of 133 kN (30 kips) was reached three days after overlay placement in ***3-WT-3D***. The interface strength continued to increase with time under wet cure. The highest peak shear load of 156 kN (35 kips) was reached 35 days after casting in ***3-WT-35D***.

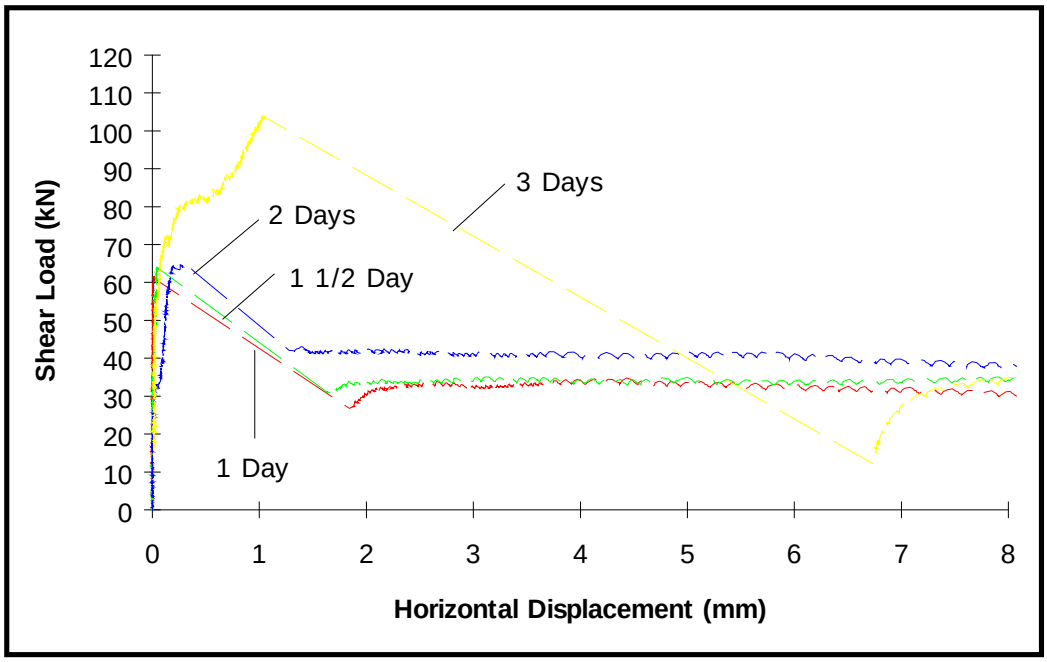

(a) 1 to 3 Days after Casting

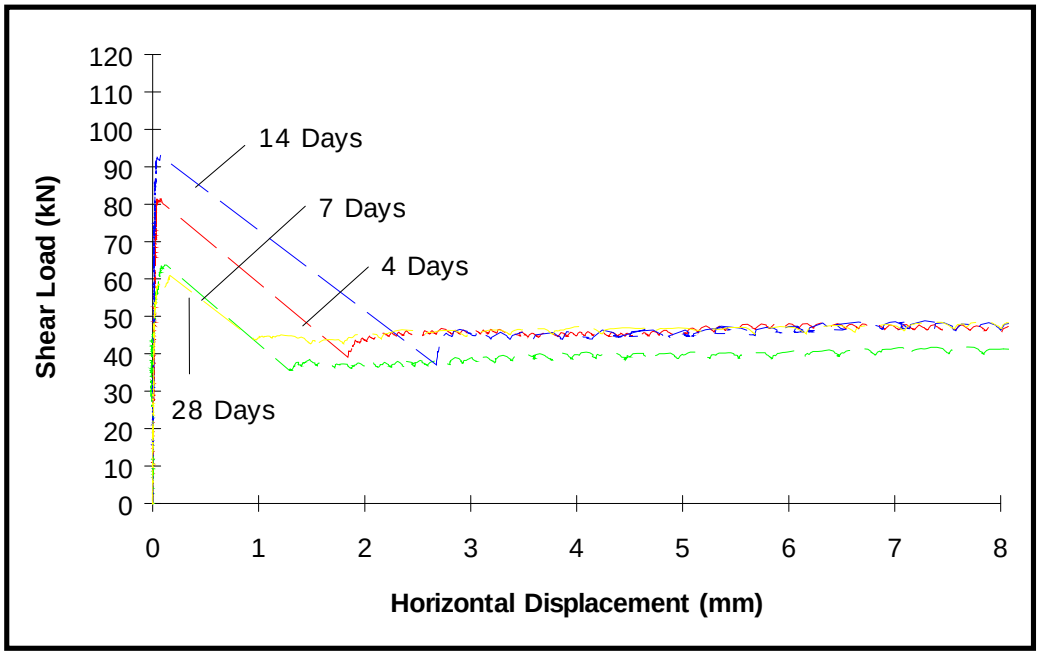

(b) 4 to 28 Days after Casting

Figure 6.2 Interface Strength Development at Early Ages

Figure 6.3 Typical Nail Pull-Out Failure from Overlay at Early Ages

6.4.2 Interface Strength in Dry-Cured Specimens

Peak shear loads of 31 kN (7 kips) and 85 kN (19 kips) were reached 12 and 24 hours after overlay placement, respectively, in the dry-cured specimens (***3-DY-HD*** and ***3-DY-1D***). The average interface shear stresses at failure were 680 kPa (100 psi) and 1,820 kPa (265 psi) after 12 and 24 hours, respectively. Test results indicated rapid initial interface strength gain for the first four days. The highest peak shear load of 126 kN (28.5 kips) was reached four days after casting in ***3-DY-4D***. Interface shear strengths determined in later tests were lower than in a specimen tested four days after casting. A peak shear load of 100 kN (22.5 kips) was reached 35 days after placement of the overlay in ***3-DY-35D*** which corresponds to a drop of 20 percent when compared to that of a specimen tested four days after casting. Test results revealed that the development of the interface shear strength was significantly influenced by the overlay curing method.

6.4.3 Wet Cure vs. Dry Cure

Figure 6.4 shows the effect of the two different overlay curing methods on the interface shear strength development. Test results are shown in terms of the average interface shear stress at failure with time. The interface strength increased continuously in the wet-cured specimens, while the strength gain stopped approximately four days after casting in the dry-cured specimens as shown in Fig. 6.4. The shear load versus overlay displacement plots of all wet-cured specimens are shown in Fig. 6.5. The stiffness in the load-displacement plot at 12 hours was low as shown in Fig. 6.5 (a). The peak shear load was 27 kN (6 kips) at a horizontal slip of 0.2 mm (0.01 in.). The initial peak of a specimen tested 24 hours after casting was associated with a relatively large horizontal displacement. Rapid

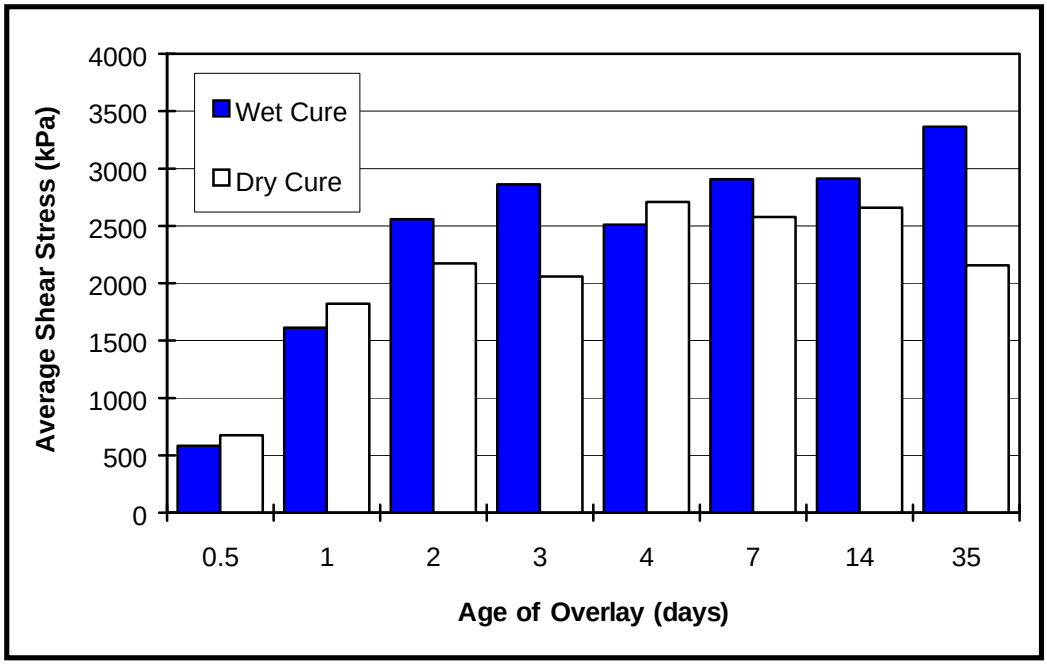

Figure 6.4 Effect of Curing Method: Wet vs. Dry, ES-II

gain of the interface shear strength was observed in specimens tested later. The interface strength kept increasing with the increasing time of the wet cure although the rate of gain was not high after three days. The shear load versus overlay displacement plots of all dry-cured specimens are shown in Fig. 6.6. The rapid initial interface strength gain for the first four days is shown. The load-displacement plot of a specimen tested 12 hours after casting shows no clear initial peak. The overlay begins to slip at a low shear load of approximately 8 kN (1.8 kips). The peak shear load of 31 kN (7 kips) was reached at a large horizontal slip of 1.7 mm (0.07 in.). It must be noted that interface shear failure would have occurred at a much lower shear load without the use of interface shear reinforcement. The initial peak of a specimen tested 24 hours after casting was

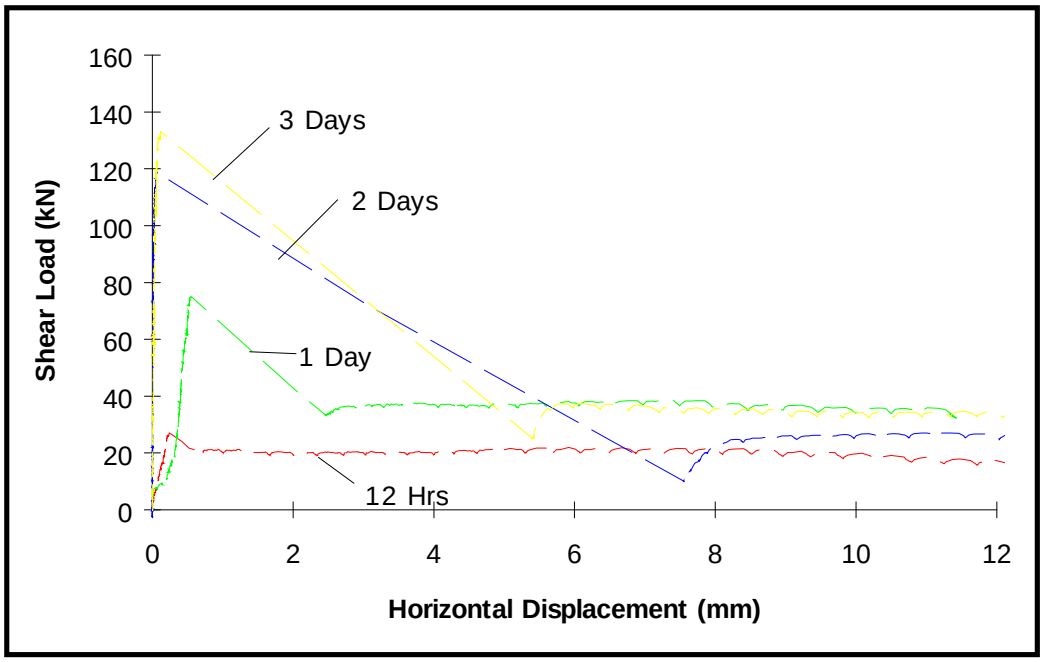

(a) 12 Hours to 3 Days after Casting

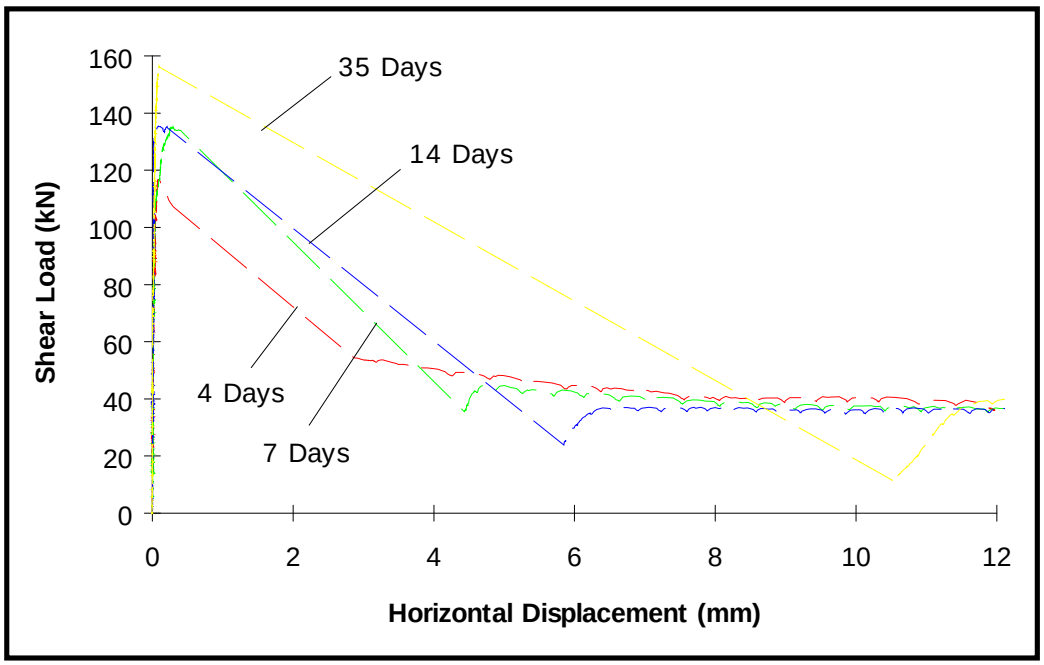

(b) 4 to 35 Days after Casting

Figure 6.5 Effect of Curing Method: Wet Cure

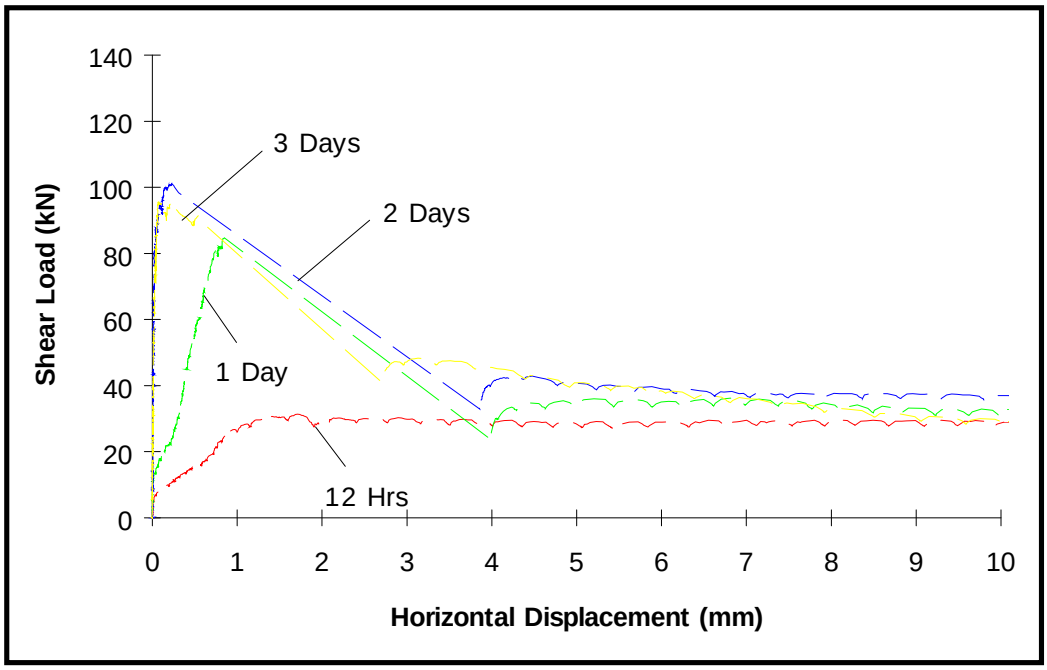

(a) 12 Hours to 3 Days after Casting

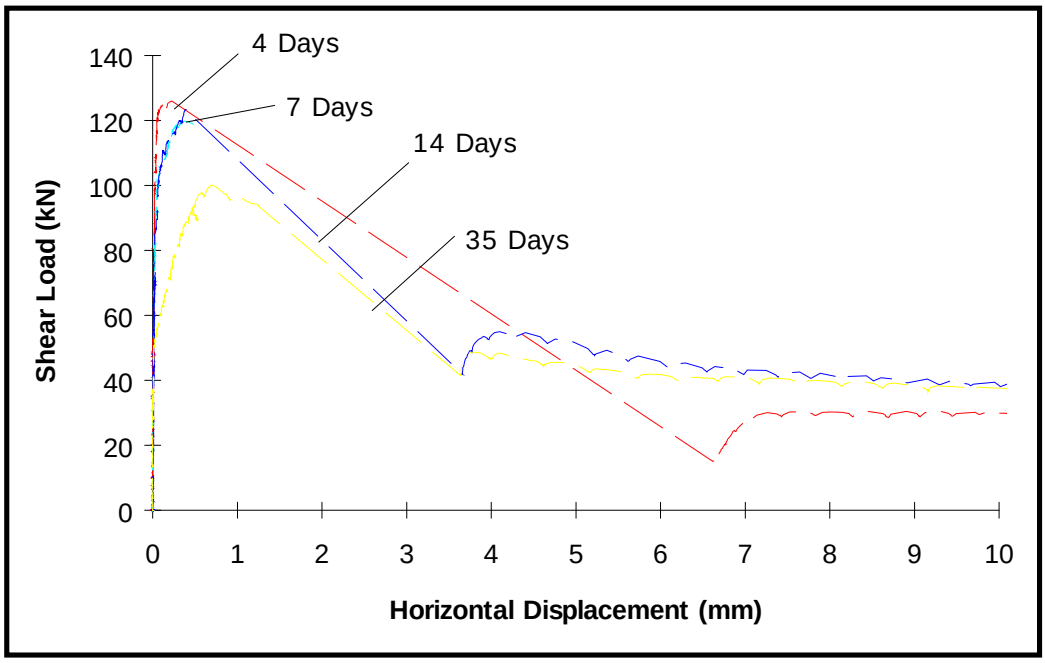

(b) 4 to 35 Days after Casting

Figure 6.6 Effect of Curing Method: Dry Cure

Figure 6.7 Change of Nail Failure Mode with Time

again associated with a relatively large horizontal displacement of the overlay. The highest peak shear load of 126 kN (28.5 kips) was reached four days after casting. Part of the plot after the peak is not shown for a specimen tested seven days after casting due to a measurement error. Nails typically failed by being pulled-out of the overlay at early ages while they failed by being pulled-out from the base concrete at later ages as shown in Fig. 6.7.

6.5 Conclusions

The early age push-off tests lead to the following conclusions:

1. Good bond developed 24 hours after overlay placement. Test results show that the shear strength of the bonded-rough interface was 1,370 kPa (200 psi) or higher 24 hours after casting,
2. Overlay delamination can initiate within the first 48 hours after overlay placement. Shear load versus displacement plots showed that overlay slipped at low shear loads for specimens tested 12 and 24 hours after the overlay placement,
3. The post peak shear resistance of the nails in specimens tested within the first 48 hours after casting was not as high as those tested 48 hours after casting,
4. The interface strength increased with time when the overlay was continuously moist cured. The rate of the strength gain was high during the first three days,
5. Test results indicated that good curing procedures of the overlays at early ages, especially for the first three days when the interface strength gain is high, resulted in higher interface shear strengths, and

6. The development of interface strength was significantly influenced by the overlay curing method. The interface strength began to decrease shortly after stopping moist curing. Tests show that the interface shear strength dropped approximately 23 percent one day after the removal of the moist cure.

CHAPTER SEVEN
BEAM TESTS FOR STATIC AND FATIGUE INTERFACE STRENGTH - EXPERIMENTAL PROGRAM AND TEST RESULTS

7.1 Introduction

Highway pavements are typically subjected to traffic producing high cycle fatigue under wheel loading. Flexural cracks develop in pavement slabs during service life since the flexural strength of concrete in fatigue is significantly lower than the static flexural strength (Stelson and Cernica 1958, Hilsdorf and Kesler 1966). Deterioration of the interface bond between the two concrete layers by fatigue loading in shear can be expected in bonded concrete overlays which may lead to the loss of composite action. The load-displacement plot determined for a push-off test specimen subjected to several loading and unloading cycles (Fig. 5.17), for example, suggested cumulative interface damage due to the cyclic loading. The possible loss of composite action due to deterioration of interface strength subjected to fatigue loading was studied in the composite beam tests. The test preparation and the results of tests are described in this chapter.

7.2 Research Scope and Objectives

The performance of the composite beam test specimens subjected to static and fatigue loading was examined. The research objectives were:

1. Determine the interface strength deterioration of composite beams subjected to the fatigue loading,
2. Determine the advantages of using jumbo nails in terms of composite action,
3. Evaluate the fatigue performance of unbonded overlays with nails, and
4. Compare interface strengths determined using push-off tests and composite beam static tests.

7.3 Preparation for Beam Tests

7.3.1 Beam Test Setup

The composite beam test setup was designed so that the interface could be subjected to shear stresses by application of the vertical force on a simple beam. The cross-sectional dimensions of the composite beams were selected to represent those of the typical bonded concrete overlays. The depths of the overlay and the base beam were 100 mm (4 in.) and 200 mm (8 in.), respectively. The beam had to be relatively wide (460 mm or 18 in.) to eliminate the possibility of tensile splitting cracks in the base beam due to nail driving. The span length of the beam was 1.83 m (72 in.). A composite test beam is shown in Figs. 7.1 and 7.2. The plan view of the beam in Fig. 7.1 (a) shows the location of interface contact region. The area other than the contact surface was unbonded using 5-mm- (3/16-in.-) thick foam core board which was also used for the push-off tests. A single line load was applied on top of the overlay at the beam midspan. The shallow saw cut shown in Fig. 7.1 (a) served as a flexural crack inducer. The neutral axis (N.A.) of the uncracked section was in the base beam in Fig. 7.1 (b). The neutral axis moved

into the overlay after development of flexural cracks. Figure 7.2 shows the equilibrium of forces acting on a cracked half beam. A couple consisting of the compression (***C***) and the tension forces (***T***) acting on the overlay and on the longitudinal reinforcing steel is shown in Fig. 7.2 (a). The shear force acting on the interface equals the compression force acting on the overlay or the sum of the tension forces in the reinforcing steel shown in Fig. 7.2 (c). It was assumed that friction between the two concrete layers in the unbonded region would be very small and could be neglected. The average interface shear stress can be quantified by measuring the strains in the longitudinal reinforcing steel, finding the tension force, and dividing by the interface area:

$$\tau = \frac{C}{ab} = \frac{T}{ab} \qquad (7.1)$$

where a = length of interface (380 mm or 15 in.) and b = width of interface (125 mm or 5 in.).

7.3.2 Preparation of Beam Specimens

Figure 7.3 (a) shows the steel cages made for the base beams. Five U.S. # 4 bars (diameter = 13 mm or 0.5 in.) were used for the longitudinal reinforcement. The longitudinal reinforcing steel was designed to produce 290 kN (65 kips) interface shear force or 6,000 kPa (870 psi) average interface shear stress at yield. The middle 250-mm (10-in.) portion on three reinforcing bars was unbonded as shown in Figs. 7.1 (a) and 7.3 (b). Strain gages were installed on the bars in the unbonded region. Relatively heavy shear stirrups were used to provide beam shear strength.

(a) Reinforcing Steel

(b) Strain Gage Installation

Figure 7.3 Base Beam Reinforcement

Six base beams were cast at the same time. V-shaped grooves were created on the top surface of two base beams while the concrete was still fresh to produce very rough grooved interfaces. The maximum texture depth was approximately 6 mm (0.25 in.). Two other beams had relatively smooth trowel finished interfaces. The interfaces of all other beams were heavily shotblasted so that the texture closely resembled that of typical bonded concrete overlays. The contact area was 475 cm^2 (75 $in.^2$) on each side of the beam. One or two jumbo nails were used across the interface on each side of eight composite beams to provide interface shear reinforcement ratios of 0.18 percent and 0.36 percent, respectively. Figures 7.4 (a) and (b) show the interface preparation before overlay placement for the beams with heavy shotblasting and two nails and for beams with V-shaped grooves and no nails. Two thin layers of general purpose grease were applied to the heavily shotblasted contact surfaces of two base beams to create unbonded interfaces. The second group of six beams was constructed in a similar manner. One monolithically cast beam (a beam with a depth equal to the beams with overlays) was made when the second group of beams was made. A reduced shear section was created by inserting a horizontal foam core board template during concrete placement when the concrete lift reached 200 mm (8 in.) measured from the bottom of the form. The "monolithically" cast beam served as a control beam.

7.3.3 Materials

7.3.3.1 Reinforcing Steel The stress versus strain relationship of the reinforcing steel was determined from coupon tests. A typical stress versus strain plot is shown in Fig. 7.5. The yield strength of the reinforcing steel was 450 MPa (65 ksi). The stiffness was 200,000 MPa (29,000 ksi). Four stress versus strain

(a) Heavy Shotblasting

(b) V-Shaped Grooves

Figure 7.4 Interface Preparation for Beam Tests

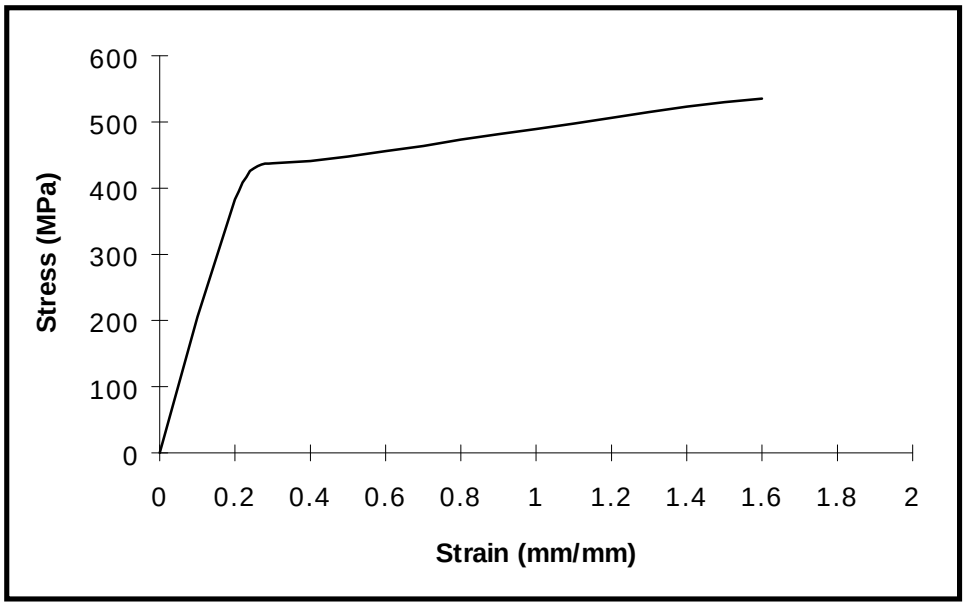

Figure 7.5 Stress vs. Strain: Reinforcing Steel

plots were used to determine the tension force in the reinforcing steel based on strain readings.

7.3.3.2 Concrete The properties of the concrete used for the base beams and the overlays are shown in Table 7.1. The maximum size of the river gravel aggregates used for both the base beams and the overlays was 20 mm (3/4 in.). The base concrete was moist cured under wet burlap and plastic sheets for seven days. Overlays were cured under a plastic sheet for three days. The compressive strength of the overlays was similar to that of the base beams as shown in Table 7.1. An attempt was made to achieve similar compressive strengths for the base beams and the overlays between the first and the second batches although there were some differences as indicated in Table 7.1. The difference in concrete strengths between the two different batches was too small to significantly affect the test results.

Table 7.1 Compressive Strength and Aggregate Types

Batch No.	Aggregate Type	28-Day Compressive Strength (MPa)	Remarks
1	River gravel	36	Base beams
	River gravel	38	Overlays
2	River gravel	31	Base beams
	River gravel	33	Overlays

7.3.4 Test Procedure

Five composite beams were tested statically until interface delamination was observed. Seven composite beams and one monolithically cast beam were subjected to two to three million cycles of load. Table 7.2 summarizes the beam tests. The specimen notation was based on interface type (M: monolithic, V: grooved, H: heavy shotblasting, N: smooth trowel finish), number of nails used in each interface (0, 1, or 2), presence of the bond (B: bonded, U: unbonded), and replicate number.

7.3.4.1 Beam Static Test A vertical line load was applied slowly at the beam midspan until interface delamination was observed. The loading rate was approximately 4.5 kN (1 kip) per minute. Interface shear stresses were determined using two different methods: (1) direct measurement of the strains in the longitudinal reinforcing steel (Eq. 7.1) and (2) the shear formula (Eq. 2.2). The

shear formula, which was used in many previous studies (Hanson 1960, Saemann and Washa 1964, Badoux and Hulsbos 1967), is based on an uncracked beam section. It must be noted that the interface shear stresses of the beams determined by Eq. 2.2 are probably not correct because of the cracked beam section and the presence of discontinuities along the interface (interface not continuously bonded as shown in Fig. 7.1). The shear formula was used in an attempt to draw comparison between the current and previous studies.

7.3.4.2 Beam Fatigue Test Sinusoidal cyclic loading was applied at the beam midspan on top of the overlay for all beams subjected to up to three million fatigue cycles. Testing frequency was 6 Hz. The average vertical load and the loading amplitude were typically 56 kN (12.5 kips) and 24 kN (5.5 kips), respectively, with a maximum of 80 kN (18 kips) and a minimum of 32 kN (7 kips). The interface shear stresses typically ranged between 2,000 kPa (290 psi) and 860 kPa (125 psi) during cycling. Interface shear stresses during cycling were much higher in magnitude than those in bonded concrete overlays subjected to typical traffic wheel loads which were suggested by Metzinger (1990) to be approximately 280 kPa (40 psi). High shear stresses were applied in an attempt to accelerate interface deterioration. Cycling was stopped two times during each one million cycles. Beam midspan deflection, reinforcing steel strains, and interface slips were measured to determine deterioration of composite action as the beams were statically loaded to the maximum fatigue load (80 kN).

7.3.4.3 Post-Fatigue Static Test All beams tested in fatigue were subjected to post-fatigue static tests after cycling. Beams were statically loaded until interface delaminations were observed. The post-fatigue static tests were performed to determine the extent of interface strength deterioration by cycling.

7.3.5 Testing Equipment and Instrumentation

The Material Testing System (MTS) had a fatigue-rated capacity of 250 kN (55 kips). Static load, loading amplitude, and cyclic frequency were controlled by a servo-controller. The output jack of the servo-controller was connected to a PC based data acquisition system. The beam midspan deflection was monitored using a linear potentiometer with 0.025 mm (0.001 in.) accuracy supported on a stand beneath the base beam. Interface slips between the overlay and the base beam were monitored using dial gages with 0.0025 mm (0.0001 in.) accuracy and linear potentiometers as shown in Fig. 7.6. A dial gage and a linear potentiometer were installed at each end of the beam. Signals from the servo-controller, strain gages, and potentiometers were recorded at a sampling rate of 20 data sets per second.

Figure 7.6 Interface Slip Measurement

7.4 Beam Static Test Results

7.4.1 Interface Shear Strength

Specimens ***V0B-1*** with very rough grooved interfaces and no jumbo nails and ***H1B-2*** with rough heavily shotblasted interfaces and one jumbo nail across the interface were tested first. Each beam was preloaded before the static test to produce flexural cracks which initiated at the beam bottom fibers and progressed upward typically ending in the overlay as shown in Fig. 7.7. Test results are summarized in Table 7.3. Applied load versus beam midspan deflection and load versus strains in the longitudinal reinforcing steels are shown in Figs. 7.8 (a) and (b). Initial flexural stiffness and development of reinforcing steel strains in the two beams were similar. The interface on one end of ***V0B-1*** delaminated at an applied load of 202 kN (45 kips). The interface shear stress was 5,930 kPa (860 psi) at failure based on strain readings. The shear stress was 3,400 kPa (495 psi) based on the shear formula which is only 57 percent of that determined directly by the strain readings. A sudden delamination failure was observed. The loss of composite section caused by the interface delamination forced the base beam to support the applied load. The deflection of the beam increased rapidly indicating failure. No delamination failure developed in ***H1B-2*** under vertical load which reached 209 kN (47 kips). The interface shear stress was 6,070 kPa (880 psi) at the maximum load based on strain readings. The interface slips on each side of the beam remained vary small as indicated in Table 7.3. Test results indicated that the bars yielded.

The interface shear strength of ***V0B-1*** (5,930 kPa or 860 psi) based on strain readings was significantly higher than typical interface strengths of 2,760 kPa (400

Figure 7.7 Flexural Cracking after Preloading

psi) reached in push-off specimens with a bonded-rough interface. It was suspected that the interfaces might be subjected to a compression force during the test due to the presence of the highly flexible foam core board used as the bond breaker. The presence of the compression force acting on the interface along with the shear force can result in a stronger interface (Mattock and Hawkins 1972, Valluvan 1993).

It was decided to modify the test beams. The purpose was to ensure that the compression force did not interact with the shear force. Two 100-mm- (4-in.-) deep saw cuts were made across the full width of the overlay at the beam center. The distance between the two saw cuts was 150 mm (6 in.). The center 150-mm portion of the overlay and the underlying foam core board were completely removed, and the space was filled with concrete or the hydrostone mortar capable

of sustaining

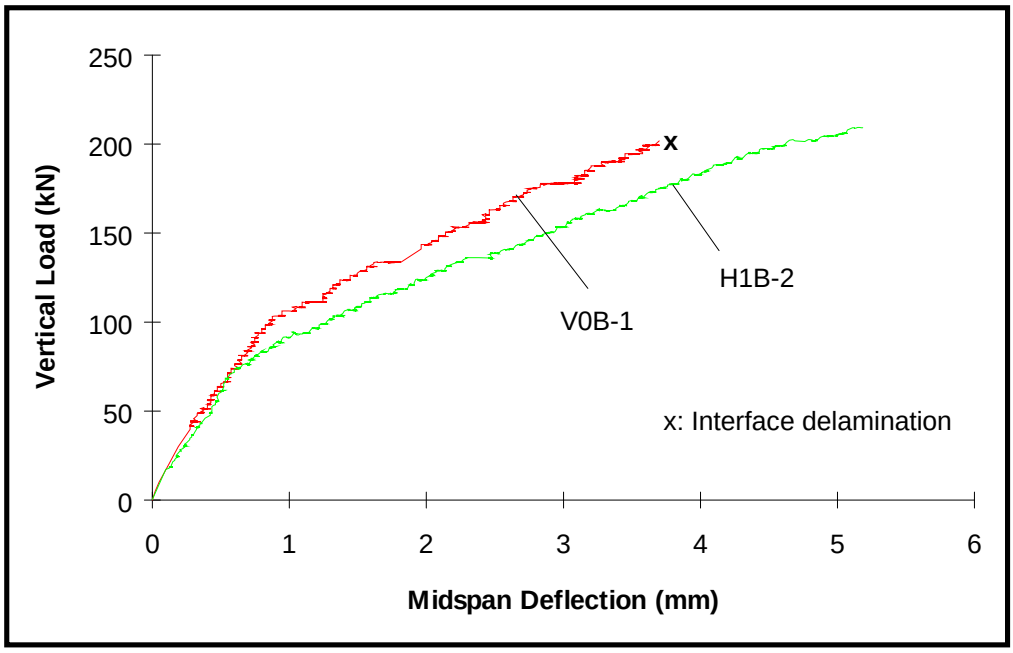

(a) Load vs. Deflection

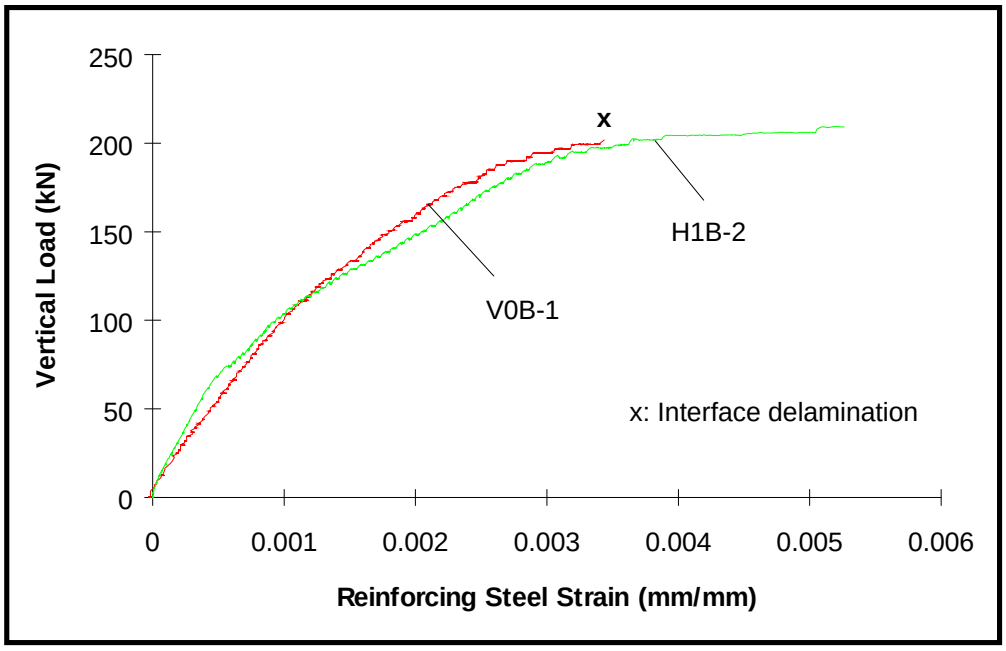

(b) Load vs. Reinforcing Steel Strain

Figure 7.8 Beam Static Tests: ***V0B-1***, ***H1B-2***

(a) Interface Delamination

(b) Failed Interface

Figure 7.9 Beam Static Test: ***V0B-1***

Figure 7.10 Test Beam for Direct Compression Transfer to Base Beam

the high compression stresses. All eleven remaining beams were modified. Figure 7.10 shows a modified beam.

Test results of the three modified composite beams are shown in Fig. 7.11. Two beams, ***V0B-2*** and ***H0B-2***, had grooved and heavily shotblasted interfaces, respectively, with no nails while the third beam, ***N1B-2***, had relatively smooth troweled interfaces with one nail across the interface on each side of the beam. The load versus beam midspan deflection plots in Fig. 7.11 (a) show that the initial flexural responses of the two composite beams with the rough interfaces were similar. ***V0B-2*** which had rougher interfaces was capable of maintaining composite section under higher vertical loads. Interface delaminations were observed in both tests. The delamination occurred at a vertical load of 205 kN (46

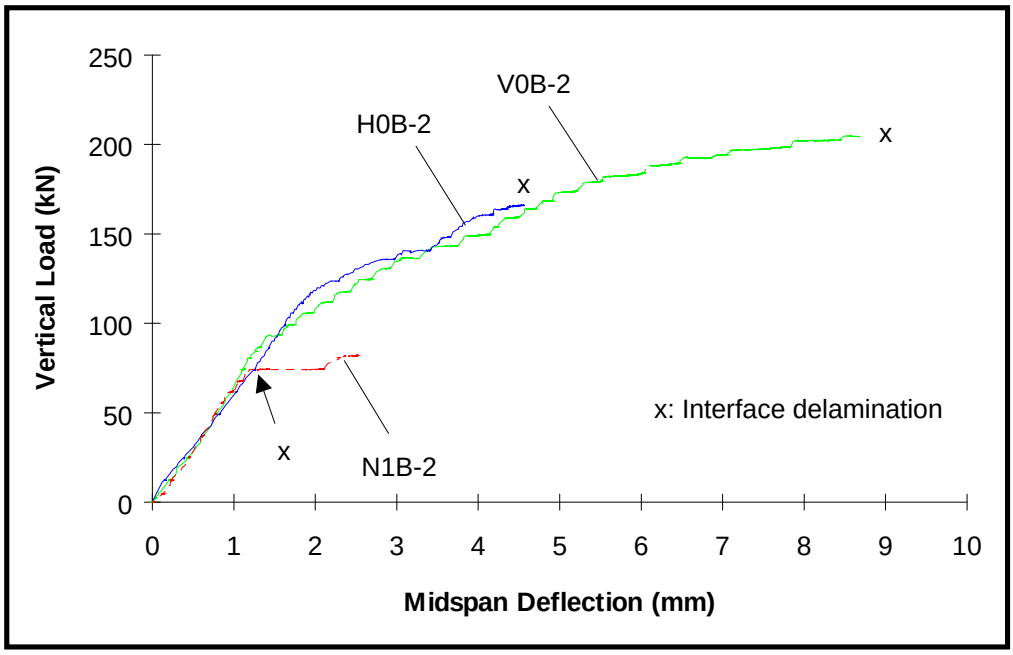

(a) Load vs. Deflection

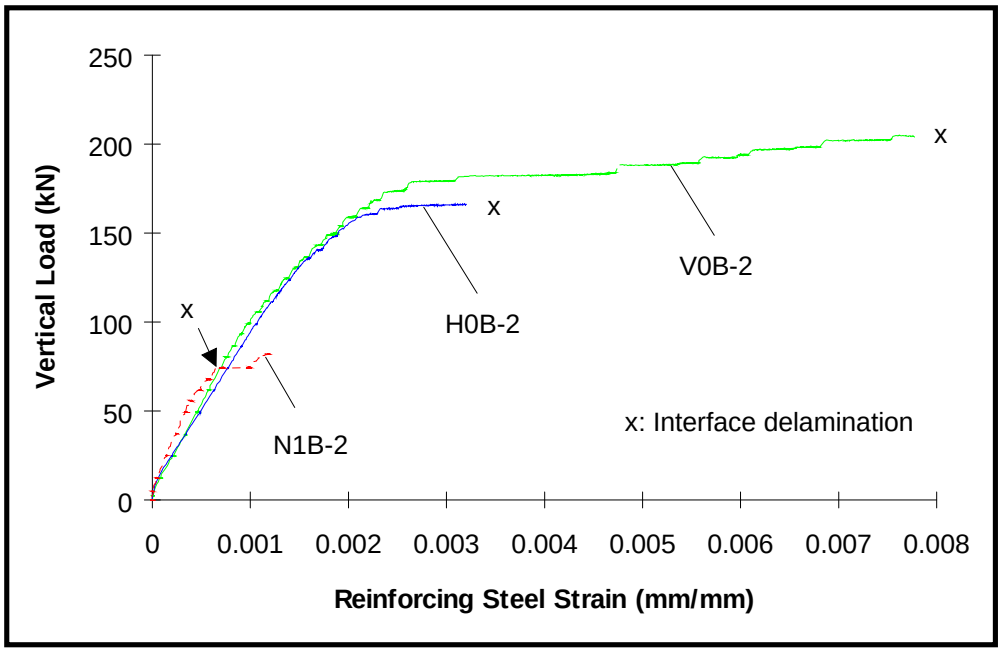

(b) Load vs. Reinforcing Steel Strain

Figure 7.11 Beam Static Tests: ***V0B-2***, ***H0B-2***, and ***N1B-2***

kips) in ***V0B-2***. The interface shear stress at failure was 6,350 kPa (920 psi) and 3,450 kPa (500 psi) based on strain readings and the shear formula, respectively. The interface delamination occurred at a lower load (166 kN or 37 kips) in ***H0B-2*** than in ***V0B-2***. The interface shear stress at failure was 5,910 kPa (860 psi) and 2,790 kPa (405 psi) based on strain readings and the shear formula, respectively. The interface slips at failure were on the order of 0.4 mm (0.015 in.). The load versus reinforcing steel strain plots in Fig. 7.11 (b) also show that the responses of the two composite beams were similar until interface delamination occurred in ***H0B-2***. The interfaces were inspected after tests. The shear failure plane was partly in the base beam in ***V0B-2*** which indicated the development of the excellent bond with the very rough grooved interface as shown in Fig. 7.12. The structural behavior of the modified beams was not significantly different from that of the unmodified beams.

Test results of ***N1B-2*** which had a relatively smooth troweled interface are also shown in Fig. 7.11. A significantly different flexural behavior was obtained. Interface delamination occurred at a significantly lower vertical load when compared with those of the composite beams with the rougher interfaces. The interface delamination occurred at a load of 74 kN (16.5 kips). ***N1B-2*** was unloaded after the initial delamination occurred and then reloaded. The two different loading curves are shown in Fig. 7.13 which indicate the loss of composite action due to the delamination. The vertical load versus interface slips are plotted in Fig. 7.14 for the initial loading and the reloading, respectively. The interface slip at failure was 0.15 mm (0.006 in.) on the west end in the initial loading. The slip suddenly increased after the delamination occurred even though the jumbo nail resisted further slip at some point in the loading as shown in Fig. 7.14 (a). Figure 7.14 (b) shows that the slip at the west end, which was already delaminated,

(a) Base Beam

(b) Overlay

Figure 7.12 Partial Failure in Base Beam: ***V0B-2***

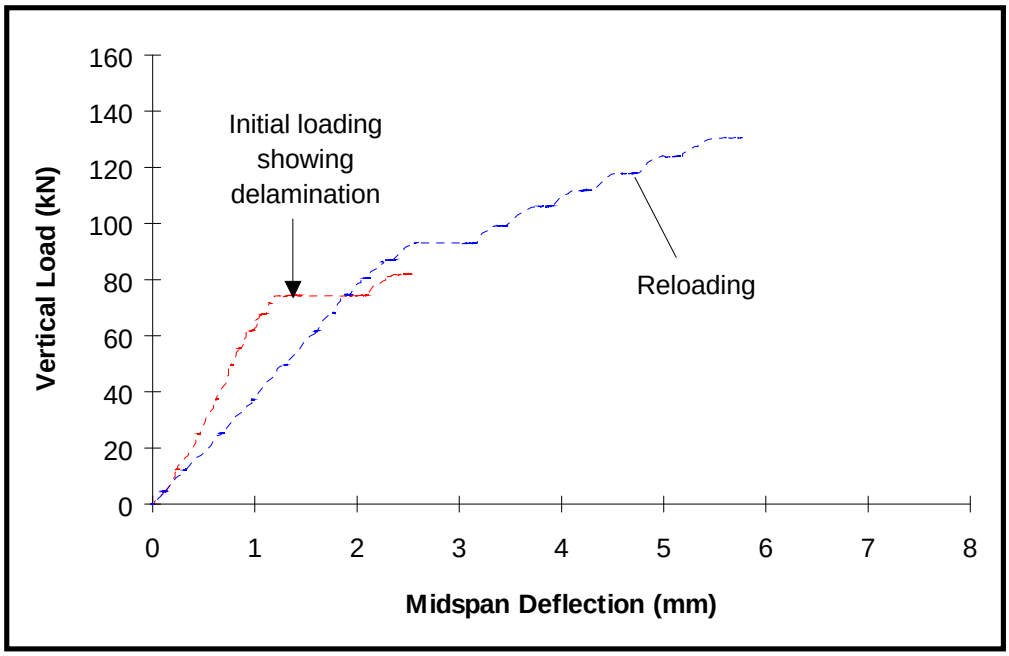

(a) Load vs. Deflection

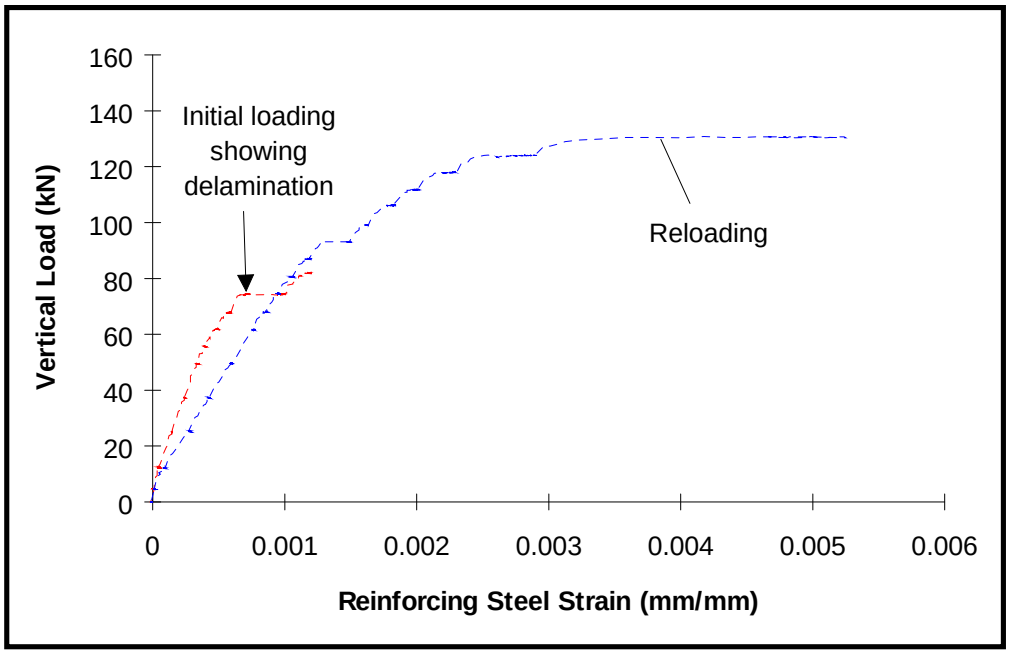

(b) Load vs. Reinforcing Steel Strain

Figure 7.13 Static Beam Test: ***N1B-2***

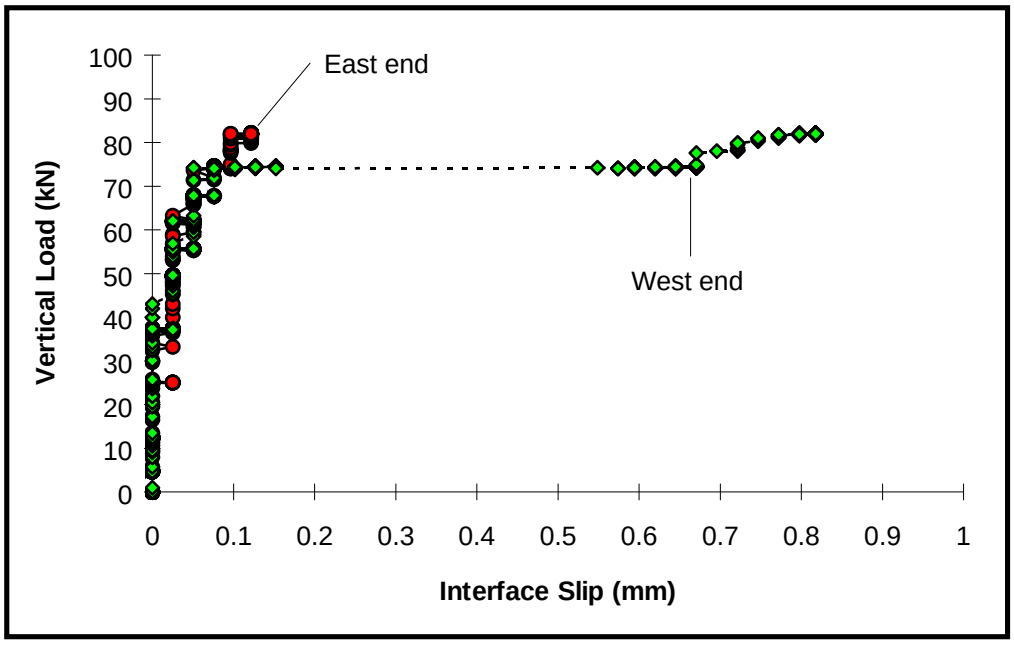

(a) Initial Loading

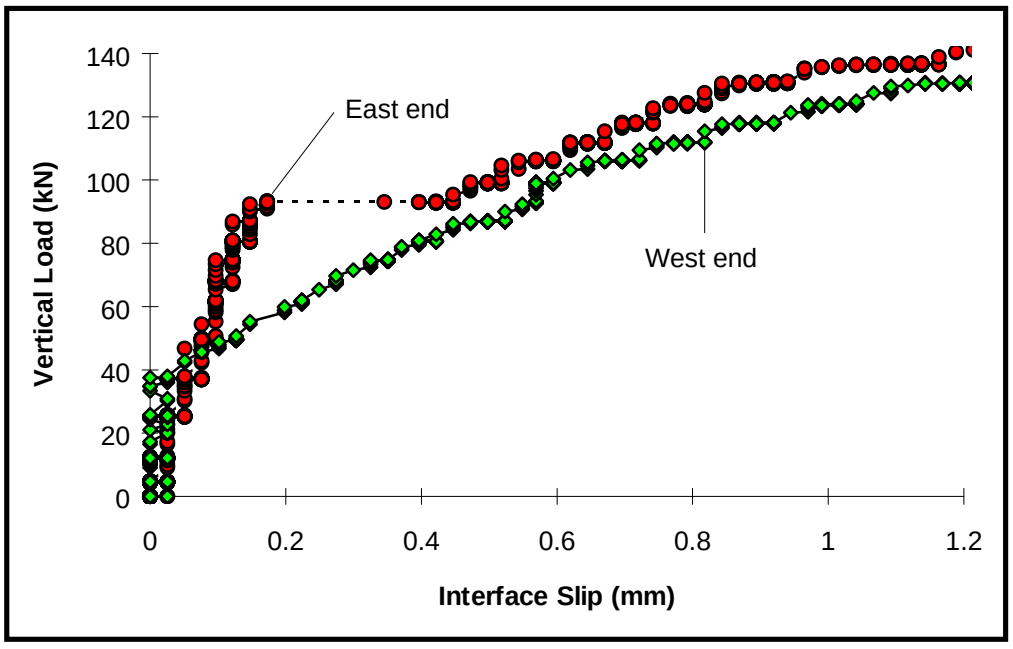

(b) Reloading

Figure 7.14 Load vs. Interface Slip: ***N1B-2***

increased under reloading. The interface at the east end also delaminated during reloading when the vertical load reached 93 kN (21 kips). The interface slip was 0.15 mm when the delamination occurred. The effect of delamination at the east end is also shown in Fig. 7.13 where the beam midspan deflection and the reinforcing steel strain suddenly increased at a vertical load of 93 kN.

7.4.2 Beam Static Test: Discussion of Test Results

The interface shear strength determined based on strain readings was significantly higher in the beam static tests than the typical interface strength of push-off specimens with a bonded-rough interface. One possibility is that the interface shear strengths determined from push-off tests are lower than those determined by the beam static tests because of tensile stresses acting on the interface along with shear. Tensile stresses are produced in the in-situ push-off tests due to an eccentricity of 20 mm (3/4 in.) between the applied loads and the interface shown in Fig. 4.3 and discussed in Chapter Four.

The shear formula was used to allow comparisons between the current study results and previously published test data. Hanson (1960), for example, after experimentally studying T-shaped girders and push-off specimens, concluded that the push-off tests gave a good representation of the character of the stress-slip curves for the girders tested. The interface shear strengths determined based on the shear formula were similar to the push-off test results in the current study. The interface shear strengths determined from direct strain measurements, however, appear to be more accurate and should be used to determine the interface shear strength.

7.5 Beam Fatigue Test Results

7.5.1 Control Beam

A monolithically cast beam, ***M0-1***, was subjected to three million fatigue cycles. Test results are summarized in Table 7.4 in terms of beam midspan deflections, reinforcing steel strains, and shear stresses at the reduced shear section. Table 7.4 shows that the reinforcing steel strain increased very slowly with increasing load cycles. The beam midspan deflection also increased slowly from 0.9 mm (0.035 in.) at the initial loading to 1.1 mm (0.045 in.) after cycling. The interface slips, however, remained less than 0.1 mm (0.004 in.) throughout fatigue cycling which suggests that there was no deterioration of the interface strength. Test results of ***M0-1*** revealed that the strength of the artificially created interface (reduced shear section) was unaffected by repeated shear loading with an applied shear stress on the order of 2,000 kPa (290 psi).

7.5.2 Beams with Bonded-Rough Interfaces

Four composite beams with bonded-rough interfaces were subjected to approximately three million fatigue cycles. The interfaces of all four beams were heavily shotblasted. No jumbo nails were used for ***H0B-1***. One nail was used across the interface on each side of ***H1B-1***. Two nails were used on each end of the two other beams, ***H2B-1*** and ***H2B-2***. Test results of ***H0B-1*** are shown in Fig. 7.15. The vertical load versus beam midspan deflection and the load versus reinforcing steel strain are shown in Fig. 7.15 for the initial loading and the static loading after 1 million, 2 million, and 3.1 million cycles. The mean vertical load and the loading amplitude were 36 kN (8 kips) and 24 kN (5.5 kips), respectively, during the first

Table 7.4 Fatigue Test Results: ***M0-1***, Values at 80 kN Vertical Load

Number of Cycles (x 1,000)	Reinforcing Steel Strain (%)	Midspan Deflection (mm)	Max. Interface Stress (kPa) by	
			Shear Formula	Strain Gages
0	0.080	0.9	1,350	2,130
500	0.075	1.0	1,350	2,000
1,000	0.077	1.1	1,350	2,050
1,500	0.077	1.0	1,350	2,050
2,000	0.078	1.1	1,350	2,080
2,500	0.081	1.1	1,350	2,160
3,000	0.082	1.1	1,350	2,190

one million cycles. The mean vertical load was later increased to 56 kN (12.5 kips) with no change in the loading amplitude which resulted in a maximum load of 80 kN (18 kips) and the minimum of 32 kN (7 kips). The beam deflection and the reinforcing steel strain did not change significantly after cycling in Fig. 7.15. The interface slip remained less than 0.1 mm (0.004 in.) when the interfaces were subjected to 2,210 kPa (320 psi) repeated shear stresses during cycling. The interface strength was not influenced by cycling based on beam deflection, reinforcing strain, and interface slip readings. Test results of ***H2B-1*** are shown in Fig. 7.16. Test results are shown for the initial loading and the static loading after 1 million, 1.8 million, and 3 million cycles, respectively. The reinforcing steel

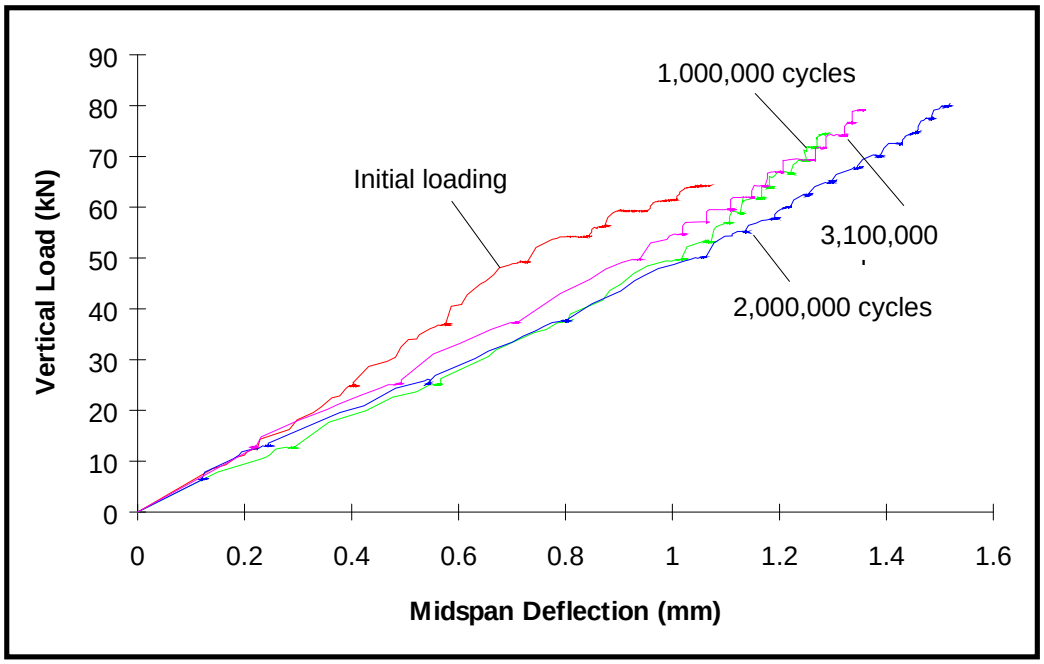

(a) Load vs. Deflection

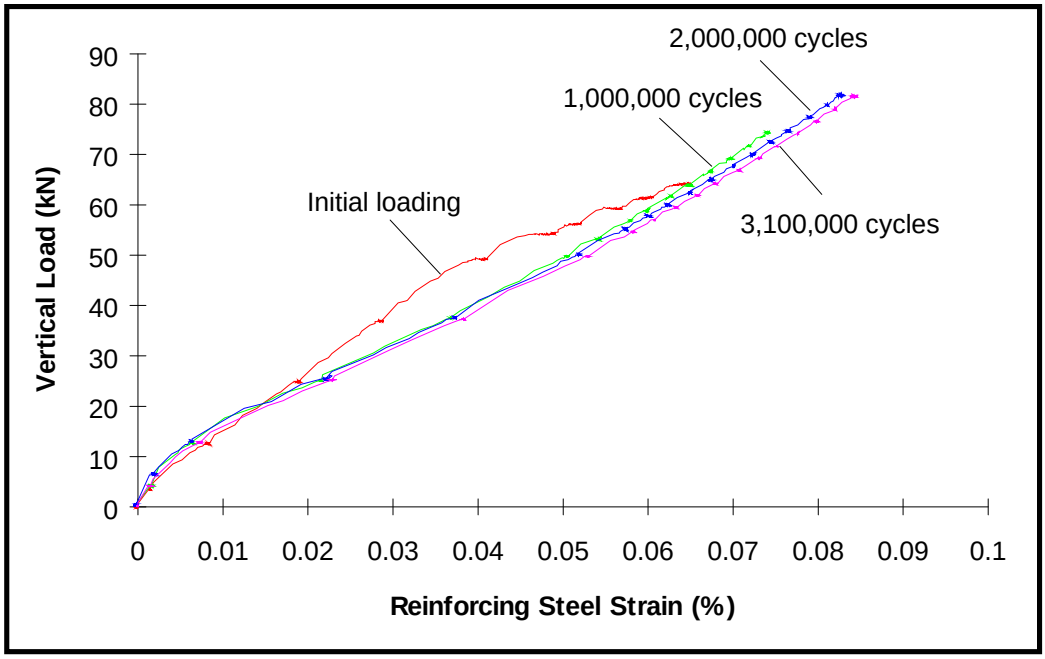

(b) Load vs. Reinforcing Steel Strain

Figure 7.15 Beam Fatigue Tests: ***H0B-1***

Table 7.5 Fatigue Test Results: ***H0B-1***, Values at 80 kN Vertical Load

Number of Cycles (x 1,000)	Reinforcing Steel Strain (%)	Midspan Deflection (mm)	Max. Interface Stress (kPa) by	
			Shear Formula	Strain Gages
0 [a]	0.058	1.0	1,030	1,550
1,000 [b]	0.073	1.3	1,230	1,950
1,500	0.081	1.4	1,350	2,160
2,000	0.082	1.5	1,350	2,190
2,500	0.083	1.3	1,350	2,210
3,100	0.083	1.4	1,350	2,210

Note a: Values at vertical load of 60 kN,
b: Values at vertical load of 73 kN.

strains remained almost the same after cycling. The beam deflection slowly increased with increasing number of cycles probably due to the development of additional flexural cracks. Interface slips remained very small, on the order of 0.05 mm (0.002 in.), during cycling. Test results indicate that no significant interface deterioration occurred after three million fatigue cycles. Table 7.6 summarizes the test results of ***H2B-1***. Similar observations were made from the fatigue tests of the two other composite beams, ***H1B-1*** and ***H2B-2***. The beam midspan deflections, reinforcing steel strains, and interface slips did not change significantly after approximately three million fatigue cycles.

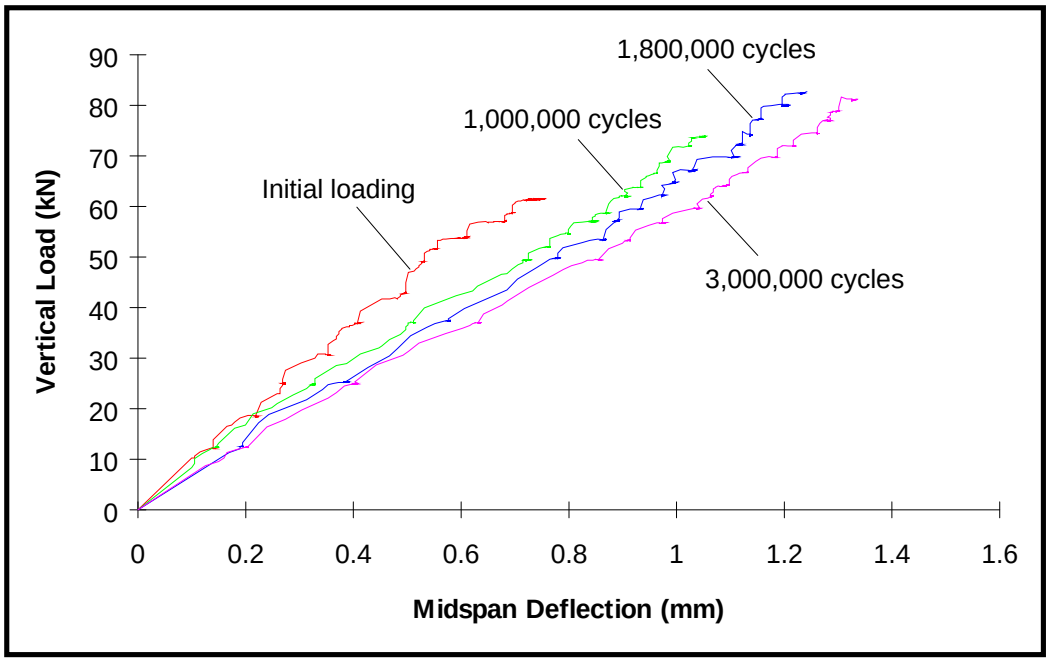

(a) Load vs. Deflection

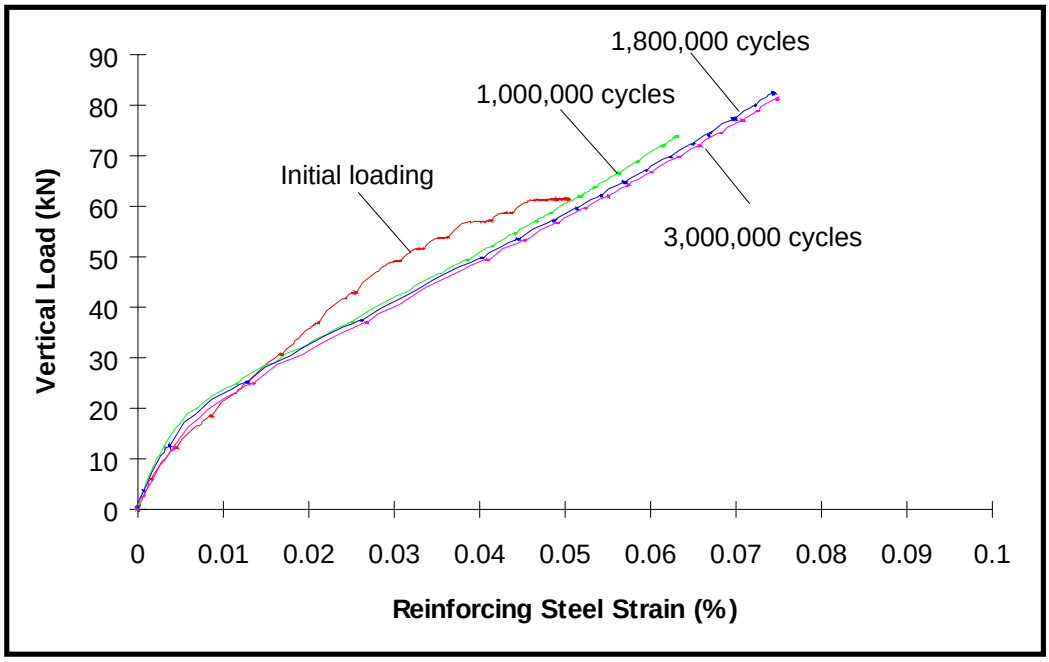

(b) Load vs. Reinforcing Steel Strain

Figure 7.16 Beam Fatigue Tests: ***H2B-1***

Table 7.6 Fatigue Test Results: ***H2B-1***, Values at 80 kN Vertical Load

Number of Cycles (x 1,000)	Reinforcing Steel Strain (%)	Midspan Deflection (mm)	Max. Interface Stress (kPa) by	
			Shear Formula	Strain Gages
0 [a]	0.045	0.7	1,030	1,200
1,000 [b]	0.063	1.0	1,230	1,680
1,250	0.070	1.2	1,350	1,870
1,800	0.073	1.2	1,350	1,950
2,300	0.074	1.3	1,350	1,970
3,000	0.073	1.3	1,350	1,950

Note a: Values at vertical load of 60 kN,
b: Values at vertical load of 73 kN.

7.5.3 Beam with Bonded-Smooth Interfaces

N1B-1 had smooth troweled interfaces. One jumbo nail was used across the interface on each side of the beam. The interface strengths were very low and, although both interfaces failed during the preloading, loading was applied for approximately two million cycles. Test results are shown in Fig. 7.17 for initial loading and for static loading after 0.4 million, 1 million, and 1.9 million cycles. The beam midspan deflections and the reinforcing steel strains were significantly larger than those of the composite beams with the bonded-rough interfaces indicating the loss of composite action due to the delamination. The change in the

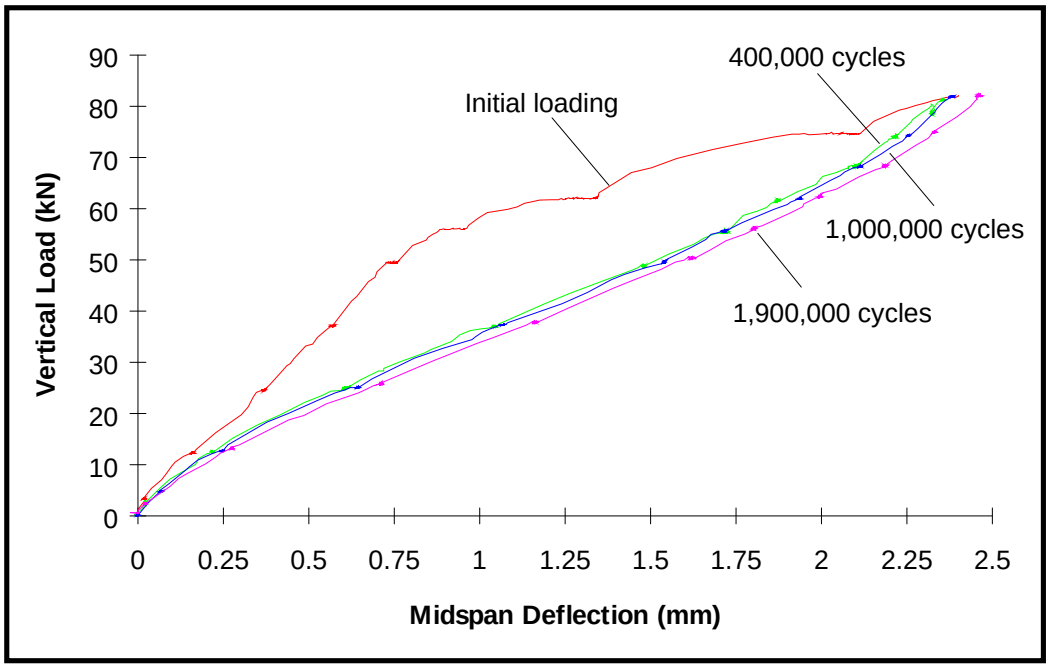

(a) Load vs. Deflection

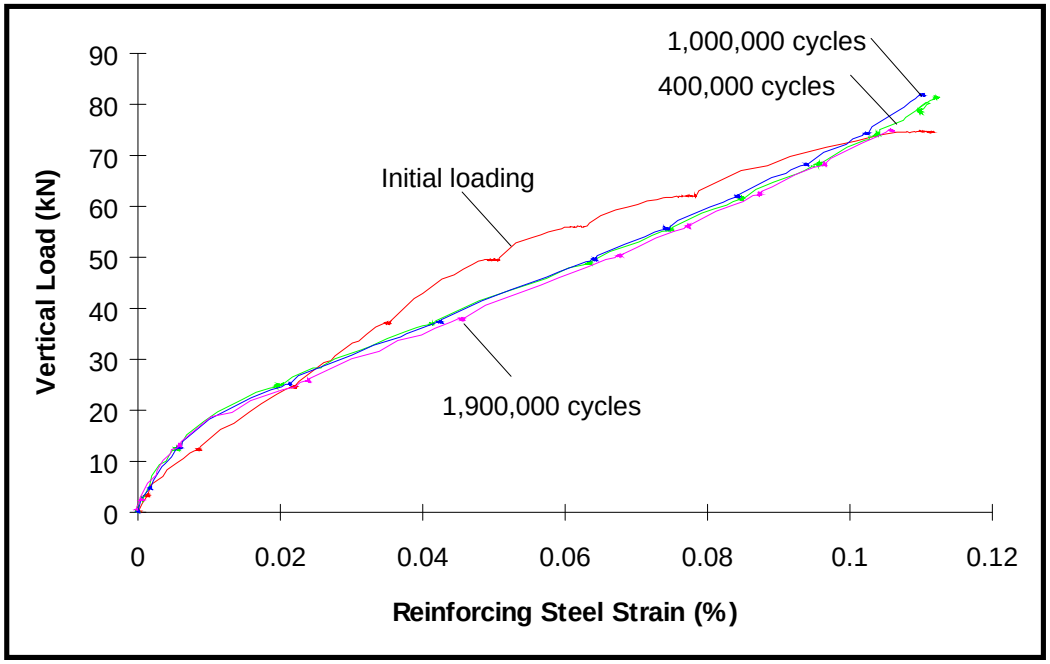

(b) Load vs. Reinforcing Steel Strain

Figure 7.17 Beam Fatigue Tests: ***N1B-1***

Table 7.7 Fatigue Test Results: ***N1B-1***, Values at 80 kN Vertical Load

Number of Cycles (x 1,000)	Reinforcing Steel Strain (%)	Midspan Deflection (mm)	Interface Slip (mm)	
			East	West
0	0.12	2.3	0.35	0.47
400	0.11	2.3	0.27	0.21
1,000	0.11	2.4	0.27	0.27
1,400	0.11	2.4	0.28	0.29
1,900	0.11	2.5	0.29	0.39

beam deflections between the initial loading and the static loading after 400,000 cycles was large as shown in Fig. 7.17 (a) which may suggest additional deterioration of the unbonded-smooth interface due to cycling. The change in the reinforcing steel strains remained relatively small between before and after cycling in Fig. 7.17 (b). Table 7.7 summarizes the test results of ***N1B-1*** in terms of beam midspan deflections, reinforcing steel strains, and interface slips.

7.5.4 Unbonded Beams

Two beams with unbonded-rough interfaces were subjected to approximately two million fatigue cycles. The interfaces of both beams were heavily shotblasted and unbonded. One and two jumbo nails were used across the unbonded interface on each side of ***H1U-1*** and ***H2U-1***, respectively. Test results are shown in Fig. 7.18 for ***H1U-1*** for the initial loading and the static loading after

0.4 million, 1.1 million, and 2 million cycles. Beam midspan deflections and reinforcing steel strains of the unbonded beam were significantly larger than those of the composite beams with the bonded-rough interfaces which suggests that the interface of the unbonded beam with nails did not maintain the full composite section after cycling. The change in the beam deflections between the initial loading and the static loading after 400,000 cycles was large as shown in Fig. 7.18 (a) probably due to the deterioration of the unbonded-rough interface with nails occurred. Similar test results were observed in ***H2U-1***. Test results of ***H1U-1*** and ***H2U-1*** are summarized in Tables 7.8 and 7.9, respectively.

7.6 Post-Fatigue Static Test Results

7.6.1 Composite Beams

Four composite beams with bonded-rough interfaces and a monolithically cast beam were subjected to post-fatigue static tests since no interface delaminations were observed during the fatigue cycling. Tests were performed in a similar manner as the beam static tests. Test results are summarized in Table 7.10. Interface delamination of ***H0B-1*** occurred at a load of 148 kN (33 kips). The interface shear stress was 4,800 kPa (695 psi) at failure based on strain readings. The interface failure stress was 81 percent of that (5,910 kPa or 860 psi) in the companion beam, ***H0B-2***, which was tested without cycling. ***H0B-1*** was unloaded after the delamination occurred and then reloaded. The two different load versus beam midspan deflection plots are shown in Fig. 7.19 which shows the difference in the flexural responses of the same beam before and after interface delamination. Higher interface shear strengths were reached in all other beams tested after fatigue

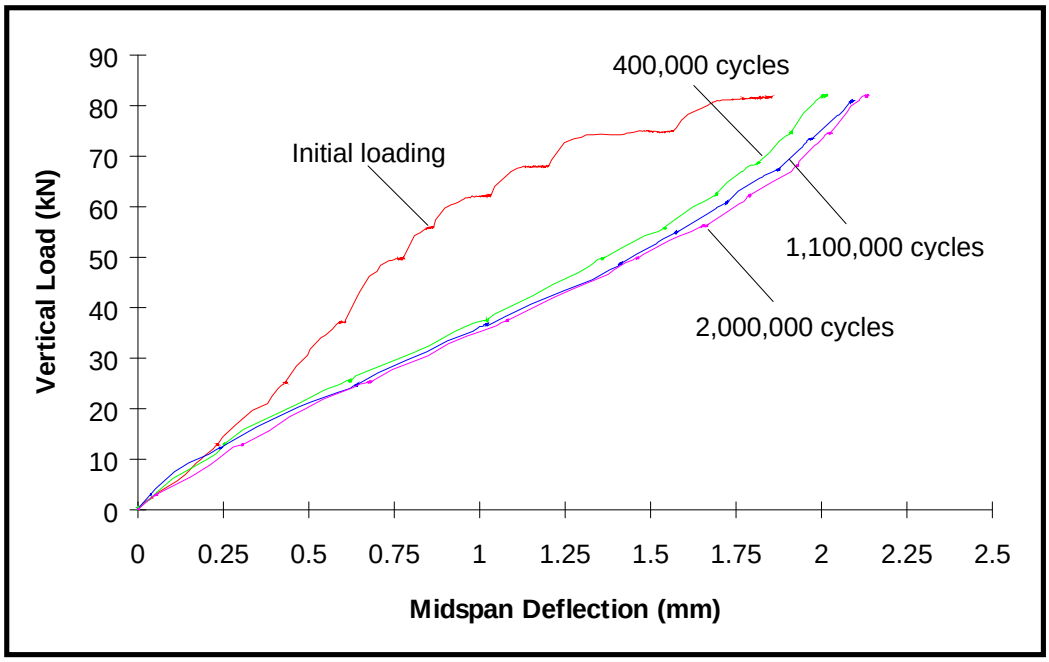

(a) Load vs. Deflection

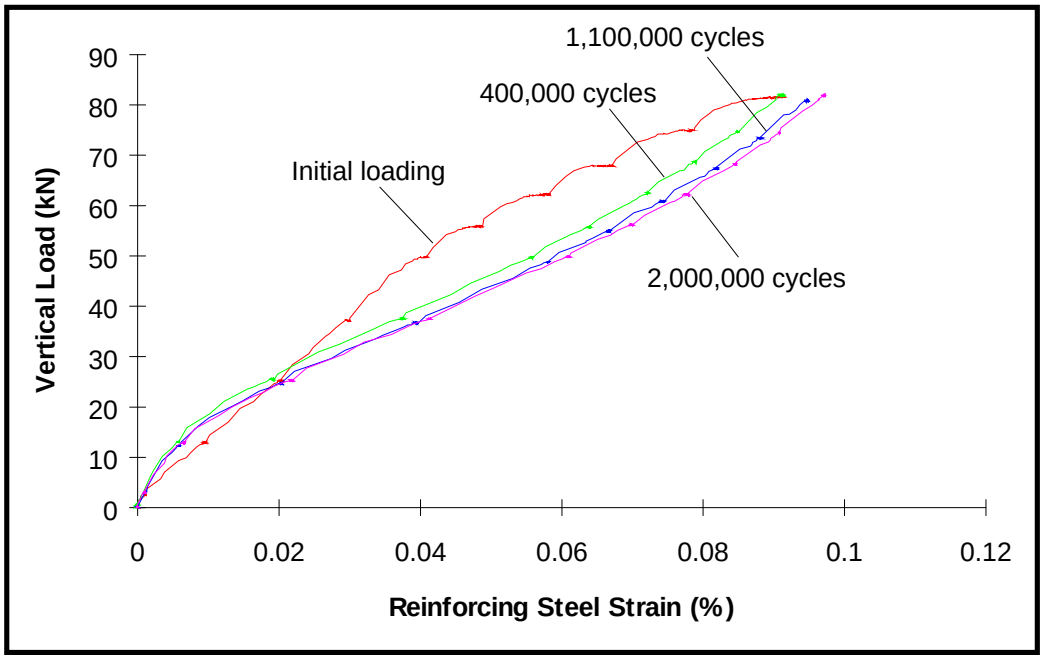

(b) Load vs. Reinforcing Steel Strain

Figure 7.18 Beam Fatigue Tests: ***H1U-1***

Table 7.8 Fatigue Test Results: ***H1U-1***, Values at 80 kN Vertical Load

Number of Cycles (x 1,000)	Reinforcing Steel Strain (%)	Midspan Deflection (mm)	Interface Slip (mm)	
			East	West
0	0.085	1.7	0.20	0.25
400	0.090	2.0	0.22	0.32
1,100	0.094	2.1	0.23	0.31
1,500	0.096	2.1	0.23	0.38
2,000	0.096	2.1	0.25	0.35

Table 7.9 Fatigue Test Results: ***H2U-1***, Values at 80 kN Vertical Load

Number of Cycles (x 1,000)	Reinforcing Steel Strain (%)	Midspan Deflection (mm)	Interface Slip (mm)	
			East	West
0	0.078	1.6	0.10	0.29
500	0.075	2.0	0.18	0.34
1,000	0.076	1.9	0.19	0.28
1,500	0.078	1.8	0.19	0.27
2,000	0.079	2.0	0.20	0.27

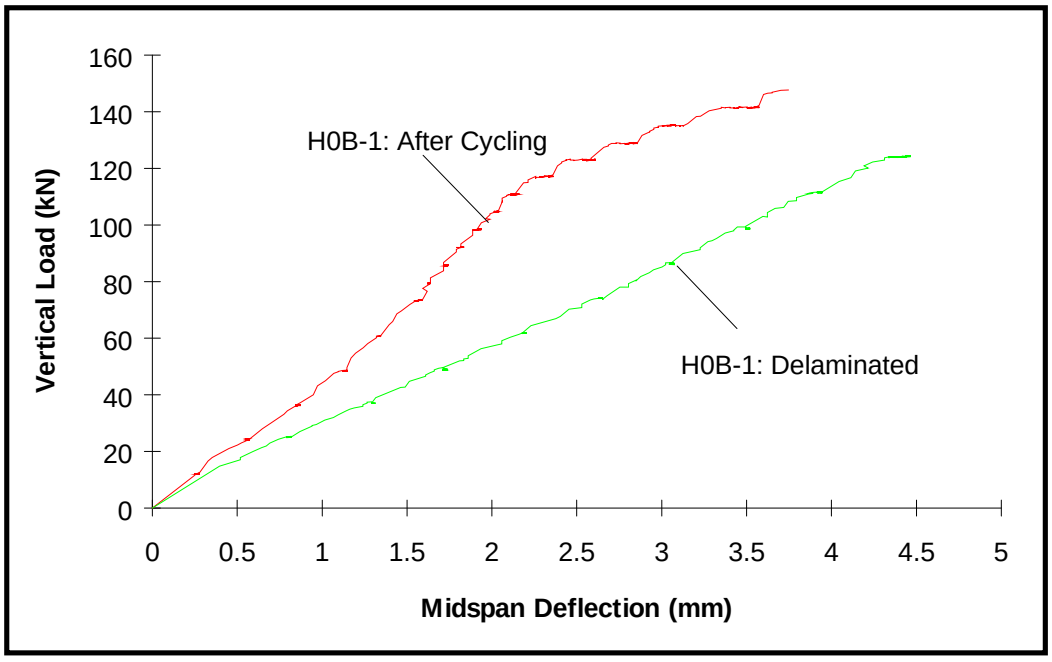

Figure 7.19 Post-Fatigue Beam Tests: ***H0B-1***

loading. Delamination occurred at an interface shear stress of approximately 6,900 kPa (1,000 psi) in ***H2B-1*** but no delamination was observed in ***H2B-2***. The peak interface shear strength was not computed in ***H2B-1*** since the strain gages failed at large strains following yielding. Delaminations occurred at interface stresses of 6,390 kPa (925 psi) and 6,890 kPa (1,000 psi) for ***M0-1*** and ***H1B-1***, respectively. High interface strengths determined in the post-fatigue static tests indicated that fatigue cycling did not significantly influence interface strength. Test results of the two composite beams with bonded-rough interfaces and the monolithically cast beam after cycling are shown in Fig. 7.20. Figure 7.20 shows that the monolithically cast beam and the composite beam with nails were capable of maintaining composite action under higher loads than the composite beam, ***H0B-1***, without nails. Figures 7.21 and 7.22 show the failure surfaces of the base beam and

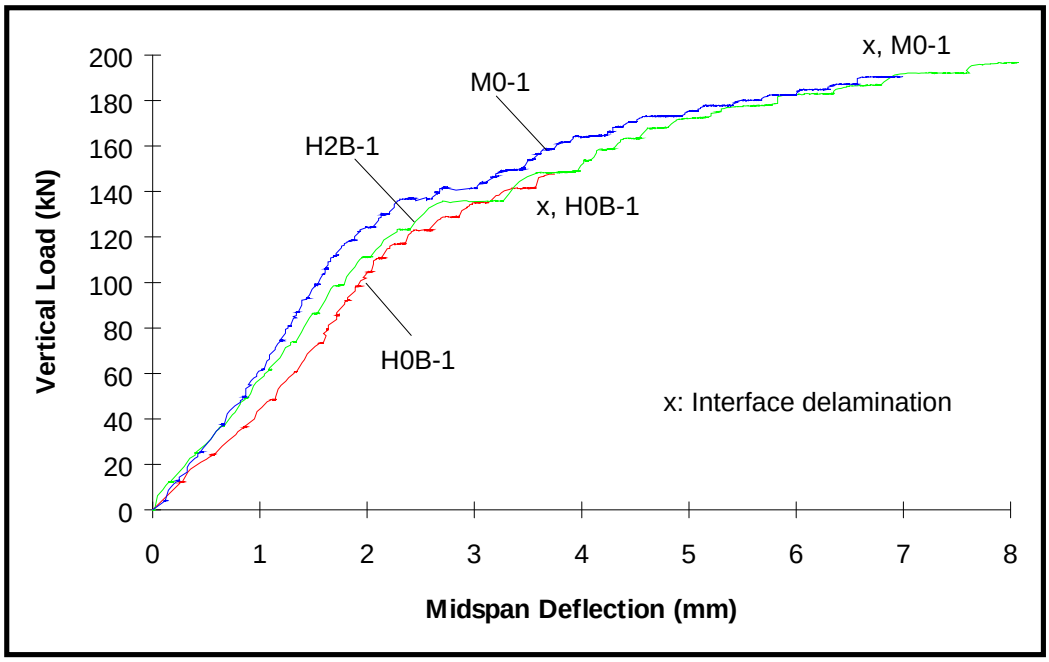

Figure 7.20 Post-Fatigue Beam Tests: ***H0B-1***, ***H2B-1***, and ***M0-1***

the overlay after delamination occurred for ***M0-1*** and ***H0B-1***. The shear failure plane was partly in the base beam and partly in the overlay in ***M0-1*** while it was along the interface in ***H0B-1***.

7.6.2 Unbonded Beams

The unbonded beams were also tested after the completion of cycling. Test results are shown in Fig. 7.24. Figure 7.24 shows that there was not any significant difference in the flexural responses between ***N1B-1*** and the delaminated beam where the behavior of the delaminated beam represented that of the base beam alone. No significant composite action was observed in ***N1B-1*** after cycling. Moderately better flexural performances were exhibited by the two unbonded

(a) Base Beam

(b) Overlay

Figure 7.21 Interface after Delamination: ***M0-1***

(a) Base Beam

(b) Overlay

Figure 7.22 Interface after Delamination: ***H0B-1***

(a) Interface Delamination

(b) Failed Interface

Figure 7.23 Post-Fatigue Static Tests

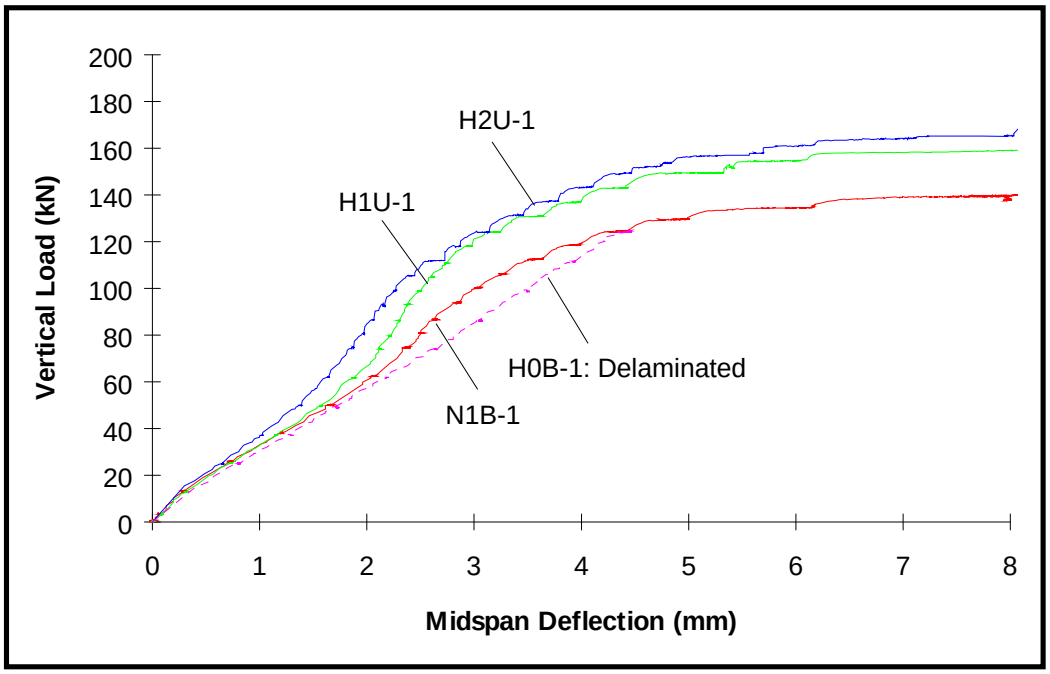

Figure 7.24 Post-Fatigue Beam Tests: Unbonded Beams

beams with nails, ***H1U-1*** and ***H2U-1***, as shown in Fig. 7.24.

7.7 Test Summary and Conclusions

7.7.1 Test Summary

Five composite beams were statically tested without cycling until interface delamination was observed. The average of interface shear strength of the three composite beams with bonded-rough interfaces was 6,060 kPa (880 psi). Four composite beams with bonded-rough interfaces and one monolithically cast beam were subjected to approximately three million fatigue cycles and then tested statically until interface delamination was observed. No interface delamination was observed after cycling. Post-fatigue static tests were completed on all beams

subjected to fatigue cycling. The average interface shear strength of the three composite beams with the bonded-rough interfaces after cycling was 6,200 kPa (900 psi). Fatigue cycling did not influence interface bond strength.

Two beams with unbonded-rough interfaces and one beam with unbonded-smooth interfaces were subjected to approximately two million cycles of fatigue loading. Beam static tests performed after approximately one-half million cycles suggested interface deterioration in the unbonded beams. All unbonded beams were subjected to post-fatigue static tests. The flexural response of a beam with unbonded-smooth interfaces was not significantly different from that of a delaminated beam, indicating the loss of the composite action after cycling. Two beams with unbonded-rough interfaces performed moderately better in flexure than the delaminated beam. The initial flexural stiffness of the two beams was approximately the same as that of the delaminated beam. The flexural stiffness of the two beams increased more than that of the delaminated beam as the vertical load increased. Test results suggest that the Hilti jumbo nails used across the unbonded-rough interface provided shear resistance only after some slip occurred between the base beam and the overlay. Local deterioration of the interface after cycling, such as crushing of unbonded surfaces and of concrete surrounding the nails may be the cause of the slip.

The interface shear strengths determined in all beam tests were much higher than those determined in the push-off tests. The mean of the interface shear strengths of the six composite beams with the bonded-rough interfaces was 6,130 kPa (890 psi) while that of all push-off specimens with similar interface preparation was 2,760 kPa (400 psi). The interface shear strengths determined by the push-off tests were low probably because of the presence of some tensile stresses acting on the interface along with shear. The current study reveals that the true interface

shear strengths may be much higher than those typically determined in push-off tests.

7.7.2 Conclusions

The composite beam static and fatigue tests resulted in the following conclusions:

1. Interface bond between base concrete and overlay was not influenced by the application of the repeated shear stresses for maximum shear stresses up to 2,000 kPa (290 psi),
2. An interface shear strength of approximately 6,130 kPa (890 psi) developed between base beams and overlays with roughened interfaces,
3. A shear strength of 6,390 kPa (930 psi) in a monolithically cast beam indicated that the development of interface bond in adequately roughened interfaces was almost the same as that of monolithically cast concrete,
4. Composite action of an unbonded interface with jumbo nails deteriorated under repeated shear loading, especially when the unbonded interface was not properly roughened, and
5. It is unlikely that the interface bond is influenced by repeated loading in bonded concrete overlays.

CHAPTER EIGHT
FULL-SCALE EXPERIMENTAL BONDED CONCRETE OVERLAY

8.1 Introduction

8.1.1 Background

A section of Interstate Highway 10 (IH-10) through downtown El Paso, Texas, is to be rehabilitated in 1996 by the Texas Department of Transportation (TxDOT). The proposed rehabilitation section is approximately 1.3 km (0.8 mile) long and is at least three lanes in each direction. The continuously reinforced concrete pavement (CRCP) highway was originally constructed in 1965. The average daily traffic is over 90,000 vehicles in each direction and about 35 percent of the total traffic volume is trucks. The feasibility of rehabilitating the 30-year-old pavement was studied by the Center for Transportation Research at the University of Texas at Austin. In the study, an expedited construction of the bonded concrete overlay (BCO) using high early-strength concrete was suggested (Allison, McCullough, and Fowler 1993). An overlay depth of 165 mm (6.5 in.) was recommended. Expedited construction was important because of the large amount of daily traffic and the fact that an alternate traffic route would not be available during construction. TxDOT decided to build a full-scale mockup pavement to simulate the BCO of IH-10 and to assist in determining proper design and construction procedures. Construction of the experimental BCO, built on an aggregate plant haul road in El Paso, started in late April and was completed in late

June 1995. Two different types of Hilti shear connectors were used to improve bond and force transfer between the BCO and the existing pavement.

8.1.2 Scope and Objectives of Experimental BCO

The construction of the experimental BCO and the results of field condition surveys conducted over a six-month period immediately following overlay placement will be described. The research objectives were as follows:

1. Determine the extent of overlay delamination, if any, in the BCO constructed under the relatively severe climate conditions existing in El Paso, Texas;
2. Compare the performance of test sections constructed with and without shear connectors; and
3. Assess the advantages of using shear connectors for the expedited BCO construction using high early-strength concrete.

8.2 Preliminary Work

8.2.1 Overlay Mix Design

The overlay concrete mixes were developed by the Construction Materials Research Group of the University of Texas at Austin while the mix design for IH-10 used in 1965 was duplicated for the base slab. Three different mixes were used for the overlay: plain concrete, polypropylene fibrous concrete, and steel fibrous concrete. Compressive strengths of approximately 48 MPa (7,000 psi) and 54 MPa (7,850 psi) were developed in two and seven days, respectively. The thermal

coefficient was on the order of 7 x 10^{-6} mm/mm/°C (4 x 10^{-6} in./in./°F). The overlay mix designs are summarized in Appendix D.

8.2.2 Shear Connectors

Two different types of Hilti shear connectors were used to enhance shear transfer between the overlay and base slab in some test sections and are summarized in Table 8.1: powder-driven jumbo nails and epoxy-bonded HIT HY 150 connectors (HY-150). The pull-out capacity of a jumbo nail is approximately 38 kN (8.5 kips) when installed in normal strength concrete (compressive strength, f'c = 32 MPa or 4,650 psi) while the ultimate shear capacity of a jumbo nail is about 50 kN (11 kips). The pull-out capacity of a HY-150 connector is approximately 30 percent higher than that of a jumbo nail.

8.2.3 El Paso Climate Study

Previous research (Neal 1983, Whitney et al. 1992) suggests that the potential for delamination in a BCO increases if the overlay is placed on a day when the ambient temperature change shortly after concrete placement is large and the water evaporation rate from freshly placed concrete is high. Whitney et al. suggested that overlay placement should be avoided when the temperature variation is more than 14 °C (25 °F) during the 24-hour period after casting and when evaporation exceeds 1 kg/m^2/hr (0.2 lb/$ft.^2$/hr). The 1 kg/m^2/hr evaporation rate is also considered an upper limit beyond which the development of plastic shrinkage cracks in fresh concrete can be expected. Evaporation rate can be determined using the Portland Cement Association (PCA) nomograph shown in Fig. 8.1 (PCA 1988).

Table 8.1 Shear Connectors Used in Experimental BCO

Connector Type	Jumbo Nail	HIT HY 150
Length (mm)	120	200
Diameter (mm)	10.6	12.0
Drill-hole Depth (mm)	60	120
Installation Method	Powder-driven using charge	Epoxy bonded

Wind velocity, air and concrete temperatures, and relative humidity are the four important variables in determining evaporation rate. An analysis of the El Paso climate for a two-year period between July 1992 and June 1994 showed that the evaporation rate rarely fell below 1 kg/m^2/hr in the month of June (Wade, Fowler, and McCullough 1995). It was decided to construct the overlay in June 1995 to provide data under the most undesirable conditions.

8.3 Construction of Bonded Concrete Overlay

8.3.1 Base Slab Construction

The base slab, constructed May 1, 1995, was 137 m (450 ft.) long with a thickness of 200 mm (8 in.) and a width of 3.66 m (12 ft.). Figures 8.2 and 8.3 show the construction site and the concrete placement for the base slab. The longitudinal reinforcing steel (16-mm or 5/8-in. diameter, U.S. # 5 bars) was placed

Figure 8.1 Nomograph for Calculating Water Evaporation Rate from Freshly Placed Concrete (PCA 1988)

Figure 8.2 BCO Construction Site

Figure 8.3 Concrete Placement: Base Slab

at 190 mm (7.5 in.) on center at the slab mid-depth while the transverse steel (13-mm or 0.5-in. diameter, U.S. # 4 bars) was placed at 760 mm (30 in.) on center to match the existing pavement on IH-10. Most of the surface area of the base slab was cured using membrane-forming curing compounds while a portion was cured using wet burlap and plastic sheets. Sawcuts were made approximately 1.5 m (5 ft.) apart to simulate the existing cracks on IH-10. Depth of the saw cuts was 50 mm (2 in.).

8.3.2 Interface Preparation

The entire base slab except a 7.6-m (25-ft.) length at the north and the south ends was overlaid. Eight test sections were placed end to end. The length was 15.24 m (50 ft.) and the width was 3.66 m (12 ft.). Test sections were numbered one through eight with section 1 being located on the south end as shown in Fig. 8.4. Shotblasting and hydrocleaning were used for interface preparation. The interface of seven test sections (all test sections except section 7) was roughened by shotblasting while section 7 was prepared by hydrocleaning. Hydrocleaning was investigated as a potential alternative to the more conventional shotblasting. Silfwerbrand (1990) studied the pull-out strength on cores. Interface was treated by three different techniques: jack-hammering, water-jetting, and sandblasting. Test results indicated the highest pull-out strengths on cores with the water-jetted interface as shown in Fig. 8.5. The average texture of the roughened interface was measured by the sand patch method shown in Fig. 8.6. The average texture of the shotblasted interfaces ranged between 1 mm (0.04 in.) and 1.5 mm (0.06 in.). A slightly rougher interface was created by hydrocleaning where the average texture ranged between 1.5 mm (0.06 in.) and 2 mm (0.08 in.). Concrete debonding agent was applied on the prepared interface along the east longitudinal edge of the base

Figure 8.5 Comparison between Pull-Out Tests on Cores (Silfwerbrand 1990)

Figure 8.6 Sand Patch Method

slab over a 300-mm (1-ft.) width to create an unbonded interface. The debonding agent was also applied either along the south or the north edge of each test section for the same 300-mm width. The debonding agent was of a type frequently used in precast concrete construction. The reason for creating an unbonded interface along the edge of the overlay was to determine if interface delamination would extend with time and if connectors would be effective in reducing the extension of delamination. Table 8.2 summarizes the test variables for the experimental BCO. The two reinforced sections 3 and 4 and the two unreinforced sections 5 and 6 were identical except for the shear connectors as shown.

8.3.3 Installation of Shear Connectors

Jumbo nails and HY-150 connectors were installed along the east and the west longitudinal slab edges in sections 4 and 5. Each test section was divided into four subsections of equal length (3.81 m or 12.5 ft.). Jumbo nails were installed in three subsections while HY-150 connectors were installed in one subsection in sections 4 and 5, respectively. Three different jumbo nail spacings were used: 380 mm (15 in.), 510 mm (20 in.), and 760 mm (30 in.). HY-150 connectors were installed using a 510-mm spacing. All shear connectors were installed 150 mm (6 in.) from the slab edge. Shear connectors were also installed 150 mm away from existing saw cuts to avoid concrete spalling during drilling and nail driving. The installation layout of shear connectors in sections 4 and 5 is shown in Appendix E.

Figure 8.7 shows the three-step installation of a jumbo nail: drilling, drill-hole cleaning, and nail driving. Figure 8.8 shows the installation steps of an epoxy-bonded HY-150: drilling, drill-hole cleaning, epoxy application, and the connector installation. A total of 94 jumbo nails and 32 HY-150 connectors was installed in

Table 8.2 Summary of Test Variables in Experimental BCO

Section No.	Interface Preparation	Use of Shear Connectors	Overlay Reinforce-ment	Concrete	Day vs. Night Casting
1	Shotblast	--	Steel	Plain [2]	Day
2	Shotblast	--	Steel	PFRC [3]	Day
3	Shotblast	--	Steel	SFRC [4]	Day
4	Shotblast	Yes [1]	Steel	SFRC	Day
5	Shotblast	Yes [1]	--	SFRC	Day
6	Shotblast	--	--	SFRC	Day
7	Hydroclean	--	--	SFRC	Day
8	Shotblast	--	--	SFRC	Night

Note 1: Jumbo nails and HY-150 connectors,
2: Plain concrete,
3: Polypropylene fibrous concrete,
4: Steel fibrous concrete using 60-mm-long steel fibers with hooked ends.

(a) Drilling

(b) Drill-Hole Cleaning

Figure 8.7 Jumbo Nail Installation

(c) Nail Driving

Figure 8.7 Jumbo Nail Installation (Cont’d.)

(a) Drilling

(b) Drill-Hole Cleaning

Figure 8.8 HIT HY 150 Connector Installation

(c) Epoxy Application

(d) Connector after Installation

Figure 8.8 HIT HY 150 Connector Installation (Cont'd.)

sections 4 and 5 by a two-men crew. Total time required to install all shear connectors was 345 minutes (210 minutes for the jumbo nails and 135 minutes for the HY-150 connectors). The average installation time was 2.2 minutes for a jumbo nail and 4.2 minutes for a HY-150. More drilling (deeper holes) and extra time for application of the epoxy accounted for the longer installation time for the HY-150 connectors. The jumbo nails protruded approximately 55 mm (2.2 in.) above the interface while the HY-150 connectors protruded 80 mm (3.1 in.) above the interface. Table 8.3 summarizes the layout of the shear connectors.

8.3.4 Overlay Reinforcement

The longitudinal reinforcing steel (13-mm or 0.5-in. diameter, U.S. # 4 bars) in sections 1 through 4 was placed at 150 mm (6 in.) on center while the transverse steel (U.S. # 4 bars) was placed at 460 mm (18 in.) on center directly on top of the roughened interface without using chairs. Longitudinal reinforcing steel was discontinued at the end of each test section. No reinforcing steel was used in sections 5 through 8. Figure 8.9 shows overlay reinforcement and jumbo nails installed in section 4. Figure 8.10 shows HY-150 connectors installed along the slab edge.

8.3.5 Overlay Placement

Plain concrete was placed in section 1. Depth of the overlay was 165 mm (6.5 in.). The concrete used in section 2 was the same as that in section 1 but polypropylene fibers were added. Steel fibrous concrete was placed in all other sections (sections 3 through 8). The concrete placement for the day-cast sections began early in the morning at the south end of section 1 and progressed north

Table 8.3 Summary of Shear Connector Installation: Sections 4 and 5

Section No.	Subsection No.	Connector Type	Spacing (mm)	Distance from South End of Section (m)
4	4A	Jumbo nail	760	0 - 3.81
	4B	Jumbo nail	510	3.81 - 7.62
	4C	HY-150	510	7.62 - 11.43
	4D	Jumbo nail	380	11.43 - 15.24
5	5A	Jumbo nail	380	0 - 3.81
	5B	HY-150	510	3.81 - 7.62
	5C	Jumbo nail	510	7.62- 11.43
	5D	Jumbo nail	760	11.43 - 15.24

Figure 8.9 Overlay Reinforcement and Jumbo Nails

Figure 8.10 HIT HY 150 Connectors

ending at section 7. Section 8 was constructed at night on the same day. Figure 8.11 shows the overlay placement. A construction joint was created between each test section as shown in Fig. 8.12. Overlays were finished with tining in the transverse direction, and TxDOT Type II white pigmented curing compound was applied on the top surface of the overlay shortly after casting. Aggregate trucks began to travel on the BCO after six days.

8.4 Instrumentation and Field Monitoring

8.4.1 Monitoring during Overlay Placement

A Campbell Scientific weather station with a data logger was installed near the pavement and recorded air temperature, relative humidity, and wind velocity during and after overlay placement. A thermocouple was placed at the interface in each test section. Data from the weather station and thermocouples were later used to determine the water evaporation rate.

8.4.2 Field Surveys

The BCO was surveyed six times during a six-month period following the overlay placement. Table 8.4 is a summary of test types and dates. The first survey was completed between June 23 and 25 immediately following overlay placement. Field coring and two different nondestructive test (NDT) methods were used in the first condition survey: spectral-analysis-of-surface-wave (SASW) and impact-echo tests. Approximately 25 cores were taken in order to investigate development of interface tensile strength at early ages. The development of transverse cracks in the overlay due to restrained drying shrinkage of concrete was investigated in the

Figure 8.11 Placement of Overlays

Figure 8.12 Construction Joint Placement between Test Sections

Table 8.4 Summary of Field Surveys on Experimental BCO

Index	Date Performed	Test Type		
		Crack Survey	Pull-Out Test (No. of Cores)	Non Destructive Tests
1	June 23~25	Yes	25 [1]	Yes [3]
2	July 25	Yes	--	--
3	Aug. 28	Yes	--	--
4	Sept. 17~19	Yes	19 [1]	Yes [4]
5	Nov. 22	--	14 [2]	--
6	Dec. 9~11	--	33 [2]	--

Note 1: Pull-out tests conducted in sections 1 through 6,
2: Pull-out tests conducted in unreinforced sections 5 and 6 only,
3: SASW and impact-echo tests,
4: SASW, impact-echo, and impulse-response tests.

second and third field surveys performed on July 25 and August 28, respectively. The fourth condition survey, conducted between September 17 and 19, was completed approximately three months after overlay placement. Field coring and three different NDT methods were used in an attempt to detect interface delaminations: SASW, impact-echo, and impulse-response tests. Nineteen cores were taken to determine interface tensile strength and existence of delaminations. A crack survey was also performed. Forty-seven additional cores were taken on November 22 and December 9~11, 1995, approximately five and six months after placement of the overlay.

8.4.2.1 Pull-Out Test The interface bond strength in tension was determined using a pull-out test. A 100-mm- (4-in.-) diameter core was drilled into the BCO past the interface to an approximate depth of 190 mm (7.5 in.). A steel cap was epoxied on the top surface of the core. The pull-out device was connected to the steel cap and the pull-out force was applied until the core failed in tension at the interface. Figures 8.13 and 8.14 show core drilling and the pull-out test.

8.4.2.2 Spectral-Analysis-of-Surface-Wave Test Stokoe et al. (1988) have studied in-situ seismic testing using the SASW method. The test configuration is shown in Figs. 8.15 and 8.16. The SASW test requires an impulse source (a hammer) and two receivers (accelerometers) spaced 200 mm (8 in.) on center on the surface of the overlay as shown in Fig. 8.16. An impulse load was applied by striking a hammer on the surface of the overlay at a point approximately 200 mm from the first receiver. The surface wave (Rayleigh wave) propagated along the surface on a circular wave front centered at the impact point. The propagation of the surface wave was monitored using the two receivers. Signals at the receivers were recorded by a Hewlett Packard 3562A dynamic signal analyzer shown in Fig. 8.17. Each recorded time signal was then transformed into the frequency domain using a Fast Fourier Transform (FFT) algorithm in the digital analyzer, and the phase angle difference between the two receivers was calculated for each frequency. A cross power spectrum was generated by the analyzer where the relative phase angle difference between the two receivers and the frequency were plotted in the y-axis and x-axis, respectively. The overlay delamination was determined by investigating the cross power spectrum. Delamination was indicated

Figure 8.13 Core Drilling

Figure 8.14 Pull-Out Test

Figure 8.15 General Configuration of Source and Receivers Used in SASW Test (Stokoe et al. 1988)

Figure 8.16 Spectral-Analysis-of-Surface-Wave Test

Figure 8.17 Hewlett Packard 3562A Dynamic Signal Analyzer

by a loss of the low frequency (large wavelength) energy, which suggested that propagation of surface waves with wavelengths greater than the overlay depth (165 mm or 6.5 in.) was disrupted. The typical cross power spectrum generated for bonded and delaminated interfaces is shown in Appendix F.

8.4.2.3 Impact-Echo Test The theoretical basis of the impact-echo test for detecting voids or cracks in plate-like structures or in layered plates was described by Sansalone and Pratt (1993). The impact-echo test required a very small hammer instrumented with a load cell and a receiver (accelerometer) as shown in Fig. 8.18. Surface waves (Rayleigh waves or R-waves) and body waves (compression waves or P-waves, and shear waves or S-waves) were generated from a transient pulse introduced by the mechanical impact on the top surface of the pavement as

Figure 8.18 Impact-Echo Test

Figure 8.19 Propagation of Surface Wave (R) and Body Waves (P and S) Generated by Impulse Load (Sansalone and Pratt 1993)

schematically shown in Fig. 8.19. The impact was applied very close to the receiver in order to measure the displacements due mostly to vertically propagating P-waves. The P-wave was reflected by the internal cracks (for the delaminated interface) and the horizontal boundaries of the layered pavement (interface and bottom fibers of the base slab for the bonded interface). Vertical displacements of the surface indicated the arrival of the reflected P-waves and were recorded by the receiver. The recorded time signal was then transformed into the frequency domain using the FFT algorithm. A displacement amplitude spectrum was generated by the analyzer where displacement and frequency were plotted in the y-axis and x-axis, respectively. The existence of interface delaminations was determined by investigating the amplitude spectrum. Good bond was indicated by resonant peaks at frequencies of approximately 12 kHz and 5 kHz, which correspond to the depth of the interface and the total depth of the overlay, respectively. An interface delamination was indicated by the absence of the return at 5 kHz indicating that the wave energy was not transmitted past the interface.

8.4.2.4 Impulse-Response Test The impulse-response test required a modal hammer and a receiver (velocity transducer or geophone) as shown in Fig. 8.20. An impulse load was applied by a large hammer hitting the top surface of the overlay close to the receiver. The flexural vibrations of the pavement in the vicinity of the impact point were measured. An amplitude spectrum similar to that of the impact-echo test was generated. The displacement amplitude and the frequency were plotted in the y-axis and x-axis, respectively. An undulating response in the amplitude spectrum indicated a lack of support at the interface (a delaminated interface). Good bond was indicated by a flat and low magnitude response.

Figure 8.20 Impulse-Response Test

8.5 Test Results

8.5.1 Weather Conditions

The lowest air temperature for June 22, 21 °C (70 °F) was recorded in the morning approximately one hour after overlay placement of section 1 started. The highest temperature, 36 °C (96 °F), was recorded in the afternoon approximately five hours after placing the last day-cast section. The relative humidity was 30 percent or higher early in the morning and then began to decrease rapidly. The relatively humidity was 15 percent or lower for the most of the afternoon. The wind velocity remained between 6 and 19 kmph (4 and 12 mph) during most of the day. The air temperature and water evaporation rate from the overlay determined using the recorded weather data are shown in Fig. 8.21. Figure 8.21 (b) shows that a high evaporation potential existed for test sections cast later in the morning.

8.5.2 Crack Survey Results

8.5.2.1 Development of Overlay Shrinkage Cracks The development of transverse cracks in the overlay due to restrained shrinkage of concrete was investigated. Crack development was typically determined on the side face of the BCO because it was difficult to identify cracks on the tined top surface of the overlay. The first crack survey was carried out immediately following overlay placement. The crack survey was not performed on the side face because the formwork was kept in place for several days after casting. No cracks were detected. It must be noted, however, that small width shrinkage cracks may have developed at early ages but could not be identified due to the tined finish. Later crack surveys revealed that many drying shrinkage cracks developed in the overlay.

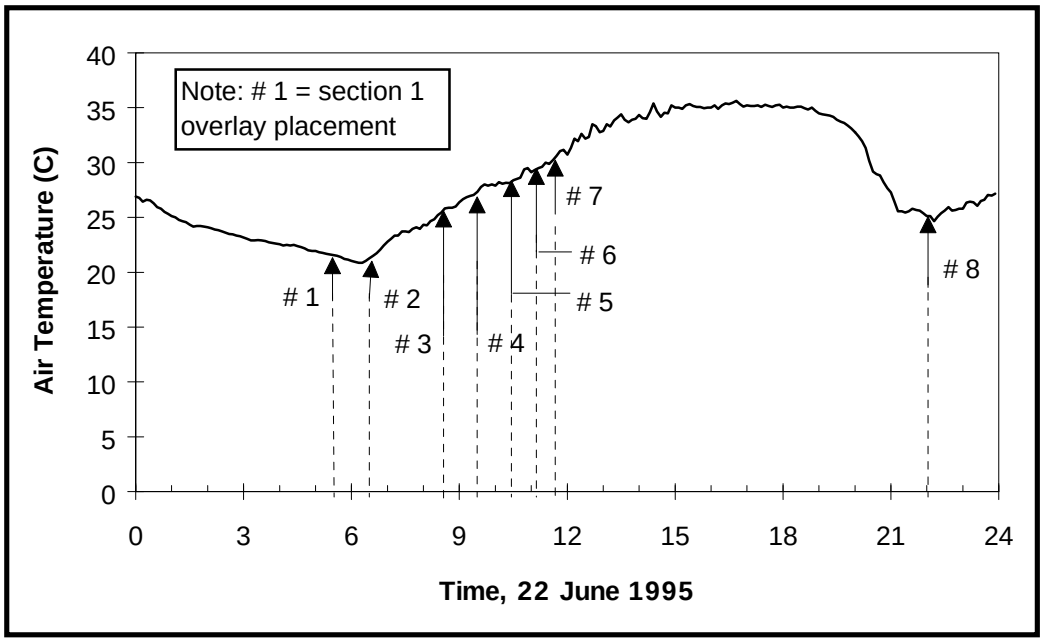

(a) Air Temperature vs. Time

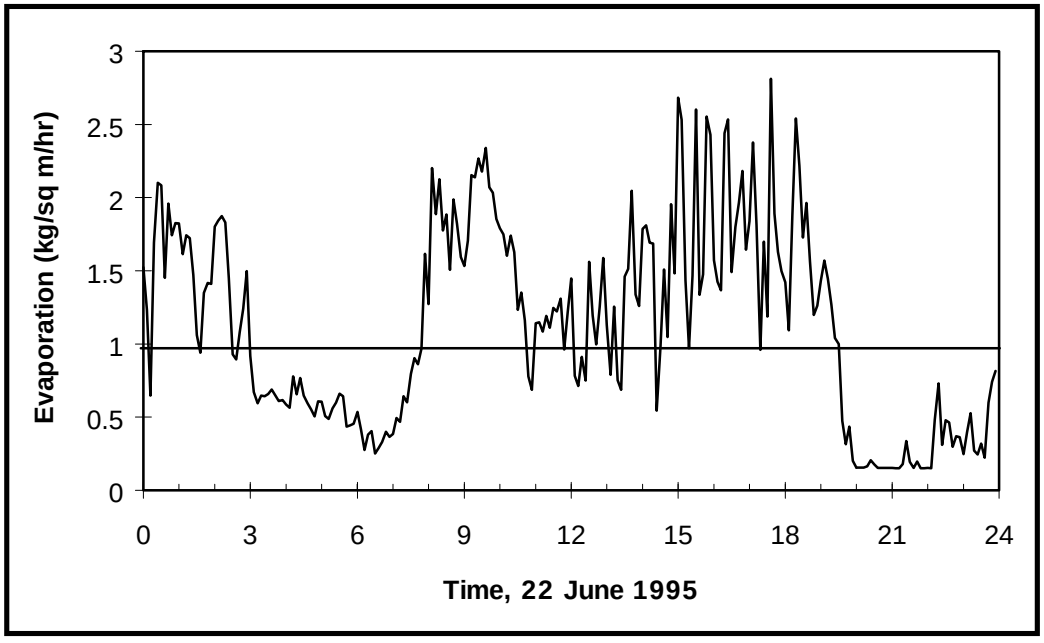

(b) Evaporation Rate vs. Time

Figure 8.21 Weather Conditions on June 22, 1995

The location of each crack was recorded while the crack width was measured using a crack comparator. Figure 8.22 shows a relatively wide drying shrinkage crack that developed in the overlay. The average crack spacing one month after the overlay placement was 1.8 m (6 ft.) and after three months was 1.2 m (4 ft.). Table 8.5 summarizes the crack survey results.

In the three crack surveys, data were collected at approximately one-month intervals after the overlay placement and are shown in Fig. 8.23 which shows development of drying shrinkage cracks with time for each test section. The cumulative and average widths of all cracks in each test section are shown in Fig. 8.24. The cumulative crack widths in sections 1 and 2, cast very early in the morning when the air temperature was the lowest of the day, are smaller than those in sections cast later in the morning in Fig. 8.24 (a). The cumulative crack width increased in test sections cast later in the morning (sections 3 through 7) while that in the night-cast section (section 8) was the smallest. The cumulative crack widths in the five test sections cast later in the morning, sections 3 through 7, were compared. The cumulative widths of cracks in the two sections with shear connectors (sections 4 and 5) one month after casting are significantly smaller than those in the three other sections (sections 3, 6 and 7) probably because the shear connectors improved shear transfer and distributed stresses from the overlay to the base slab more uniformly. The results of crack surveys performed later also revealed similar results. The cumulative crack widths in sections 4 and 5 are again significantly smaller than those in sections 3 and 6 two and three months after casting as shown in Fig. 8.24 (a). The mean of the cumulative crack widths in sections 4 and 5 is 1.3 mm (0.05 in.) while that in sections 3 and 6 is 1.7 mm (0.07 in.) one month after casting in Table 8.5. The mean of the cumulative crack widths

Figure 8.22 Drying Shrinkage Crack in Overlay

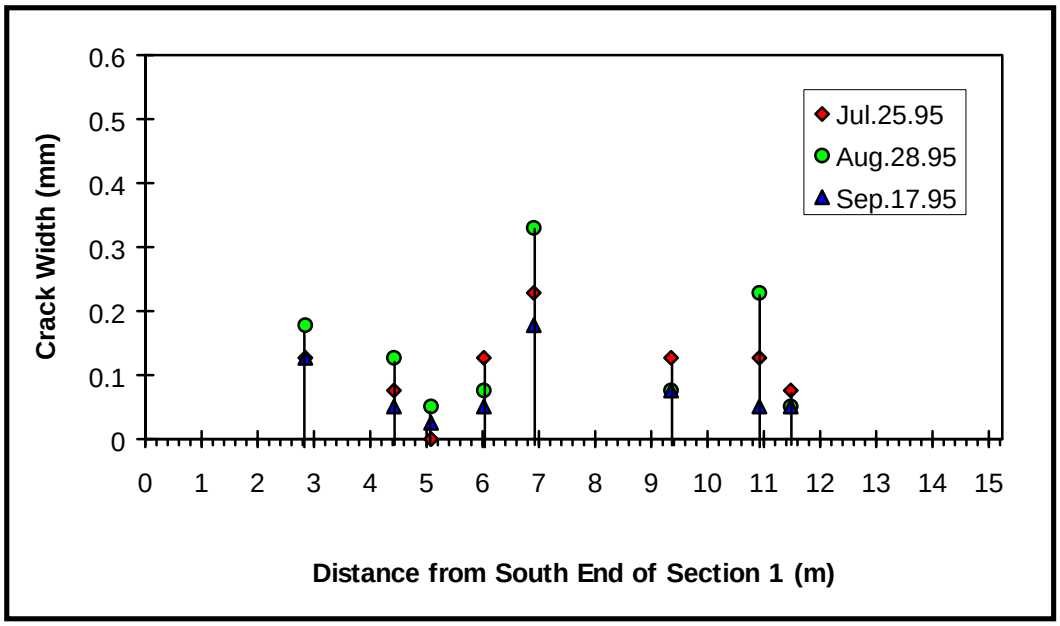

(a) Section 1

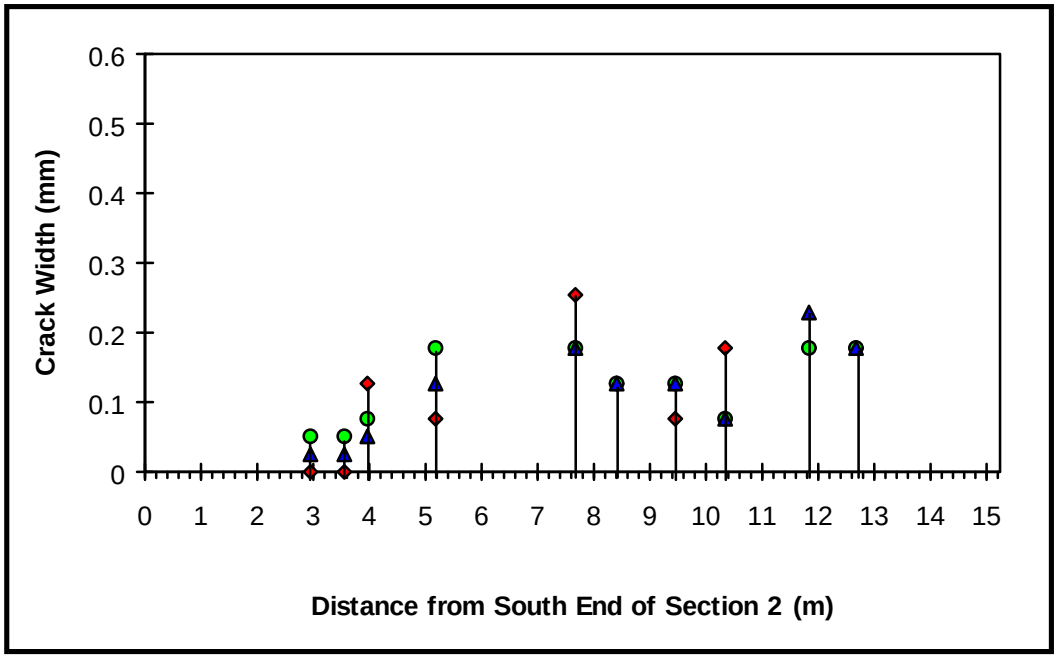

(b) Section 2

Figure 8.23 Overlay Shrinkage Crack Development with Time

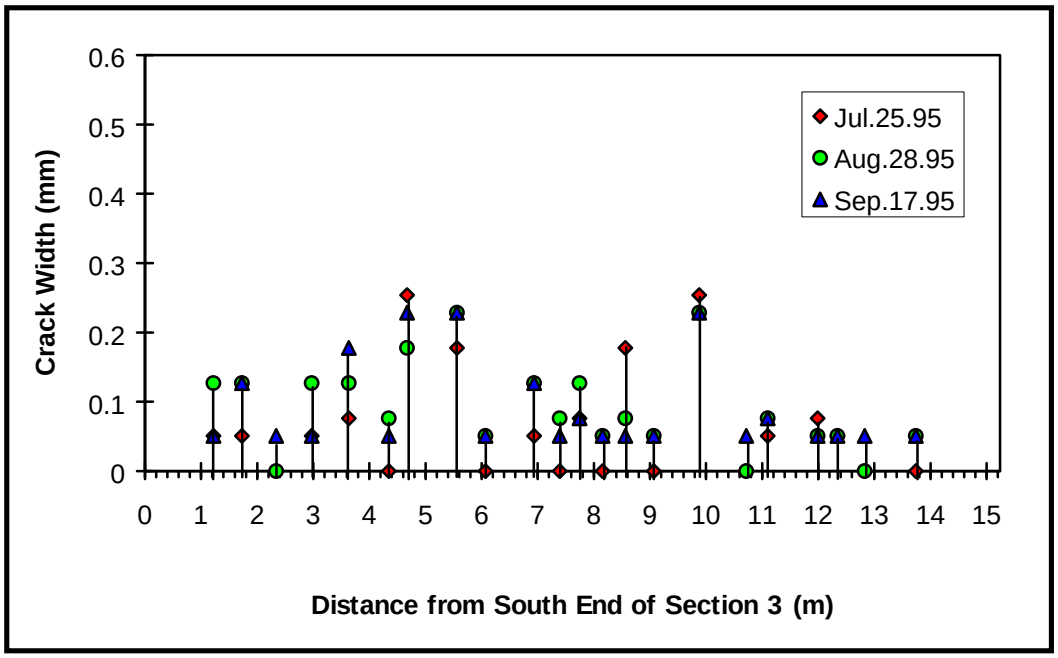

(c) Section 3

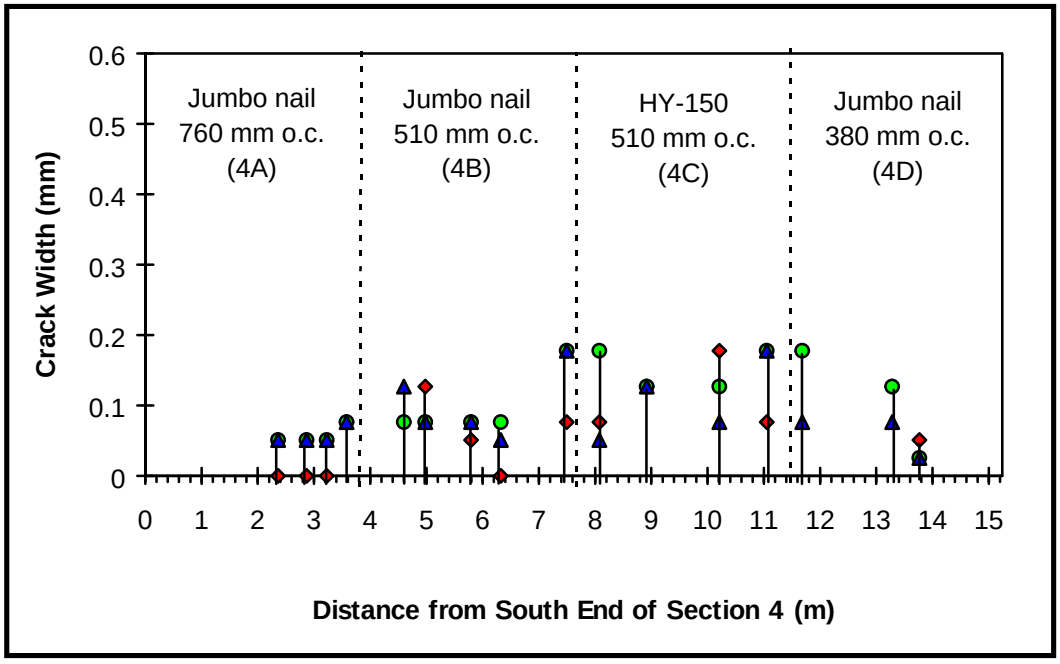

(d) Section 4

Figure 8.23 Overlay Shrinkage Crack Development with Time (Cont'd.)

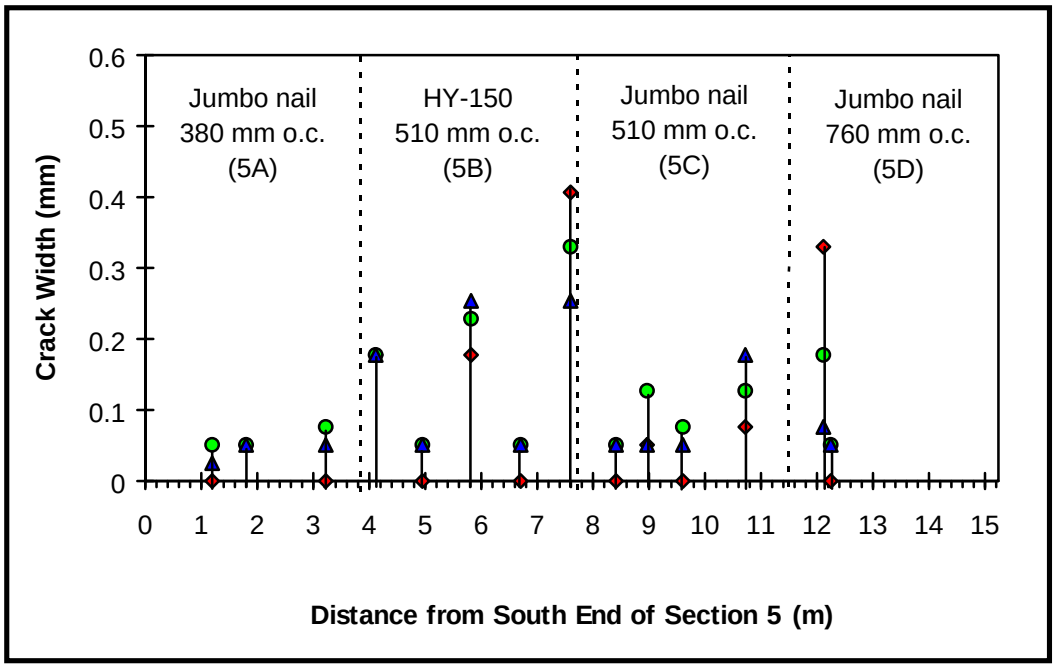

(e) Section 5

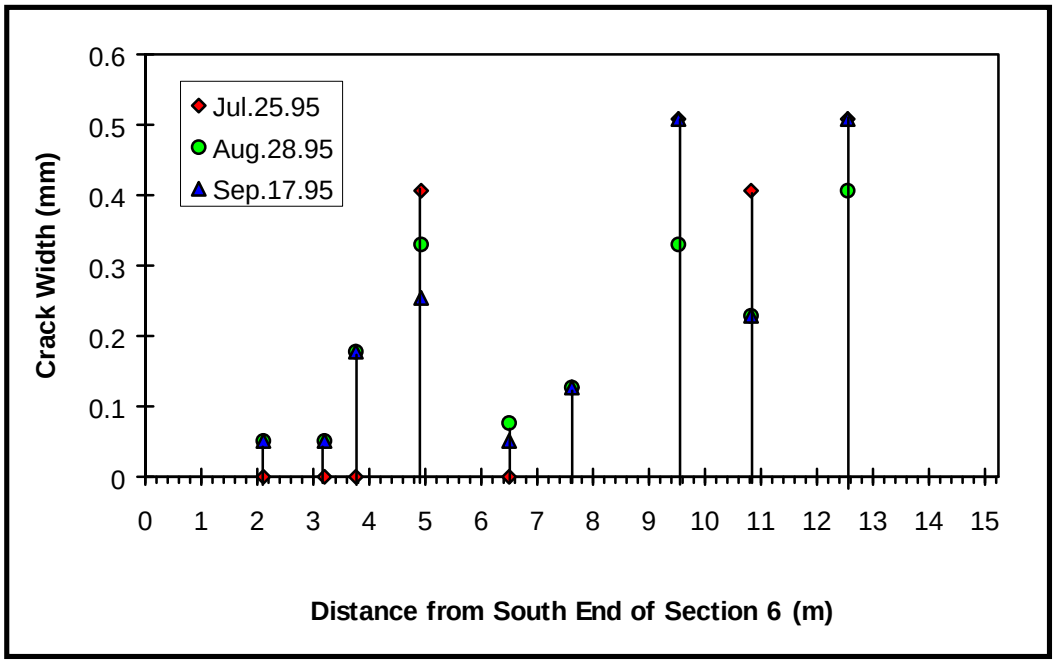

(f) Section 6

Figure 8.23 Overlay Shrinkage Crack Development with Time (Cont'd.)

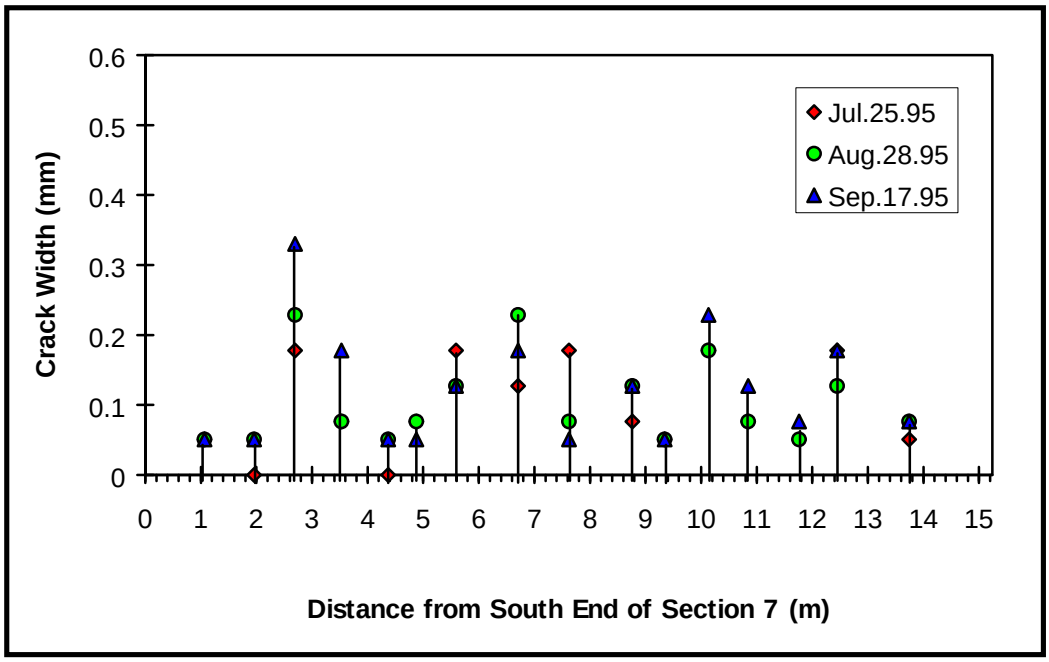

(g) Section 7

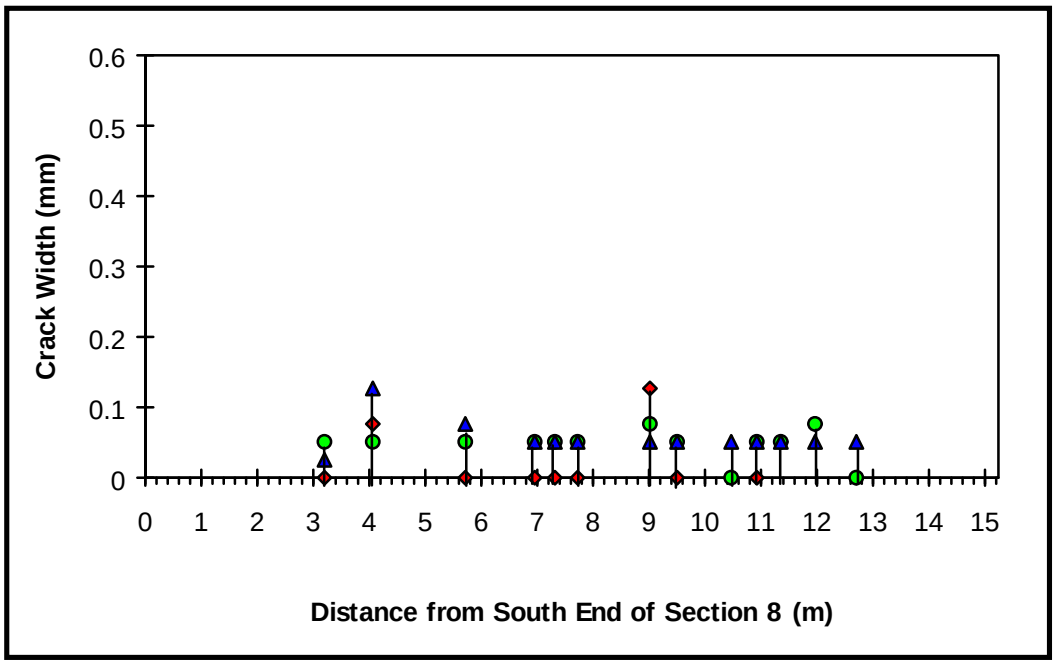

(h) Section 8

Figure 8.23 Overlay Shrinkage Crack Development with Time (Cont'd.)

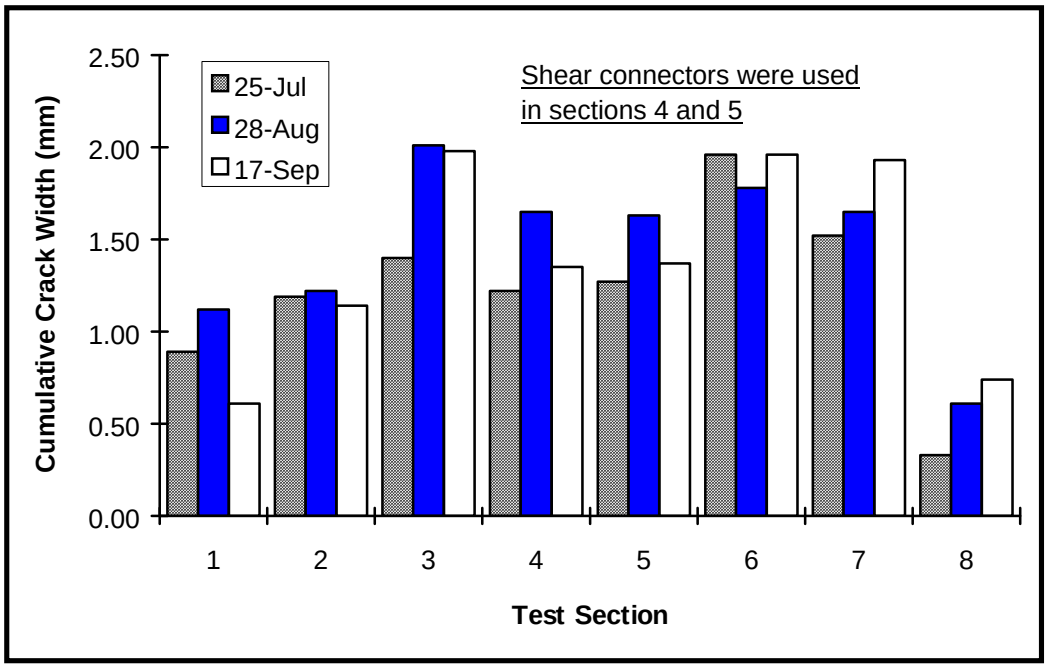

(a) Cumulative Width of Cracks

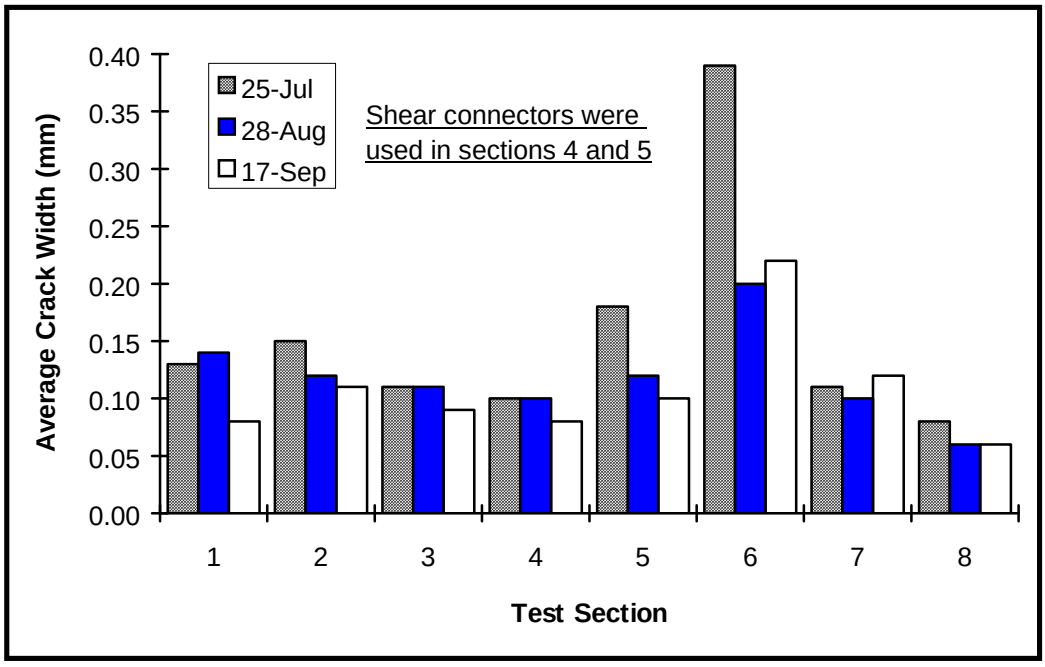

(b) Average Width of Cracks

Figure 8.24 Development of Overlay Drying Shrinkage Cracks

in sections 4 and 5 is 1.4 mm (0.055 in.) while that in sections 3 and 6 is 2 mm (0.08 in.) three months after casting. Test results indicate that the shear connectors helped to control the development of drying shrinkage cracks in the overlay. It is noteworthy that the cumulative and the average crack widths in section 6, where neither the overlay reinforcement nor the shear connectors were used, were much larger than those in section 5 in Figs. 8.24 (a) and (b), respectively.

8.5.2.2 Comparison between Different Shear Connectors Development of the drying shrinkage cracks in the overlay for the different connector spacings in sections 4 and 5 was compared. Table 8.6 is a summary the three crack survey results. Figures 8.23 (d) and (e) also show the overlay drying shrinkage crack development with time in sections 4 and 5, respectively. A comparison of the crack survey results between subsections 5A (jumbo nail, 380 mm o.c.) and 5D (jumbo nail, 760 mm o.c.) reveals that more cracks of smaller width develop with a smaller connector spacing as shown in Fig. 8.23 (e). Similar results are also shown in Fig. 8.23 (d) for section 4. It must be noted that a comparison between nail spacings of 380 mm (15 in.) and 510 mm (20 in.) was not possible due to the different boundary conditions created by the presence of the construction joint placed at the end of each test section. The construction joint influenced the crack development pattern in sections 4 and 5. The drying shrinkage cracks are more evenly spaced in the two middle subsections (4B and 4C, or 5B and 5C) than the two subsections located next to the construction joints (4A and 4D, or 5A and 5D) in Figs. 8.23 (d) and (e). The cumulative and the average crack widths in subsections which used the two different shear connectors with 510-mm spacing were compared. The cumulative and the average crack widths in subsection 5B (HY-150, 510 mm o.c.) are larger than those in 5C (jumbo nail, 510 mm o.c.) in Fig. 8.23 (e) while they are

not significantly different between subsections 4B(jumbo nail, 510 mm o.c.) and 4C (HY-150, 510 mm o.c.) in Fig. 8.23 (d) and Table 8.6.

8.5.3 Results of Pull-Out Tests on Cores

8.5.3.1 Pull-Out Tests at Early Ages Approximately 25 pull-out tests on cores were attempted when the overlay was between 16 and 50 hours old. The purpose was to determine development of the interface tensile strength at early ages. Reliable test results were not obtained due to many technical problems encountered during the coring and the pull-out tests. Problems included difficulties in coring due to the presence of the overlay reinforcing steels in sections 1 through 4, improper surface preparation for the placement of steel caps using epoxy, and difficulties with relatively deep coring (190 mm or 7.5 in.) at early ages when the interface bond strength was low. Test results achieved from several successful pull-out tests indicated that the interface strength in tension was approximately 550 kPa (80 psi) or higher 30 hours after the overlay placement.

8.5.3.2 Pull-Out Tests: September 1995 Nineteen cores were taken to determine the development of the interface tensile strength and the presence of interface delaminations in a field survey conducted three months after the overlay placement. Coring attempted in reinforced sections 1 through 4 was again not successful because all cores failed at the interface due to the severe vibrations when the core bit cut through reinforcing steel placed on top of the interface. Figure 8.25 shows all pull-out test results in section 5. A control pull-out test (no. 11) was conducted in the interior region. The epoxy failed during the test but a pull-out strength of at least 1,400 kPa (200 psi) was reached before epoxy failure. Three pull-out tests (no. 8 through 10) were performed in subsection 5A along the south

slab edge as shown. Jumbo nails were installed at 380 mm (15 in.) spacing along the east and the west longitudinal slab edges. No significant pull-out strength was determined in core no. 8 where the pull-out test was performed very close to the intentionally unbonded area, while a very low pull-out strength (97 kPa or 14 psi) was determined in core no. 9. Figure 8.26 (a) shows that core no. 9 was located next to a construction joint and Fig. 8.26 (b) shows the profile of the failed interface. Delamination did not seem to have occurred along the entire edge since a high pull-out strength (1,020 kPa or 150 psi) was determined in core no. 10 at the southwest corner. Figure 8.27 shows core no. 10 located in the corner area. Two more pull-out tests were made in subsection 5D near the slab edge where the jumbo nails were installed at 760-mm (30-in.) spacing as shown in Fig. 8.25. A high pull-out strength of 1,050 kPa (150 psi) was determined in core no. 13. The epoxy failed during the test of core no. 12 but a pull-out strength of at least 1,500 kPa (215 psi) was determined even though the core was very close to the intentionally unbonded region. Figure 8.28 shows all pull-out test results conducted in section 6. The pull-out strength of 1,360 kPa (200 psi) was determined at the middle of section 6 (no. 17) three months after the overlay placement. Three pull-out tests (no. 14 through 16) were completed in the intentionally unbonded area along the south edge which revealed that the applied bond breaker successfully prevented bond from developing between the two concrete layers. Two more pull-out tests (no. 18 and 19) were made very close to a relatively wide crack (0.5 mm or 0.02 in.) as shown in Figs. 8.28 and 8.29. Relatively low pull-out strengths of 560 kPa (80 psi) and 390 kPa (55 psi) were determined in cores no. 18 and 19, respectively.

8.5.3.3 Pull-Out Tests: November and December 1995 Figure 8.30 shows the test results of twenty-three additional cores taken in section 5 (no. 20 through 23 and 34 through 52) five and six months after the overlay placement. Interface

(a) Core No. 9

(b) Interface after Tension Failure

Figure 8.26 Pull-Out Test near Slab Edge: Section 5

Figure 8.27 Pull-Out Test in Slab Corner: Section 5

delaminations were found in two cores near the intentionally unbonded area and near a 0.4-mm- (0.02-in.-) wide shrinkage crack. The delamination may have spread from the intentionally unbonded northwest corner in one core (no. 23) and the development of the interface bond appears to have been influenced by the stresses developed on the interface neighboring the crack in the other core (no. 37). The pull-out test results of all other cores in section 5 with shear connectors, however, indicated the development of good interface bond. Figure 8.31 shows the test results of twenty-four additional cores (no. 24 through 33 and 53 through 66) in section 6. Interface delaminations were more often found in section 6 constructed without shear connectors than in section 5 with shear connectors. Delaminated interfaces were found in six cores taken near 0.5-mm- (0.02-in.-) wide cracks (no. 26, 27, 59, 60, 63, and 64). The interface delaminations appear to have spread

Figure 8.29 Pull-Out Tests near a Crack: Section 6

along the crack for less than 300-mm (1-ft.) width starting from pavement edges. Delaminated interfaces were also found at the southeast and southwest corners (no. 24 and 54) and cores taken at two north-side corners had very low pull-out strengths as shown in Fig. 8.31. In addition to the delaminated cores, cores taken near the slab edges typically had significantly lower pull-out strength than the control cores taken in the interior region away from cracks. It must be noted that the interface strengths of cores taken in section 6 without shear connectors were often significantly lower than those in section 5 with shear connectors at similar locations. The pull-out test results clearly indicated that interface delaminations occurred in the experimental BCO approximately five months after the overlay construction. The interface conditions of the experimental BCO need to be monitored on a continuing basis to determine if delaminations found in the corner

region and along overlay drying shrinkage cracks further spread with time. All pull-out test results are summarized in Appendix G.

8.5.4 Nondestructive Test Results

Several different NDT methods were used in this study in an attempt to detect the overlay delamination. The NDT test results, using SASW and impact-echo techniques, conducted in the first field survey completed immediately following the overlay placement were rather difficult to verify since pull-out tests were not performed. The results are summarized in the Appendix. The overlay delaminations in six test sections (sections 1 through 6) were investigated using three different NDT methods (SASW, impact-echo, and impulse-response tests) on September 17, approximately three months after the overlay placement. The first series of the NDT tests was completed during the day. The second test series was performed at night on the same day. It was theorized that the delaminated interface would be closed during the day when the temperature of the overlay was higher than that of the base slab. Expansion of the concrete may close the crack and create difficulties in detecting the existence of delaminations. Most tests were conducted in the corner region and along the slab edges where the interface delamination was most likely to occur.

Table 8.7 summarizes the locations and the results of the NDT tests in sections 5 and 6. Test results presented in Table 8.7 show that there are differences in the test results determined using the different test methods. The results of the same NDT test performed during the day and at night are not often the same which indicates that the NDT test results may be highly sensitive to the temperature change in the pavement. A comparison between the NDT and the pull-out test

results can be made from Table 8.7. The comparison seems to indicate that the SASW test was the most erratic. The SASW test results agree with the pull-out test results in four out of eight locations during the day while the two test methods agree only in one out of five locations at night in Table 8.7. The impact-echo test results agree with the pull-out test results in five out of eight locations during the day and in three out of five locations at night. Much better agreement was seen between the pull-out test and the impulse-response test. The impulse-response test results agree with the pull-out test results in six out of eight locations during the day and in all five locations at night as shown in Table 8.7. Figures 8.32 and 8.33 compare the pull-out and the NDT test results in sections 5 and 6, respectively. Thirteen NDT investigations were made on eight pull-out test locations in sections 5 and 6 as shown in Figs. 8.32 and 8.33. The SASW and the pull-out test results agree at five locations while the impact-echo and the pull-out test results agree at eight locations. The impulse-response and the pull-out test results agree at eleven out of thirteen locations.

Table 8.8 summarizes the results of the NDT tests in sections 1 through 4. The NDT test results were compared with the known interface conditions (intentionally unbonded interface using the bond breaker) where applicable as shown in Table 8.8. The SASW test results agree with the known interface conditions at two out of four locations during the day and in two out of three locations at night. The impact-echo test results agree at three out of four locations during the day and in one out of three locations at night. Much better agreement was again observed using the impulse-response test. The impulse-response test results agree with the known delaminated interface condition at two out of four locations during the day and in all three locations at night as shown in Table 8.8. Test results seem to indicate that the impulse-response test is effective in detecting

the delaminated interface. The SASW and the impact-echo tests can also determine the existing interface condition but are not as effective as the impulse-response test.

8.6 Conclusions

8.6.1 Overlay Drying Shrinkage Crack Development

Restrained drying shrinkage of overlays resulted in the development of cracks in the overlay in the transverse direction. Crack surveys conducted for the three-month period after the overlay placement revealed the following:

1. The overlay shrinkage crack development rate was highest during the first month following the overlay placement.
2. Average crack spacing in the overlay one and three months after the overlay placement was 1.8 m (6 ft.) and 1.2 m (4 ft.), respectively.
3. Overlay crack development was closely related to the time the overlay was placed. Total and average widths of cracks in a night-cast section were significantly smaller than those in day-cast sections. Cumulative crack widths in test sections cast early in the morning were also smaller than those in test sections cast later in the morning.
4. Shear connectors effectively controlled development of the overlay drying shrinkage cracks at early ages. Drying shrinkage cracks which developed in test sections with shear connectors were evenly distributed and the width of cracks was typically smaller than in sections without connectors.
5. Cumulative and average crack widths in section 6, where neither overlay reinforcement nor shear connectors were used, were much larger than those in section 5 which had the same test variables but with connectors.

6. A comparison between jumbo nail spacing of 380 mm (15 in.) and 760 mm (30 in.) revealed that more cracks of smaller width developed with a smaller nail spacing.

8.6.2 Interface Strength Development

A total of fifty-nine cores was made to determine the development of the interface strength and the interface delaminations in unreinforced sections 5 and 6. The pull-out test results on cores revealed the following:

1. Interface tensile strength of 550 kPa (80 psi) or higher developed 30 hours after overlay placement and 1,360 kPa (200 psi) or higher strength developed three months after overlay placement.
2. Interface delaminations occurred in the experimental BCO.
3. Delaminated interfaces were typically found near relatively wide (0.5 mm or 0.02 in.) shrinkage cracks in sections 5 and 6. The development of shrinkage in the concrete neighboring the crack seems to have caused the interface delamination.
4. Delaminated interfaces were also found in cores taken very close to the intentionally unbonded area in the corner region. Interface delaminations appeared to spread from the unbonded area.
5. Interface strengths of cores taken along the edge, at corners, and close to cracks were significantly lower than those of cores taken in the interior region away from cracks.
6. Interface strength of cores taken in a test section with nails (section 5) was significantly higher than that of cores taken at similar locations in a test section without nails (section 6).

7. Interface conditions of the experimental BCO need to be monitored on a continuing basis to determine if delaminations continue to spread with time.

8.6.3 Delamination Detection by Nondestructive Tests

Three different NDT methods (SASW, impact-echo, and impulse-response tests) were used to determine interface conditions. Test results were verified by pull-out tests in some locations. Test results revealed the following:

1. The impulse-response test was effective in detecting delaminations. A comparison between the NDT and the pull-out test results showed that the impulse-response test results agreed with the pull-out test results in 16 out of 20 locations.
2. The SASW and the impact-echo tests were not as effective in determining interface conditions as the impulse-response test. The SASW and impact-echo test results agreed with the pull-out test results in nine out of 20 locations and in twelve out of 20 locations, respectively.
3. The NDT test results were sensitive to temperature changes in the pavement. The delaminated interface was more difficult to detect when the temperature of the overlay was higher than that of the base slab. The best test results were obtained when the testing was done both during the day and at night.

CHAPTER NINE
CONCLUSIONS AND RECOMMENDATIONS

9.1 General

An experimental study conducted to determine the performance of large powder-driven nails (jumbo nails) used as "shear connectors" in bonded concrete overlays (BCOs) is summarized in this chapter. The experimental program was divided into four parts (1) nail pull-out tests, (2) interface shear transfer tests or push-off tests, (3) beam tests for static and fatigue interface shear strength, and (4) a full-scale experimental BCO. The BCO was constructed in El Paso, Texas, as an experimental pavement for the large scale BCO on IH-10 planned for construction in 1996. All other tests were conducted in the laboratory.

9.2 Conclusions

9.2.1 Pull-Out Tests

The pull-out capacity of jumbo nails was investigated to determine the level of tensile forces in the nail that can be developed to prevent separation of bonded overlays from the base layer. The pull-out capacity of nails had to be established before other tests could be designed. A total of 366 pull-out tests was completed. The nail installation position on concrete test slabs was grouped into three categories: installation near the slab edge (edge), installation near an existing crack

(cracked concrete), and installation where the nail is not driven near a crack or a slab edge (standard). Test results revealed the following:

1. Jumbo nail pull-out strength was strongly influenced by the concrete compressive strength (f'c). The nail pull-out strengths were linearly related to the square root of the concrete compressive strength.
2. Average pull-out strength of nails installed in normal strength concrete (f'c = 28 MPa or 4,100 psi) was 36 kN (8 kips), 20 kN (4.5 kips) in low strength concrete (f'c = 19 MPa or 2,750 psi), and 44 kN (10 kips) in high strength concrete (f'c = 51 MPa or 7,400 psi).
3. Displacement at the peak pull-out load typically ranged between 0.25 mm (0.01 in.) and 0.5 mm (0.02 in.) for all concrete strengths investigated.
4. The pull-out strength decreased with decreasing distance of the nail from an edge or crack. The average pull-out strengths of nails installed at a distance of 100 mm (4 in.) and 150 mm (6 in.) from the edge of test slabs were 80 percent and 95 percent of the standard-test pull-out strength. The average pull-out strength of nails installed at 75 mm (3 in.) from cracks was 75 percent of the standard-test pull-out strength.
5. Average pull-out strength of nails driven directly into cracks was approximately 70 percent of the standard-test pull-out strength.

9.2.2 Direct Shear Transfer Tests

The interface shear force transfer between old and new concrete layers was investigated by push-off tests. An eccentricity on the order of 20 mm (3/4 in.) between the applied load and the interface produced a small moment on the interface in the in-situ push-off test. It was assumed that the magnitude of the stresses on the interface due to the eccentric loading would be negligible. Eighty-

four push-off tests were completed when the age of overlays was at least 28 days or when the compressive strength of the overlay was approximately equal to that of base slabs. Thirty-two additional push-off tests were conducted to investigate the interface shear strength development for the first several weeks after the placement of the overlay.

9.2.2.1 Bonded Interface Test results of specimens with bonded-rough and bonded-smooth interfaces revealed the following:

1. Average of the interface shear strengths of all push-off specimens with the bonded-rough interface was 2,760 kPa (400 psi). The maximum value was 4,530 kPa (660 psi) and the minimum was 1,660 kPa (240 psi).
2. Specimens which used two nails across the interface (a shear reinforcement ratio of 0.38 percent) had approximately 16 percent higher average shear strength than those without nails. Interface strengths of specimens with 0.19 percent reinforcement ratio were about the same as that in specimens without nails.
3. Overlay horizontal displacement of specimens without nails was on the order of 0.1 mm (0.004 in.) at failure while that of specimens with nails was considerably larger because nails redistributed stresses across the interface when adhesion was lost.
4. No significant differences in the interface shear strengths were found between specimens with nails in which the levels of surface preparation (average texture depth) varied between 0.3 mm (0.012 in.) and 0.8 mm (0.03 in.). Overlay slip, however, sometimes occurred at fairly low shear stresses when the interface roughness was low (0.3 mm).
5. Interface shear strengths were related to the concrete compressive strength. The average interface shear strength was 2,570 kPa (370 psi) in specimens

placed on a low strength base slab (f'c = 19 MPa or 2,750 psi) which was 88 percent of that in specimens (2,930 kPa or 425 psi) on a normal strength base slab (f'c = 32 MPa or 4,650 psi).

6. Interface shear strength was low in specimens with a smooth troweled interface, and slip began at relatively low shear stresses.
7. There were reductions in the interface strength and the post peak shear resistance of nails in cracked specimens (specimens with nails driven into or close to cracks) compared with crack-free specimens. Interface strength of the cracked specimens was approximately 90 percent of that of the crack-free specimens in normal strength slabs. Interface strength of the cracked specimens was between 70 and 85 percent of the crack-free specimens in a high strength slab.
8. No premature nail failure in pull-out was observed in any push-off tests which indicated that the development of pull-out resistance by jumbo nails used as shear connectors was adequate.

9.2.2.2 Unbonded Interface The investigation of the shear behavior of the unbonded-rough and unbonded-smooth interfaces with nails revealed the following:

1. A specimen with an unbonded-rough interface could effectively resist the shear force and limit the interface slip.
2. Shear capacity of an unbonded-rough specimens with one nail was approximately 50 kN (11 kips) at displacement of 1.5 mm (0.06 in.). Comparison between test results of the unbonded-rough specimens with one and two nails indicated that the contribution of an extra nail in resisting shear was additional 30 kN (6.5 kips).

3. Load-slip behavior of the unbonded-smooth specimens was distinctively different from that of the unbonded-rough specimens. The contribution of shear reinforcement across the interface became significant only after large slip occurred, and a dowel strength of approximately 30 kN (6.5 kips) developed at 1.5 mm slip.

9.2.2.3 Early Age Interface Shear Strength Gain Investigation of the interface strength development for the first several weeks after the placement of the overlay resulted in the following conclusions:

1. Significant bond developed 24 hours after overlay placement. Interface shear strength was 1,400 kPa (200 psi) or higher 24 hours after casting.
2. Development of interface strength was significantly influenced by the overlay curing method. Interface strength began to decrease shortly after moist curing was stopped due to drying shrinkage of the overlays. Strength increased with time when the overlay was continuously moist cured.
3. Good curing was important at early ages, especially for the first three days when interface strength gain was rapid.
4. Overlay delamination can initiate within the first 48 hours after overlay placement in bonded concrete overlays. The overlay slipped at low shear loads for some specimens tested 12 and 24 hours after the overlay placement.

9.2.3 Beam Tests for Static and Fatigue Interface Shear Strength

The possible loss of composite action due to deterioration of interface strength subjected to fatigue traffic loading in bonded concrete overlays was studied in the composite beam fatigue tests. Interface strengths determined using composite beam static tests were compared with the push-off test results.

9.2.3.1 Beam Fatigue Tests The interface strength deterioration of seven composite beams and one monolithically cast beam subjected to fatigue loading in shear was investigated. Beams with bonded-rough interfaces were subjected to approximately 3,000,000 load cycles and those with unbonded interfaces with nails to approximately 2,000,000 cycles. Test results lead to the following conclusions:

1. No interface delaminations were observed during the fatigue cycling of four composite beams with bonded-rough interfaces and a monolithically cast beam for maximum shear stress of 2,000 kPa (290 psi) during cycling. Post-fatigue static tests revealed that interface bond between base concrete and overlay was not influenced by application of the repeated loading in shear.
2. Deterioration of composite action of unbonded interfaces with nails was observed after approximately half a million cycles. Jumbo nails used across unbonded-rough interfaces provided shear resistance only after some slip occurred between the base beam and overlay. Local deterioration of the interface after cycling, such as crushing of unbonded surfaces and of concrete surrounding the nails can be the cause of slip.

9.2.3.2 Beam Static Tests Five composite beams were tested statically without cycling. Test results revealed the following:

1. Average interface shear strength of approximately 6,130 kPa (890 psi) developed between the base beam and the overlay in roughened interfaces. A shear strength of 6,390 kPa (930 psi) determined in a monolithically cast beam indicated that development of interface bond in adequately roughened interfaces was almost the same as that of monolithically cast concrete.
2. Interface shear strengths determined in all beam tests were much higher than those determined in the push-off tests probably because of the presence of some tensile stresses acting on the interface due to slight eccentricities between the applied load and the shear plane along with shear in the in-situ push-off test.

9.2.4 Full-Scale Experimental Bonded Concrete Overlay

An experimental BCO was constructed between April and June 1995 in El Paso, Texas, when the local weather conditions were considered most favorable for overlay delamination. Field condition surveys were conducted over a six-month period immediately following overlay placement. The condition of overlays in test sections with and without shear connectors was compared in terms of overlay crack development, interface tensile strength development as well as the extension of delaminated interfaces.

9.2.4.1 Overlay Drying Shrinkage Crack Development Restrained drying shrinkage of overlays resulted in development of cracks in the overlay in the transverse direction. Crack surveys revealed the following:

1. The overlay shrinkage crack development rate was highest during the first month following overlay placement.
2. Average crack spacing in the overlay one and three months after overlay placement was 1.8 m (6 ft.) and 1.2 m (4 ft.), respectively.

3. Overlay crack development was closely related to the time the overlay was placed. Total and average crack widths in a night-cast section were significantly smaller than those in day-cast sections. The cumulative crack widths in test sections cast early in the morning were also smaller than those in test sections cast later in the morning.
4. Shear connectors effectively controlled development of overlay drying shrinkage cracks at early ages. Drying shrinkage cracks which developed in test sections with shear connectors were evenly distributed while the width of cracks was typically smaller than in test sections without connectors.

9.2.4.2 Interface Strength Development Fifty-nine cores were tested to determine development of interface strength and interface delaminations. The pull-out test results revealed the following:

1. Interface tensile strength of 550 kPa (80 psi) or higher developed 30 hours after the overlay placement and 1,360 kPa (200 psi) or higher strength developed three months after overlay placement.
2. Interface delaminations occurred in the experimental BCO.
3. Delaminated interfaces were typically found near relatively wide (0.5 mm or 0.02 in.) overlay drying shrinkage cracks. The development of shrinkage in the concrete neighboring the crack seems to have caused the interface delamination.
4. Delaminated interfaces were also found in cores taken very close to the intentionally unbonded area in the corner region. Interface delaminations appeared to spread from the unbonded area.
5. Interface strengths of cores taken along the edge, at corners, and close to cracks were significantly lower than those of cores taken in the interior region away from cracks.

6. Interface strength of cores taken in a test section with nails (section 5) was significantly higher than that of cores taken at similar locations in a test section without nails (section 6).

9.2.4.3 Delamination Detection by Nondestructive Tests Three different nondestructive test (NDT) methods (SASW, impact-echo, and impulse-response tests) were used to determine interface conditions. Test results were verified by pull-out tests in some locations. Test results revealed the following:

1. The impulse-response test was effective in detecting delaminations.
2. The SASW and the impact-echo tests were not as effective in determining interface conditions as the impulse-response test.
3. The NDT test results were sensitive to temperature changes in the pavement. The delaminated interface was more difficult to detect when the temperature of the overlay was higher than that of the base slab. The best test results were obtained when the testing was done both during the day and at night.

9.3 Recommendations for Use of Jumbo Nails in BCO

Pull-out test results conducted over a six-month period following the overlay placement (June to December 1995) on an experimental BCO in El Paso, Texas, clearly indicated that a potential for interface delaminations existed under the severe local weather conditions. Delaminations can further extend during winter months due to large daily temperature change (on the order of 20°C or 35 °F) and interface conditions of the experimental BCO need to be monitored on a continuing basis. The results of the current experimental study lead to the conclusion that jumbo nails can effectively be used as “shear connectors” in the large-scale BCO to be constructed on IH-10. Nails installed along pavement edges

and longitudinal sawcuts can deter interface delaminations in the area where they are most likely to occur. An installation distance of 150 mm (6 in.) from an edge or sawcut and several different nail spacings similar to those used in the experimental BCO (380 mm to 760 mm) seem to be adequate but need further study. Although nails can be installed close to existing transverse pavement structural cracks where reflection cracking in the overlay is most likely to occur, it can be more labor intensive than installation along the edges. In case when nails are installed only in the longitudinal direction it is theorized that smaller crack widths will develop in BCO with nails and will reduce the potential for interface delaminations.

APPENDIX A
PULL-OUT TEST DATA

APPENDIX B
JUMBO NAIL DESIGN CRITERIA IN PULL-OUT

Colecchia (1994) reported the jumbo nail pull-out test results and developed the design equations with which the nail pull-out strength can be predicted. The design equations included the effect of the concrete compressive strength and the effect of the edge and crack distances on the nail pull-out strength.

B1 Pull-Out Strength in Standard Condition: No Edge or Crack Effects

When nails were tested in the standard condition (near neither an edge or a crack), the only factor which had a strong influence on pull-out strength was the concrete compressive strength. Figure B1 shows the pull-out strength versus concrete strength for all nails tested in the standard condition. A line was plotted such that 95 percent of the data points lie above it. The equation of the line is

$$Ps = f'c / 820 \qquad \text{(B1a)}$$

where Ps = pull-out strength in kips, and f'c = concrete compressive strength in psi, and it is recommended that Eq. B1a not be used for concrete strengths lower than 2700 psi or greater than 7500 psi since the recorded data did not include such concrete strengths. The SI equivalent to the above equation is

$$Ps = 0.78\ f'c \qquad \text{(B1b)}$$

Figure B1 Pull-Out Strength vs. Concrete Compressive Strength: Standard Test

where Ps = pull-out strength in kN, and f'c = concrete strength in MPa.

B2 Edge Effect

The pull-out strength decreased with decreasing edge distance when nails were installed close to the slab edges. Figure B2a shows the average pull-out strength (as a percentage of the standard strength) versus edge distance for each test slab. An average rate of increase shown in Fig. B2a was used in determining the edge effect. The concrete strength also influenced the pull-out strength. Figure B2b shows the pull-out strength versus concrete compressive strength when nails were driven at 4 in. away from the slab edges. The dashed line in Fig. B2b (linear regression line) was used to obtain the rate of reduction in pull-out strength with increasing concrete strength. The solid line in Fig. B2b has the same slope as the

(a) Pull-Out Strength vs. Edge Distance

(b) Pull-Out Strength vs. Concrete Compressive Strength at 4-in. Edge Distance

Figure B2 Edge Effect on Pull-Out Strength

dashed line but is plotted such that 95 percent of recorded data lie above it. The edge effect can be represented as a percentage of the standard pull-out strength:

$$Ee = [105 - 0.01\ f'c + 8\ (De - 4)] / 100 \leq 1.0 \qquad \text{(B2a)}$$

where Ee = edge effect (less than unity), f'c = concrete compressive strength in psi, and De = edge distance in inches (not less than 4 in.). Equation B2a is useful for determining the minimum edge distance necessary such that the edge effect has no effect on the pull-out strength. By setting Ee equal to 1.0 and solving for De in terms of f'c, the minimum edge distance can be determined by the following equation:

$$De = f'c / 800 + 3.5 \qquad \text{(B2b)}$$

The SI equivalents to above equations are

$$Ee = [105 - 1.45\ f'c + 3.15\ (De - 10)] / 100 \leq 1.0 \qquad \text{(B3a)}$$

$$De = 0.46\ f'c + 9 \qquad \text{(B3b)}$$

where De = edge distance in cm (not less than 10 cm) and f'c = concrete compressive strength in MPa.

B3 Crack Effect

Nails driven near an existing crack also had reduced pull-out strengths. As with the edge effect, the pull-out strength decreased as the distance from a crack decreased. Figures B3a and B3b show the average pull-out strength (as a

percentage of the standard strength) versus the crack distance and the pull-out strength versus existing crack width, respectively. The design equations were derived in a similar fashion as those for the edge effect and the crack effect can be determined by

$$Ec = [64 - 1.25\ Wc + 11.65\ (Dc - 1)] / 100 \leq 1.0 \qquad \text{(B4a)}$$

where Ec = crack effect (less than unity), Wc = crack width in 1/1000 inch, and Dc = distance from a crack in inches. The SI equivalent to Eq. B4a is

$$Ec = [64 - 49\ Wc + 4.6\ (Dc - 2.5)] / 100 \leq 1.0 \qquad \text{(B4b)}$$

where Wc = crack width in mm and Dc = distance from a crack in cm.

B4 Formulation of Design Equation

The design equation for the pull-out strength of a nail with a 95 percent confidence level takes the following form:

$$Pn = (Ps)\ (Ee)\ (Ec) \qquad \text{(B5)}$$

where, Pn = nominal pull-out strength, Ps = pull-out strength in standard condition (Eq. B1), Ee = edge effect (Eqs. B2a and B3a), and Ec = crack effect (Eq. B4).

(a) Pull-Out Strength vs. Crack Distance

(b) Pull-Out Strength vs. Crack Width at 1-in. Crack Distance

Figure B3 Crack Effect on Pull-Out Strength

APPENDIX C

PUSH-OFF TESTS: SUMMARY OF CONCRETE MATERIAL PROPERTIES

Table C1 Base Slabs: Test Slab Number and Material Properties

Slab No.	Aggregate Type	28-Day Compressive Strength (MPa / psi)	56-Day Compressive Strength (MPa / psi)	Date Cast	Initial Test
1	River gravel	30.1 / 4,375	32.0 / 4,650	Nov. 6, 1992	Jan. 5, 1994
2	Soft limestone	18.5 / 2,690	18.7 / 2,710	Dec. 3, 1992	Jan. 5, 1994
3	Hard limestone	26.6 / 3,865	28.2 / 4,090	Dec. 11, 1992	Nov. 13, 1993
4	Soft limestone	47.2 / 6,850	51.3 / 7,440	Jan. 15, 1993	Nov. 10, 1993

Table C2 Overlay Material Properties

Test Series	Base Slab No.	Overlays			
		28-Day Strength (MPa / psi)	Aggregate Type	Date Cast	Initial Test
DS-I	1	30.4 / 4,410	River gravel	Feb. 15, 1994	Mar. 16, 1994
DS-II	2	19.5 / 2,830	River gravel	Feb. 22, 1994	Mar. 28, 1994
DS-III	1	37.8 / 5,480	River gravel	Aug. 17, 1994	Aug. 26, 1994
	3	30.5 / 4,420	River gravel	Sept. 22, 1994	Oct. 4, 1994
DS-IV	4	26.7 / 3,870	River gravel	May 31, 1994	--
DS-V	1	29.3 / 4,260	River gravel	Dec. 14, 1993	Jan. 5, 1994
	2	ditto	ditto	ditto	ditto
	3	28.1 / 4,085	Soft limestone	Oct. 15, 1993	Nov. 13, 1993
	4	ditto	ditto	ditto	Nov. 5, 1993
ES-I	4	28.7 / 4,170	River gravel	Mar. 9, 1994	Mar. 10, 1994
ES-II	3	25.4 / 3,690	River gravel	May 25, 1994	May. 26, 1994

APPENDIX D

EXPERIMENTAL BCO: OVERLAY MIX DESIGNS

Table D1 Overlay Mix Proportions per Cubic Meter [a]

Mix Constituents	Plain Concrete	Polypropylene Fibrous Concrete (PFRC)	Steel Fibrous Concrete (SFRC)
Water	151 kg	151 kg	151 kg
Cement, Type I/II	520 kg	520 kg	520 kg
Coarse Aggregate	1,061 kg	1,061 kg	1,010 kg [b]
Fine Aggregate	653 kg	653 kg	653 kg
Fibers	--	1.78 kg [c]	44.5 kg [d]
Air Entrainment	16.1 ml/100 kg cement	16.1 ml/100 kg cement	16.1 ml/ 100 kg cement
High Range Water Reducer	53.7 ml/100 kg cement	53.7 ml/100 kg cement	53.7 ml/100 kg cement

Note a: Water cement ratio = 0.29
b: Contains 404 kg intermediate size aggregate
c: Fibrillated polypropylene fibers
d: 60-mm long steel fibers with hooked ends

APPENDIX E
LAYOUT OF SHEAR CONNECTORS

APPENDIX F

EXAMPLES OF NONDESTRUCTIVE TEST RESULTS

Figure F1 SASW Tests Showing Bonded Interface

Figure F2 SASW Tests Showing Delaminated Interface

Figure F3 Impact-Echo Tests Showing Bonded Interface

Figure F4 Impact-Echo Tests Showing Delaminated Interface

Figure F5 Impulse-Response Tests

APPENDIX G

EXPERIMENTAL BCO: PULL-OUT TEST RESULTS

Table G1 Summary of Pull-Out Test Results: September 1995

Section No.	Core No.	Location [a]		Pull-out		Area of Section
		North	West	Load (lbs)	Strength (psi)	
5	8	7 in.	14 in.	0	0	Corner
	9	6 in.	6 ft.	200	14	Edge
	10	6 in.	10 ft. 9 in.	2,100	148	Corner
	11	22 ft. 2 in.	6 ft.	2,550	203	Interior
	12	43 ft. 4 in.	1 ft. 4 in.	> 3,100	> 219	Edge
	13	42 ft. 11 in.	10 ft. 8 in.	2,150	152	Edge
6	14 [b]	6 in.	16 in.	0	0	Corner
	15 [b]	6 in.	5 ft. 9 in.	0	0	Edge
	16 [b]	6 in.	10 ft. 8 in.	0	0	Corner
	17	24 ft. 10 in.	6 ft. 4 in.	2,800	197	Interior
	18	30 ft. 11 in.	11 ft. 3 in.	1,150	81	Near crack
	19	31 ft. 7 in.	11 ft. 3 in.	800	56	Near crack

Note a: Distance measured from south-east corner of each test section,
b: Pull-out test performed in the intentionally unbonded area using bond breaker.

Table G2 Summary of Pull-Out Test Results: November 1995

Section No.	Core No.	Location [a]		Pull-out		Area of Section
		North	West	Load (lbs)	Strength (psi)	
5	20	24 ft. 6 in.	6 ft.	2,100	167	Near crack
	21	25 ft. 2 in.	6 ft.	1,650	116	Near crack
	22	47 ft. 8 in.	11 ft. 8 in.	1,400	111	Edge
	23	48 ft. 8 in.	11 ft. 8 in.	0	0	Corner
6	24	1 ft. 4 in.	11 ft. 8 in.	0	0	Corner
	25	2 ft. 4 in.	11 ft. 8 in.	900	72	Edge
	26	40 ft. 10 in.	11 ft. 8 in.	0	0	Near crack
	27	41 ft. 6 in.	11 ft. 8 in.	0	0	Near crack
	28	48 ft.	11 ft. 8 in.	950	76	Edge
	29	49 ft. 8 in.	11 ft. 8 in.	> 800	> 64	Corner
	30	49 ft. 8 in.	6 ft.	1,100	88	Edge
	31	49 ft. 8 in.	1 ft. 4 in.	430	34	Corner
	32	40 ft. 10 in.	10 ft. 8 in.	650	52	Near crack
	33	41 ft. 6 in.	10 ft. 8 in.	250	20	Near crack

Note a: Distance measured from south-east corner of each test section.

Table G3 Summary of Pull-Out Test Results: December 1995

Section No.	Core No.	Location [a]		Pull-out		Area of Section
		North	West	Load (lbs)	Strength (psi)	
5	34	21 ft. 2 in.	6 ft.	> 2,800	> 223	Interior
	35	4 ft. 5 in.	11 ft. 8 in.	3,950	314	Edge
	36	6 ft. 10 in.	11 ft. 8 in.	2,550	203	Edge
	37	24 ft. 8 in.	11 ft. 8 in.	0	0	Crack
	38	25 ft. 4 in.	11 ft. 8 in.	900	72	Crack
	39	39 ft. 6 in.	11 ft. 8 in.	1,600	127	Crack
	40	40 ft. 2 in.	11 ft. 8 in.	1,750	139	Crack
	41	42 ft. 11 in.	11 ft. 8 in.	1,850	147	Edge
	42	43 ft. 11 in.	11 ft. 8 in.	3,400	271	Edge
	43	1 ft. 4 in.	1 ft. 4 in.	> 2,650	> 211	Corner
	44	1 ft. 4 in.	6 ft.	2,150	171	Edge
	45	7 ft.	1 ft. 4 in.	> 2,200	> 175	Edge
	46	31 ft. 10 in.	11 ft. 8 in.	> 2,250	> 179	Edge
	47	33 ft. 6 in.	11 ft. 8 in.	1,900	151	Edge
	48	45 ft.	1 ft. 4 in.	> 1,100	> 88	Edge
	49	48 ft. 4 in.	1 ft. 10 in.	2,500	199	Corner
	50	48 ft. 8 in.	6 ft.	1,550	123	Edge
	51	39 ft. 6 in.	1 ft. 4 in.	Bonded [b]	--	Crack
	52	40 ft. 2 in.	1 ft. 4 in.	> 1,750	> 139	Crack

Note a: Distance measured from south-east corner of each test section,
b: Pull-out strength not tested.

Table G3 Summary of Pull-Out Test Results: December 1995 (Cont'd.)

Section No.	Core No.	Location [a]		Pull-out		Area of Section
		North	West	Load (lbs)	Strength (psi)	
6	53	1 ft. 4 in.	6 ft.	> 1,200	> 95	Edge
	54	1 ft. 8 in.	1 ft. 10 in.	0	0	Corner
	55	5 ft.	1 ft. 4 in.	> 2,150	> 171	Edge
	56	16 ft.	1 ft. 4 in.	> 1,500	> 119	Crack
	57	10 ft. 8 in.	11 ft. 8 in.	1,550	123	Edge
	58	11 ft. 8 in.	11 ft. 8 in.	2,600	207	Edge
	59	16 ft.	11 ft. 8 in.	0	0	Crack
	60	16 ft. 8 in.	11 ft. 8 in.	0	0	Crack
	61	23 ft. 10 in.	6 ft. 4 in.	> 2,900	> 231	Interior
	62	39 ft. 10 in.	1 ft. 4 in.	Bonded [b]	--	Edge
	63	40 ft. 10 in.	1 ft. 4 in.	0	0	Crack
	64	40 ft. 10 in.	2 ft. 10 in.	0	0	Crack
	65	40 ft. 10 in.	6 ft.	Bonded [b]	--	Crack
	66	42 ft. 6 in.	11 ft. 8 in.	450	36	Edge

Note a: Distance measured from south-east corner of each test section,
b: Pull-out strength not tested.

APPENDIX H

NONDESTRUCTIVE TEST RESULTS: JUNE 1995

REFERENCES

1. "Standard Specifications for Highway Bridges." (1989). American Association of State Highway and Transportation Officials, Washington D.C.

2. ACI Committee 318 (1989). "Building Code Requirements for Reinforced Concrete and Commentary (ACI 318-89)." American Concrete Institute, Detroit, MI.

3. Allison B.T., McCullough B.F., and Fowler D.W. (1993). "Feasibility Study for a Full-Scale Bonded Concrete Overlay on IH-10 in El Paso, Texas." The University of Texas at Austin, Center for Transportation Research, Report No. 1957-1F.

4. Al-Negheimish A.I. (1988). "Bond Strength, Long Term Performance and Temperature Induced Stresses in Polymer Concrete-Portland Cement Concrete Composite Members." Ph.D. Dissertation, The University of Texas at Austin.

5. Anderson A.R. (1960). "Composite Designs in Precast and Cast-in-Place Concrete." *Progressive Architecture*, 41(9), pp. 172-179.

6. "ASTM E 965 Measuring Surface Macrotexture Depth Using a Sand Volumetric Technique." (1990). 1990 Annual Book of ASTM Standards, 04.02, American Society for Testing and Materials, Philadelphia, Penn.

7. Badoux J.C. and Hulsbos C.L. (1967). "Horizontal Shear Connection in Composite Concrete Beams under Repeated Loads." *Journal of American Concrete Institute*, 64, pp. 811-819.

8. Bagate M., McCullough B.F., Fowler D.W., and Muthu M. (1985). "An Experimental Thin-Bonded Concrete Overlay Pavement." The University of Texas at Austin, Center for Transportation Research, Report No. 357-2F.

9. Bass R.A., Carrasquillo R.L., and Jirsa J.O. (1989). "Shear Transfer across New and Existing Concrete Interfaces." *ACI Structural Journal*, 86(4), pp. 383-393.

10. Birkland P.W. and Birkland H.W. (1966). "Connections in Precast Concrete Construction." *Journal of American Concrete Institute*, 63(3), pp. 345-368.

11. Breuss M. and Gassmann H.D. (1992). “Jumbo Nail Test Results - Phase 0.” The University of Texas at Austin: Hilti Corporate Research, Report No. IBEb/25.9.92.

12. Calvert G. (1990). “Thin Bonded Concrete Overlay with Fast Track Concrete.” Iowa Department of Transportation, Final Report for IDOT Proj. HR-531.

13. Campbell R.L. Sr. (1994). “Overlays on Horizontal Concrete Surfaces: Case Histories.” US Army Corps of Engineers, Technical Report REMR-CS-42.

14. Chen D., Cheng S., and Gerhardt T.D. (1982). “Thermal Stresses in Laminated Beams.” *Journal of Thermal Stresses*, 5(1), pp. 67-84.

15. Choi D. (1992). “An Analytical Investigation of Thermally-Induced Stresses in Polymer Concrete-Portland Cement Concrete Composite Beams.” M.S. Thesis, The University of Texas at Austin.

16. Choi D., Fowler D.W., and Wheat D.L. (1996). “Thermal Stresses in Polymer Concrete Overlays.” Special Publication in press, American Concrete Institute, Detroit, MI.

17. Colecchia M. Jr. (1994). “Tensile Behavior of Large Powder-Driven Fasteners in Concrete.” M.S. Thesis, The University of Texas at Austin.

18. Dulacska H. (1972). “Dowel Action of Reinforcement Crossing Cracks in Concrete.” *Journal of American Concrete Institute*, 69(12), pp. 754-757.

19. Felt E.J. (1956). “Resurfacing and Patching Concrete Pavements with Bonded Concrete.” *Proceedings*, Highway Research Board, 35, pp. 444-469: PCA Development Bulletin D8.

20. Felt E.J. (1960). “Repair of Concrete Pavement.” *Journal of American Concrete Institute*, 32(2), pp. 139-153.

21. Ferguson P.M., Breen J.E., and Jirsa J.O. (1988). *Reinforced Concrete Fundamentals*. 5th Edition, John Wiley & Sons, Inc.

22. Friberg B.F. (1938). “Design of Dowels in Transverse Joints of Concrete Pavements.” *Proceedings*, ASCE, pp. 1076-1116.

23. Gambarova P.G. and Prisco M.D. (1991). "Behavior and Analysis of R.C. Structures under Alternate Actions Inducing Inelastic Response: Chapter 5 - Interface Behavior." CEB-GTG 22, Draft presented at CEB plenary session, Wien.

24. Gillette R.W. (1963). "Performance of Bonded Concrete Overlays." *Journal of American Concrete Institute,* 60(1), pp. 39-49.

25. Goodman J.R. and Popov E.P. (1968). "Layered Beam Systems with Interlayer Slip." *Journal of Structural Division,* ASCE, 94(11), pp. 2535-2547.

26. Grimado P.B. (1978). "Interlaminar Thermoelastic Stresses in Layered Beams." *Journal of Thermal Stresses,* 1(1), pp. 75-86.

27. Grossfield B. and Birnstiel C. (1962). "Tests of T-Beams with Precast Webs and Cast-in-Place Flanges." *Journal of American Concrete Institute,* 59(6), pp. 843-851.

28. Hanson N.W. (1960). "Precast-Prestressed Concrete Bridges 2. Horizontal Shear Connections." *Journal,* PCA Research and Development Laboratories, 2(2), pp. 38-58.

29. Harris G. (1992). "Performance of a Nongrouted Thin Bonded PCC Overlay." Iowa Department of Transportation, Final Report for Highway Research Advisory Board, Proj. HR-291.

30. Hassan S., Meyer A.H., and Fowler D.W. (1991). "Establishment of Acceptance Limits for 4-Cycle MSS and Modified Wet Ball Mill Tests for Aggregates Used in Seal Coats and HMAC Surfaces." The University of Texas at Austin, Center for Transportation Research, Report No. 1222-1F.

31. Hess M.S. (1969). "The End Problem for a Laminated Elastic Strip: Differential Expansion Stresses." *Journal of Composite Materials,* 3, pp. 630-641.

32. Hilsdorf H.K. and Kesler C.E. (1966). "Fatigue Strength of Concrete under Varying Flexural Stresses." *Journal of American Concrete Institute,* 63(10), pp. 1059-1075.

33. Hofbeck J.A., Ibrahim I.O., and Mattock A.H. (1969). "Shear Transfer in Reinforced Concrete." *Journal of American Concrete Institute,* 66(2), pp. 119-128.

34. Hsu T.C. and Slate F.O. (1963). "Tensile Bond Strength between Aggregate and Cement Paste or Mortar." *Journal of American Concrete Institute*, 60(4), pp. 465-485.

35. Hutchinson R.L. (1982). "Resurfacing with Portland Cement Concrete." NCHRP Synthesis of Highway Practice 99, Transportation Research Board, National Research Council, Washington D.C.

36. Jimenez R., White R.N., and Gergely P. (1979). "Bond and Dowel Capacities of Reinforced Concrete." *Journal of American Concrete Institute*, 76, pp. 73-92.

37. Johnston D.W. and Zia P. (1971). "Analysis of Dowel Action." *Journal of Structural Division*, ASCE, 97(5), pp. 1611-1630.

38. King W.M. Jr. (1992). "Design and Construction of a Bonded Fiber Concrete Overlay of CRCP." Louisiana Transportation Research Center, Report No. FHWA/LA-92/266.

39. Krauthammer T. (1992). "Minimum Shear Reinforcement Based on Interface Shear Transfer." *ACI Structural Journal*, 89(1), pp. 99-105.

40. Krefeld W.J. and Thurston C.W. (1966). "Contribution of Longitudinal Steel to Shear Resistance of Reinforced Concrete Beams." *Journal of American Concrete Institute*, 63(3), pp. 325-343.

41. Lau C.M., Fwa T.F., and Paramasivam P. (1994). "Interface Shear Stress in Overlaid Concrete Pavements." *Journal of Transportation Engineering*, ASCE, 120(2), pp. 163-177.

42. Lundy J.R. (1990). "Delamination of Bonded Concrete Overlays at Early Ages." Ph.D. Dissertation, The University of Texas at Austin.

43. Lundy J.R., McCullough B.F., and Fowler D.W. (1991). "Delamination of Bonded Concrete Overlays at Early Ages." The University of Texas at Austin, Center for Transportation Research, Report No. 1205-2.

44. Marcus H. (1951). "Load Carrying Capacity of Dowels at Transverse Pavement Joints." *Journal of American Concrete Institute*, 23(2), pp. 169-184.

45. Marks V.J. (1990). “Thin Bonded Portland Cement Concrete Overlay.” Iowa Department of Transportation, Final Report for IDOT Proj. HR-520.

46. Mast R.F. (1968). “Auxiliary Reinforcement in Concrete Connections.” *Journal of Structural Division*, ASCE, 94(6), pp. 1485-1504.

47. Mattock A.H. (1974). “Shear Transfer in Concrete Having Reinforcement at an Angle to the Shear Plane.” *Shear in Reinforced Concrete*, Special Publication SP-42, American Concrete Institute, Detroit, MI., pp. 17-42.

48. Mattock A.H. and Hawkins N.M. (1972). “Shear Transfer in Reinforced Concrete: Recent Research.” *PCI Journal*, 17(2), pp. 55-75.

49. Mattock A.H., Johal L., and Chow H.C. (1975). “Shear Transfer in Reinforced Concrete with Moment or Tension Acting across the Shear Plane.” *PCI Journal*, 20(4), pp. 76-93.

50. McGhee K.H. (1994). “Portland Cement Concrete Resurfacing.” NCHRP Synthesis of Highway Practice 204, Transportation Research Board, National Research Council, Washington D.C.

51. van Metzinger W.A. (1990). “An Empirical-Mechanistic Design Method Using Bonded Concrete Overlays for the Rehabilitation of Pavements.” Ph.D. Dissertation, The University of Texas at Austin.

52. van Metzinger W.A., McCullough B.F., and Fowler D.W. (1991). “An Empirical-Mechanistic Design Method Using Bonded Concrete Overlays for the Rehabilitation of Pavements.” The University of Texas at Austin, Center for Transportation Research, Report No. 1205-1.

53. Millard S.G. and Johnson R.P. (1984). “Shear Transfer across Cracks in Reinforced Concrete due to Aggregate Interlock and to Dowel Action.” *Journal*, Magazine of Concrete Research, 36(126), pp. 9-21.

54. Millard S.G. and Johnson R.P. (1985). “Shear Transfer in Cracked Reinforced Concrete.” *Journal*, Magazine of Concrete Research, 37(130). pp. 3-15.

55. Mindess S. and Young J.F. (1981). *Concrete*. Prentice-Hall Inc., Englewood Cliffs, NJ.

56. Mitsui K., Li Z., Lange D.A., and Shah S.P. (1994). "Relationship between Microstructure and Mechanical Properties of the Paste-Aggregate Interface." *ACI Materials Journal*, 91(1), pp. 30-39.

57. Neal B.F. (1983). "California's Thin Bonded PCC Overlay." California Department of Transportation, Report No. FHWA/CA/TL-83/04.

58. Neville A.M. (1981). *Properties of Concrete*. 3rd Edition, Longman Scientific & Technical, Longman Group Limited, England.

59. Newmark N.M., Siess C.P., and Viest I.M. (1951). "Tests and Analysis of Composite Beams with Incomplete Interaction." *Proceedings*, Society for Experimental Stress Analysis, 9(1), pp. 75-92.

60. Paulay T., Park R., and Phillips M.H. (1974). "Horizontal Construction Joints in Cast-in-Place Reinforced Concrete." *Shear in Reinforced Concrete*, Special Publication SP-42, American Concrete Institute, Detroit, MI., pp. 599-616.

61. Poli S.D., Prisco M.D., and Gambarova P.G. (1992). "Shear Response, Deformations, and Subgrade Stiffness of a Dowel Bar Embedded in Concrete." *ACI Structural Journal*, 89(6), pp. 665-675.

62. *Design and Control of Concrete Mixtures*. (1988). Portland Cement Association, Skokie, IL.

63. Richart F.E. Jr., Hall J.R. Jr., and Woods R.D. (1970). *Vibrations of Soils and Foundations*. Prentice-Hall Inc., Englewood Cliffs, NJ.

64. Saemann J.C. and Washa G.W. (1964). "Horizontal Shear Connections between Precast Beams and Cast-in-Place Slabs." *Journal of American Concrete Institute*, 61(11), pp. 1383-1409.

65. Sansalone M. and Pratt D.G. (1993). "Theory and Operation Manual for the Impact-Echo Field System." 2nd. Edition, Cornell University Structural Engineering Report, Report No. 92-2.

66. Seible F. and Latham C.T. (1990). "Horizontal Load Transfer in Structural Concrete Bridge Deck Overlays." *Journal of Structural Engineering*, ASCE, 116(10), pp. 2691-2710.

67. Seible F. and Latham C.T. (1990). "Analysis and Design Models for Structural Concrete Bridge Deck Overlays." *Journal of Structural Engineering*, ASCE, 116(10), pp. 2711-2728.

68. Silfwerbrand J. (1990). "Improving Concrete Bond in Repaired Bridge Decks." *Journal*, Concrete International, American Concrete Institute, pp. 61-66.

69. Slater R.E. (1993). "Highway Statistics 1992." Federal Highway Administration, Publication No. FHWA-PL-93-023 HPM-40/10-93(4.2M)P.

70. Soroushian P., Obaseki K., Rojas M.C., and Sim J. (1986). "Analysis of Dowel Bars Acting against Concrete Core." *Journal of American Concrete Institute*, 83(4), pp. 642-649.

71. Soroushian P., Obaseki K., and Rojas M.C. (1987). "Bearing Strength and Stiffness of Concrete under Reinforcing Bars." *ACI Materials Journal*, 84(3), pp. 179-184.

72. Stelson T.E. and Cernica J.N. (1958). "Fatigue Properties of Concrete Beams." *Journal of American Concrete Institute*, 30(2), pp. 255-259.

73. Stokoe K.H. II et al. (1988). "In Situ Seismic Testing of Hard-to-Sample Soils by Surface Wave Method." American Society of Civil Engineers, Specialty Conference on Earthquake Engineering and Soil Dynamics II - Recent Advances in Ground Motion Evaluation, Park City, Utah.

74. Tassios T.P. and Vintzeleou E.N. (1987). "Concrete-to-Concrete Friction." *Journal of Structural Engineering*, ASCE, 113(4), pp. 832-849.

75. Taylor M.A. and Broms B.B. (1964). "Shear Bond Strength between Coarse Aggregate and Cement Paste or Mortar." *Journal of American Concrete Institute*, 61(8), pp. 939-956.

76. Temple W.H. and Cumbaa S.L. (1985). "Thin Bonded P.C.C. Resurfacing." Louisiana Department of Transportation and Development Research and Development Section, Report No. FHWA/LA-85/181.

77. Teo K.J., Fowler D.W., and McCullough B.F. (1989). "Monitoring and Testing of the Bonded Concrete Overlay on Interstate Highway 610 North in Houston, Texas." The University of Texas at Austin, Center for Transportation Research, Report No. 920-3.

78. Timoshenko S. (1926). "Analysis of Bi-Metal Thermostats." *Journal of Strain Analysis*, 11, pp. 233-255.

79. Valluvan R. (1993). "Issues Involved in Seismic Retrofit of Reinforced Concrete Frames Using Infilled Walls." Ph.D. Dissertation, The University of Texas at Austin.

80. Vanderbilt M.D., Goodman J.R., and Criswell M.E. (1974). "Service and Overload Behavior of Wood Joist Floor Systems." *Journal of Structural Division*, ASCE, 100(1), pp. 11-29.

81. Vintzeleou E.N. and Tassios T.P. (1986). "Mathematical Models for Dowel Action under Monotonic and Cyclic Conditions." *Journal*, Magazine of Concrete Research, 38(134), pp. 13-22.

82. Vintzeleou E.N. and Tassios T.P. (1987). "Behavior of Dowels under Cyclic Deformations." *ACI Structural Journal*, 84(1), pp. 18-30.

83. Wade D.M., Fowler D.W., and McCullough B.F. (1995). "Concrete Bond Characteristics for a Bonded Concrete Overlay on IH-10 in El Paso." The University of Texas at Austin, Center for Transportation Research, Report No. 2911-2.

84. Whiting et al. (1993). "Synthesis of Current and Projected Concrete Highway Technology." SHRP-C-345, Strategic Highway Research Program, National Research Council, Washington D.C.

85. Whitney D.P., Isis P., McCullough B.F., and Fowler D.W. (1992). "An Investigation of Various Factors Affecting Bond in Bonded Concrete Overlays." The University of Texas at Austin, Center for Transportation Research, Report No. 920-5.